Università degli Studi di Torino

PhD Programme in Complex Systems For Life Sciences

Department of Oncology

Title of the thesis:

"Three-dimensional collective migration of cancer cells *in vitro*"

Cycle: XXXIII

Academic years: 2017-2020

PhD Programme Coordinator: Prof. Enzo Medico

Candidate: Miriam Palmiero **Tutor: Prof. Luca Primo**

"Within the shadow of the ship
I watched their rich attire:
Blue, glossy green, and velvet black,
They coiled and swam; and every track
Was a flash of golden fire."

Samuel Taylor Coleridge,
"The Rime of the Ancient Mariner", Part IV

ABSTRACT

Metastatization occurs through the acquisition of invasive and survival capabilities that allow tumour cells to colonize distant sites. In tumours of epithelial origin detachment from the primary site is associated with the acquisition of mesenchymal traits, at least partial. A wide literature exists on the so-called epithelial to mesenchymal transition observed in single tumour cells, but the evidence of collective phenomena is also compelling.

It was recently shown that metastasis originating clusters can derive from the detachment of oligoclonal groups of cells from the primary tumour site and that circulating tumour clusters, albeit much rarer than single circulating tumour cells, are associated with a significantly higher metastatic potential. However, while the role of multicellular aggregates in cancer dissemination is acknowledged, the mechanisms that drive the formation of multi-clonal cell aggregates are not fully elucidated.

Here we show that 6 cancer cells of different tissue of origins can perform collective directional migration and can actively form heteroclonal aggregates in 3D.

Coalescence of distant cell clusters is mediated by subcellular actin-rich protrusions and multicellular outgrowths that directionally extend towards neighbouring aggregates. Coherently, perturbation of cytoskeletal dynamics impairs collective migration while myosin II activation is necessary for multicellular movements.

We put forward the hypothesis that cluster attraction is mediated by secreted soluble factors and show, consistently, that the inhibition of master downstream effectors PI3K/AKT/mTOR and MEK/ERK results in the abrogation of aggregation, coupled to a significant decrease of cell proliferation. Our hypothesis is supported by the evidence that conditioned culture media act as chemoattractant. Moreover, cells that respond chemotactically to conditioned media of other cells are also performing collective directional migration towards them.

Our results present a novel collective migration model and shed light on the mechanisms of formation of heteroclonal aggregates in cancer.

AKNOWLEDGEMENTS

My sincere gratitude goes to all those who, in various ways and in different roles, have accompanied me all along my PhD:

Professor Luca Primo, for welcoming me into his laboratory, trusting me and supporting my scientific growth with valid and highly-experienced advice, proving to be a precious guide.

Alberto Puliafito, without whom this work would not have existed and I would not be neither the researcher nor the person I am today. Thank you for the countless moments of high-quality scientific discussion, for the constructive criticisms about the work done and for the encouragement not to give up just because the road ahead was winding. I would have missed so many beautiful landscapes! Thank you for being there, even at "unlikely" times and in so many days red on the calendar.

Professors Stefano Di Talia and Giorgio Scita who have read and critically reviewed this work.

My colleagues Laurina, Vale and Barbara, for sharing this experience with me and for providing me indispensable tools to face the doctorate path, with scientific and moral support.

The colleagues of the Institute, who contributed to make enjoyable the interludes of the day. A special thanks to Desy, Giulia and Mele, the "former colleagues", with whom I shared not only my work experience, but also a piece of life, including various joys and delusions! Ilenia and Edo, who lightened the hardest days, made the ordinary ones more fun and put up with my outbursts, and Laura, for her complicity in the ups and downs of the everyday working life.

The friends scattered here and there, for staying so close albeit so far.

My family, for having made possible for me to get this far, for their ceaseless and unconditional support.

My brother Christian, uncle Pietro and my grandparents, for the love they taught me and that make me feel, always.

Enrico, the one who has been by my side.

TABLE OF CONTENTS

INTRODUCTION

CHAPTER 1: CANCER INVASION AND METASTASIS

Cancer has been known to humans since ancient times. One of the earliest historical evidence of the existence of this disease dates back to ancient Egypt, around 3000 BC, and consists in the finding of fossilised bone tumours in mummies [1, 2]. The disease was considered incurable already at that time. The word cancer appeared for the first time in the medical literature around 400 BC thanks to Hippocrates, who named the tumour "*karkinos*", from the Greek term for "crab" [1]. This name brings to our mind a vivid image, which recalls one of the main features of cancer: its capability to spread and invade.

Even if today we know many more things about cancer, we are still unable to cope with its destructive course, mainly because in a variety of human tumour types, the dissemination of cancer cells throughout the body occurs long before the primary tumour is diagnosed; indeed the 90% of patients die following the formation of metastases [3].

During the travel from the primary site to distant organs, both tumour cells and associated stromal cells undergo multiple biochemical and biological changes. The various steps accomplished by tumour cells to complete the metastatization process, schematically resumed under the name of "invasion-metastasis cascade" [4, 5] (Fig. 1), will be described in the following section.

The discussion will be focused on carcinomas, i.e., tumour arising from epithelial tissues, since the majority of the experiments presented in this thesis were conducted on epithelial tumours and the aspects treated in this section will provide preliminary notions to the proper understanding of the work.

Particular emphasis will be given to the mechanisms through which tumour cells detach from the primary site and acquire invasive and survival capability, including single-cell and collective migration and the contribution of paracrine and autocrine signalling, from the early stages of the metastatic cascade to the colonization of distant organs.

1.1 From primary tumour to distant site

1.1.1 The metastatic cascade

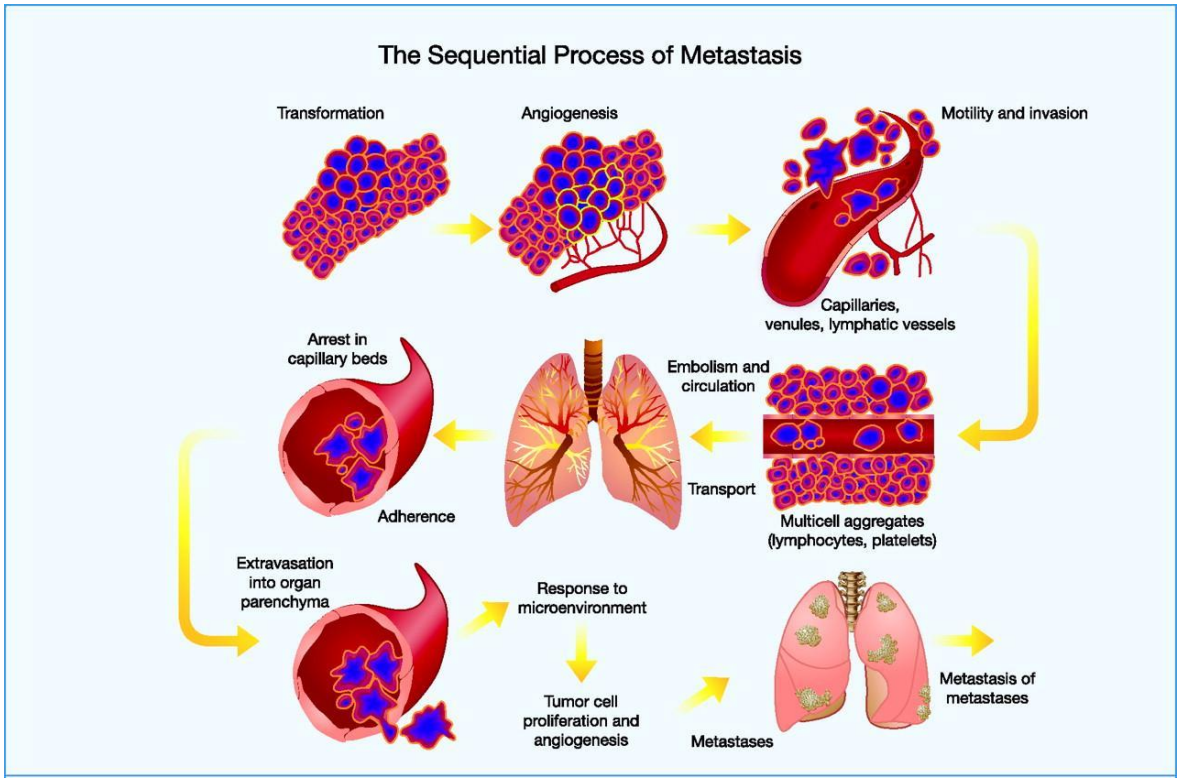

Figure 1 The metastatic cascade
This figure resumes the main steps of metastatic cascade. Clinically detectable metastases represent the result of a series of events which include the detachment of tumour cells from the primary site, the entrance in the circulation, the survival until the arrest in the capillary beds, the extravasation and the colonization of the secondary site.
From "AACR centennial series: the biology of cancer metastasis: historical perspective" [6]

1) The detachment from the epithelium

The great majority of the epithelial tissues are constituted by thin sheets of epithelial cells leaning on a layer of stroma. Between the epithelial cells and the stroma there is the basement membrane (BM), a specialised type of extracellular matrix (ECM), constituted by proteins secreted by both epithelial and stromal cells. As long as carcinoma cells remain on the epithelial side of the BM, a tumour is considered to be benign [7].

The detachment of individual or grouped cancer cells from the primary tumour and the invasion into the surrounding stroma, characterized by perforation of the BM, marks the onset of malignancy. Even if the invasion is not necessarily followed by metastasis, e.g., in the basal cell carcinomas of the skin and in glioblastoma multiforme [8], this process is considered to be a prerequisite for metastasis.

Notably, unlike normal epithelial cells, which undergo apoptosis upon losing contact to the extracellular matrix, tumour cells develop mechanisms to detach from the primary tumour [9].

The disruption of BM, necessary to allow the passage of tumour cells, is mediated by active proteolysis exerted mainly by matrix metalloproteinases (MMPs), which are secreted or activated by tumour and stromal cells. At the same time, MMP-secreting cells also produce growth factors, which enhance tumour cell proliferation [10]. Following the perforation of the BM, tumour cells enter into the surrounding stroma, where the interaction with stromal cells is fundamental to promote the invasive behaviour of tumour. Indeed, when in contact with tumour cells, stromal cells produce various heterotypic signals, activating a response which resembles what happens in wound healing or in chronical inflammation [11]. For example, in breast cancer, adipocytes present in the tumour stroma contribute to the invasion by secreting interleukin-6 (IL-6) [12]. Moreover, stromal $CD4^+$ T-lymphocytes regulate mammary carcinomas invasion by enhancing pro-tumour properties of tumour-associated macrophages (TAMs), i.e., promoting the activation of the epidermal growth factor (EGF) signalling in tumour cells [13]. The interaction is bidirectional since tumour cells send stimuli to the stroma and the tumour-stimulated stroma reacts, producing tumour-stimulating molecules, thus generating a positive feedback loop.

The migration of tumour cells that detach from the epithelium can occur by single cells (Fig. 2a), or more frequently by cohorts of cells which maintain a certain degree of cell-cell adhesion (Fig. 2b,c).

Once detached from the epithelium, cancer cells need to enter the circulation to reach distant organs. As a primary tumour grows, even before the disruption of the BM, it needs to receive a blood supply that can support its metabolic needs. Already

in the 1950s pathologists noticed that tumour cells grow preferentially nearby blood vessels, observing that they stopped their growing if more than 0.2 mm away from the vessels and died if even farther away [14]. To secure this necessary blood supply, cells of the tumour-associated stroma have again a crucial role. For example, myofibroblasts release chemotactic factors which attract endothelial precursor cells into the stroma and they also compensate the eventual loss of vascular endothelial growth factor (VEGF) in tumour cells, which promotes the maturation of the precursor in functional endothelial cells [15]. Similar mechanisms regulate also the formation of lymphatic vessels [16].

Importantly, continually emerging researches indicate that tumours can support their growth also by non-angiogenic mechanisms. For example, they can utilize pre-existing blood vessels of the surrounding normal tissues, a process that is called vessel co-option [17, 18]. Alternatively, tumour cells can organize themselves to form vascular-like channels, independently of angiogenesis. This process was first described in uveal melanomas and takes the name of vasculogenic mimicry [19].

Both the pre-existing and the newly-formed blood and lymphatic vessels serve also to provide an escape route by which cells can leave the primary tumour site.

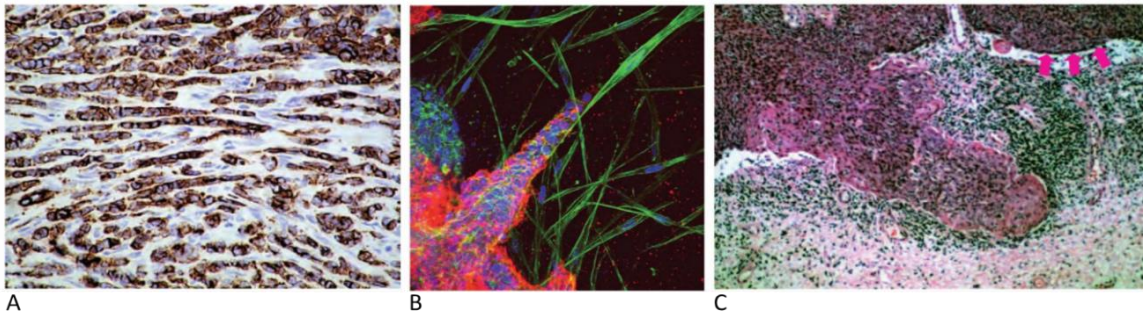

Figure 2 Different patterns of invasion

(A) Invasive mammary carcinoma cells (in brown) which have left the primary tumour and proceed one by one in single file in the surrounding stroma. **(B)** More typical than single cell migration is the collective invasion performed by carcinoma cells which detach from the primary tumour. In this picture an *in vitro* experiment made to model collective migration is represented. MCF7 human breast cancer cells were cultured together with cancer in a 3D collagen gel. Breast cancer cells invade the matrix preserving E-cadherin containing adherens junctions (red) between one cell and another. Actin stress fibres and fibroblast are labelled with phalloidin (in green) and nuclei with DAPI (in blue). **(C)** Here is shown the collective behaviour of squamous cell carcinoma of the cervix (in pink and brown), which disrupt the BM (the dark brown line pointed by pink arrows) and invade the stroma (in dark green).
From "The biology of Cancer" (second edition) [7]

2) The intravasation

Following the perforation of the epithelial basement membrane, the majority of tumour cells enter the vasculature or, to a lesser extent, the lymphatic system, by a process called intravasation.

The intravasation can both involve active cell migration or can be achieved by the passive entrance of tumour cells in the vessels, depending on the tumour type, the structure of the blood vessels and the tumour microenvironment [20].

The entrance in the lumina of the vessels occurs following the cross of their walls, constituted by pericyte and endothelial cell barriers. This ability is acquired by tumour cells thanks to the release of signalling molecules and of proteases, e.g., MMPs, by other cells in the tumour microenvironment and by tumour cells themselves [21]. The structural properties of the new blood vessels formed by tumours facilitate the access into the lumina since, unlike the blood vessels in normal tissues, the peri-tumour neovasculature is prone to leakiness and lacks of a dense coverage of pericytes [22].

It is reported that the endothelial barrier leakage, which occurs both in intravasation and in extravasation (when tumour cells leave the vasculature), is mediated by tumour-cell secreted factors and receptor-ligand interactions. For example, in metastatic melanoma cells the formation of a gap in the walls of the vessels occurs through the activation of Src in endothelial cells. Src activation is mediated by the tumour cell-derived interleukin 8 (IL-8) and by the interaction between the vascular cell adhesion molecule-1 (VCAM-1) and its receptor VLA-4. Their interaction leads to VE-cadherin disassembly and consequently to the disruption of the endothelial barrier [23].

To intravasate, tumour cells undergo changes in their cytoskeletal activity, determined by chemotactic gradients, which facilitate the reaching of the walls of vessels [24]. To mediate the attachment of tumour cells to endothelial cells, adhesion molecules and in particular integrins, found upregulated in many tumour types during intravasation [25], play an important role.

3) The arrest in the capillary bed and the extravasation

Tumour cells that have entered the circulation are known as circulating tumour cells (CTCs). They need to survive physical stress and immune surveillance they face in the circulation to spread in distant organs. Very few CTCs flowing in the blood will survive and have a chance to produce distant metastasis [26].

CTCs that survive will arrest in the capillaries at the site where they will give rise to metastasis, by binding onto the apical surface of the endothelium and the vascular extracellular matrix, a phenomenon that is facilitated by platelets through the formation of thrombi and the activation of the endothelium [27].

Here, they might leave the circulation and enter in the surrounding tissue, a step that is called extravasation, that is achieved by secretion of factors that promote vascular hyperpermeability, such as some MMPs [5].

A crucial process involved in the extravasation is the release of specific chemokines by the target organ and the expression of the cognate chemokine receptors by tumour cells. One of the best-studied couples of chemokine/receptor in the context of cancer spread is constituted by the stromal cell-derived factor 1 (SDF1), also known as C-X-C motif chemokine 12 (CXCL12), and its corresponding receptor C-X-C chemokine receptor type 4 (CXCR4). It has been reported that CXCR4 is highly expressed in congenial sites for breast cancer metastasis, such as liver, lung and bone marrow and that breast cancer cells, which express the ligand CXCL12, migrate towards those organs by means of chemotaxis [28, 29].

4) Metastatic colonization

To form metastasis, tumour cells might find a niche where they can survive and eventually grow, carrying out the colonization of the organ they have reached. Metastatic colonization is the final and the most critical step of the whole cascade. Most of the tumour cells that successfully complete the extravasation phase, are eliminated by tissue parenchyma or remain for long periods in a state of dormancy, sometimes even for years [30]. The environment that tumour cells find at the site of destination is different from that at the primary site; it does not have the same stromal cells and growth factors to which tumour cells were adapted to in the

primary tumour site. Moreover, once in the new environment, tumour cells need to resist the host tissues defences and immunitary response [31].
The dormancy phase could reflect the failure of tumour cells to adapt to this new environment or could be activated by a series of anti-proliferative stimuli that tumour cells encounter in the new environment [32]. To start the colonization process, tumour cells need to activate adaptive programs that are achieved only rarely, explaining the extremely low efficiency of metastasis formation.
All of the steps of the metastatic cascade must be successfully completed to give rise to a metastatic tumour.

1.2 Epithelial to Mesenchymal Transition

1.2.1 The EMT is at the basis of many biological processes, including cancer progression

EMT indicates a number of cellular and biological changes by which epithelial cells lose cell-cell adhesions and cell polarity and acquire mesenchymal traits, such as migratory and invasive properties. These changes occur in a broad range of tissues, both in physiological and in pathological conditions. For example, during the embryonic development, there are many processes in which cells undergo transcriptional and phenotypical transition from an epithelial to a mesenchymal state. Such transition underlies the specialization of all the distinct cell types required in metazoans, e.g., it is observed in various organisms during gastrulation or in the promotion of the cell movements necessary for the closure of the neural tube and for the migration of cells from the neural crest to other parts of the embryo [33]. Other physiological processes in the adult rely on the acquisition by cells of mesenchymal characteristics as well; examples of such processes are wound healing [34], tissue fibrosis [35] and cancer [36]. In all these processes, cells that initially form a tightly packed epithelium move elsewhere, thanks to the loss of epithelial traits and the gain of mesenchymal ones, which support cell migration.

Evidence of EMT was first reported by Gary Greenburg and Elizabeth Hay in 1982 [37]. They discovered that EMT has an important role in embryonic morphogenesis; during an experimental control for which they put epithelial tissue of chick embryo into a collagen gel, they observed by chance that cells elongated, detached from the explant and spread as single cells into the gel. Differentiated epithelial cells had acquired functional and phenotypical features of mesenchymal cells. Some years later, in the late 80s, Jean Paul Thiery and his research group noticed the transformation of rat bladder carcinoma cells into invasive mesenchymal cells, observing for the first time the EMT in the context of cancer [38].

In the following years, many discoveries contributed to the understanding of the factors involved in the EMT. Its importance in tumour progression is now largely documented.

For many tumours, the detachment of a tumour cell from its epithelium is accompanied by the loss of some epithelial traits and the acquisition of invasive capabilities [7]. Indeed, in many primary benign carcinomas, the epithelial layers maintain the same organization we found in normal epithelia: they usually form the covering of the cavities of organs and of the body surface, therefore they are formed by tightly packed cells, kept together by abundant cell junctions. Besides the detachment from the primary site, various steps of the metastasis cascade, including the local invasion at the primary tumour site, the entry and the exit from the circulation and the survival at the secondary site are supported by changes from the epithelial to mesenchymal state, as well.

However, recent studies demonstrate that the partial maintenance of epithelial features is required for cancer cells to invade and metastasize [39-41], as it will be discussed later in the chapter.

1.2.2 Morphological and molecular changes which occur in EMT

The phenotypic changes occurring in EMT are associated with alterations in the gene expression profiles, which are driven by the activity of a series of transcription

factors the most known and important among which are Snail, Slug, Twist, and Zeb1 [42, 43].

One of the main features observed during EMT both in cancer and in normal processes, such as embryogenesis, is that the expression of E-cadherin and cytokeratins, which distinguishes epithelial cells, is lost. The same happens to other proteins such as β catenin that in epithelial cells has the role to form a link between E-cadherin, which constitutes adherens junctions (AJs), and the actin cytoskeleton, holding together two adjacent cells. In the cells of many primary carcinomas, E-cadherin is expressed on the plasma membrane while as the tumour starts the invasion, the expression of E-cadherin at the leading edge of the tumour is gradually lost. Following the loss of expression of E-cadherin, β catenin is free to translocate to the nucleus and determine the expression of genes implicated in EMT-associated phenotypic changes [44].

On the other hand, the expression of vimentin, one of the main components of the cytoskeleton of mesenchymal cells, and that of fibronectin, an ECM protein usually secreted by mesenchymal cells, is induced. Moreover, E-cadherin is often replaced by the typical fibroblast marker N-cadherin, which normally forms AJs in mesenchymal cells. This replacement helps tumour cells to invade the surrounding stroma since augments the affinity between tumour cells and stromal cells, in particular fibroblasts, that normally express N-cadherin [7].

To invade adjacent tissues, tumour cells need to migrate through the ECM and push aside cells they encounter on their path. The ability to degrade the ECM is another important feature associated with the acquisition of mesenchymal traits of tumour cells [45]. Among the proteins that take part in the EMT, MMPs have a fundamental role, since they are responsible for tissue remodelling, the degradation of many components of the ECM and the conversion of certain growth factors from latent into activated forms [7, 46].

A wide literature exists on the EMT observed in single tumour cells, but the evidence of collective phenomena in tumour progression is also compelling and it is further supported by the detection of circulating tumour clusters in the blood

circulation, which partially retain epithelial features and whose contribution to metastasis is relevant, as discussed below.

1.3 Circulating tumour cells and collective migration

1.3.1 Circulating tumour clusters and their contribution to metastasis

Once detached from primary tumour, invasive cells enter into the blood or lymphatic circulation to move towards distant organs. CTCs have been found both as single cells (single CTCs) or as collectives formed by two or more cells (CTC clusters). Their presence in surgical specimens was noticed already in the 19th century [47, 48], but their biological properties have been studied only in recent years. One of the major problems regarding the role of CTCs in cancer is their scarcity in peripheral blood samples. The ratio between CTCs and normal blood cells in the bloodstream has been estimated as low as 1:1 billion [49] and suitable detection technologies have only been emerging during the last few years.

One of the most interesting things we know about CTCs is that their presence in the blood of cancer patients is associated with a worse prognosis in comparison to patients where no CTCs arefound [50, 51].

Recent works showed that CTC clusters, even if rarer in the bloodstream in comparison to single CTCs, are associated with a higher metastatization capacity [41, 49, 52]. This finding is newsworthy and opens to many questions aimed at understanding the biology and the relevance of CTC clusters in cancer spread.

Particularly compelling in this regard are the data by Aceto et al, [49]. In this paper mouse models were used to study the origin and the functional properties of CTCs.

They injected 1:1 mixture of a lung-metastatic human breast cancer cell line tagged in green or in red into the mammary fat pad of immunodeficient mice (Fig. 3).

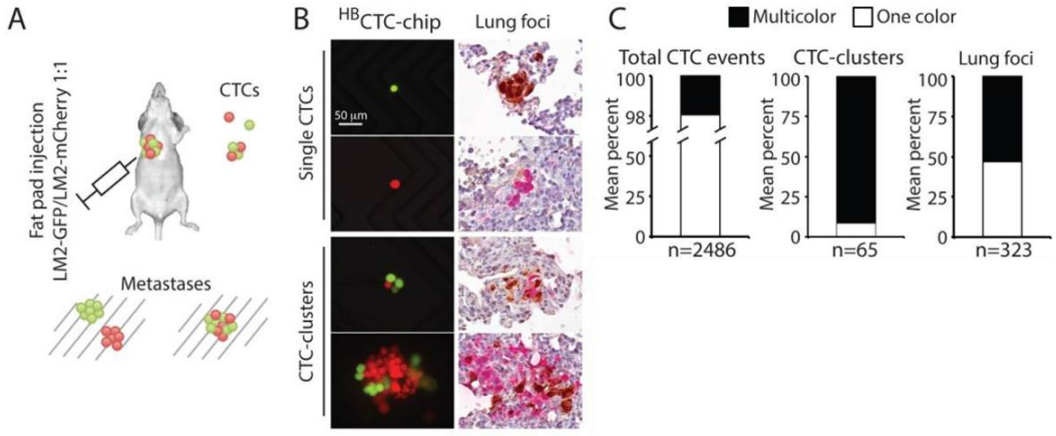

Figure 3 CTC clusters originate from the aggregation of neighbouring cells

(A) Schematic representation of the experiment. 1:1 mixture of green and red cells were injected in the right mammary gland of immunodeficient mice to generate one-color single CTCs and two-coloured CTC clusters. One-coloured metastases derived from a single CTC, while two-coloured metastases derived from a CTC cluster. **(B)** Representative images of single CTCs (green or red) and CTC clusters (mixed colours) are shown on the left; corresponding lung metastatic foci are shown on the right, whit GFP in brown and mCherry in red. **(C)** The bar graphs show the mean percentage of one-colour versus two-colour CTC events revealed with a microfluidic device on the left, the mean percentage of one-colour versus two-colour CTC clusters in the middle and the mean percentage of one-colour versus two-colour lung foci on the right.
From "Circulating tumor cell clusters are oligoclonal precursors of breast cancer metastasis." [49]

They drew the blood and analysed the lungs for the presence of metastatic deposits. They found both purely green and purely red metastasis but the majority of CTC clusters, that were rare in comparison with single CTCs found in the blood, were dual positive for green and red fluorescent proteins. This result indicated that CTC clusters did not originate from the proliferation of a single cell, otherwise one would have observed clusters of one colour since all the cells would have derived from the same precursor. CTC clusters were instead the result of the assembling of neighbouring cells, most likely in the primary tumour mass.

To further validate the hypothesis that CTC clusters originate from the detachment of a group of cells from the primary tumour and not from the grouping of single cells in the bloodstream, they did a second experiment: they seeded green cells in

left and red cells in right mammary gland (Fig. 4). The result confirmed the hypothesis since the vast majority of clusters they found in the blood were of a single colour.

Moreover, they calculated that the ability to form a metastasis by CTC clusters was 23-fold higher than that of single CTCs, and that CTC clusters contribute to approximately half of all metastatic lesions in their models.

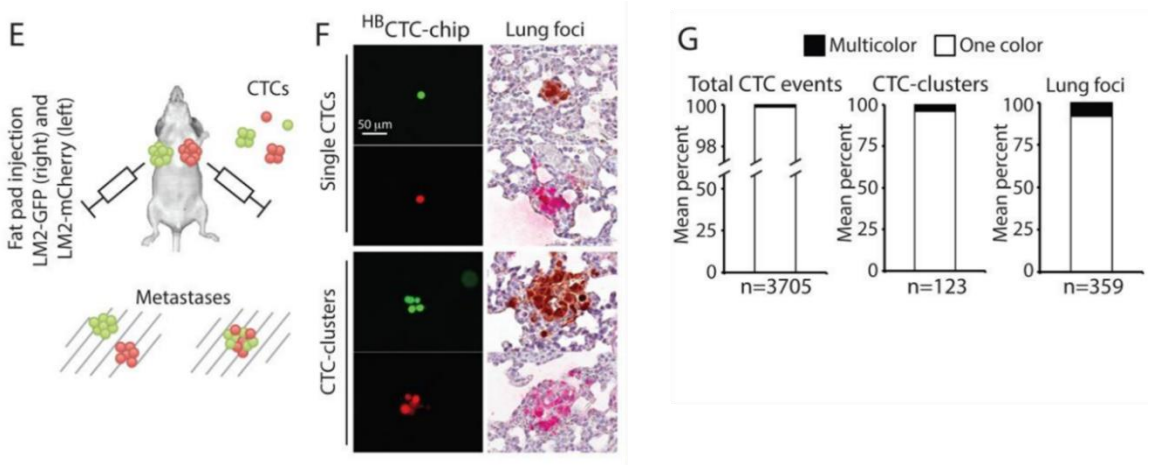

Figure 4 The majority of CTC clusters are derived from individual primary tumours

(E) Schematic representation of the second experiment. Green cells were injected in the right mammary gland and red cells in the left one to generate one-colour single CTCs and CTC clusters and rare two-colour CTC clusters (resulting from aggregation events). Accordingly, one-colour metastatic foci derive from a single CTC or a CTC cluster, while two-colour foci derive from CTC aggregates. **(F)** The same of figure 3 panel (B) after the second experiment. **(G)** The same of figure 3 panel (C) after the second experiment.
From "Circulating tumor cell clusters are oligoclonal precursors of breast cancer metastasis." [49]

Similar results were achieved in the study conducted by Maddipati et al, in pancreatic cancer [52]. To understand the origin of metastatic lesions, the authors used multi-colour lineage tracing technology in an autochthonous mouse model of pancreatic cancer, i.e., a model obtained by initiating tumours in a normal cell *de novo* and within the intact organism, for example by inducing the overexpression of an oncogene [53]. By using tamoxifen-dependent or independent Cre-mediated recombination, they were able to perform lineage tracing of pancreatic tumour cells based on the expression of four different fluorescent proteins, where each colour corresponded to a different sub-clonal population within the tumour.

First, they showed that the 80% of diaphragmatic and peritoneal micro and macro-metastases were polychromatic, indicating that they were polyclonal, i.e., they came

from more than one clone in the primary tumour. Moreover, they found multi-coloured clusters in the ascites fluids of mice, indicating that the polyclonal metastases originated from polyclonal clusters, i.e., from clusters which were polyclonal at the time of seeding and not from the seeding by one clone and the subsequent recruitment by another.

Similarly to Aceto et al, they also injected intraperitoneally in mice 1:1 mixture of red and yellow metastatic cells, or two-colour clusters (derived from two-colour diaphragmatic metastasis and then sorted by FACS to isolate red components and yellow components), as sketched in figure 5. After 3 weeks, they harvested and analysed diaphragmatic tissue for the presence of one-colour or two-colour lesions. They found that following the injection of cell clusters, two-colour metastases were the majority (70%) and that following injection of single cells, only one-colour metastases were found (Fig. 5B and C). These results demonstrated once again that polyclonal metastases derive from polyclonal clusters detached from the primary tumour.

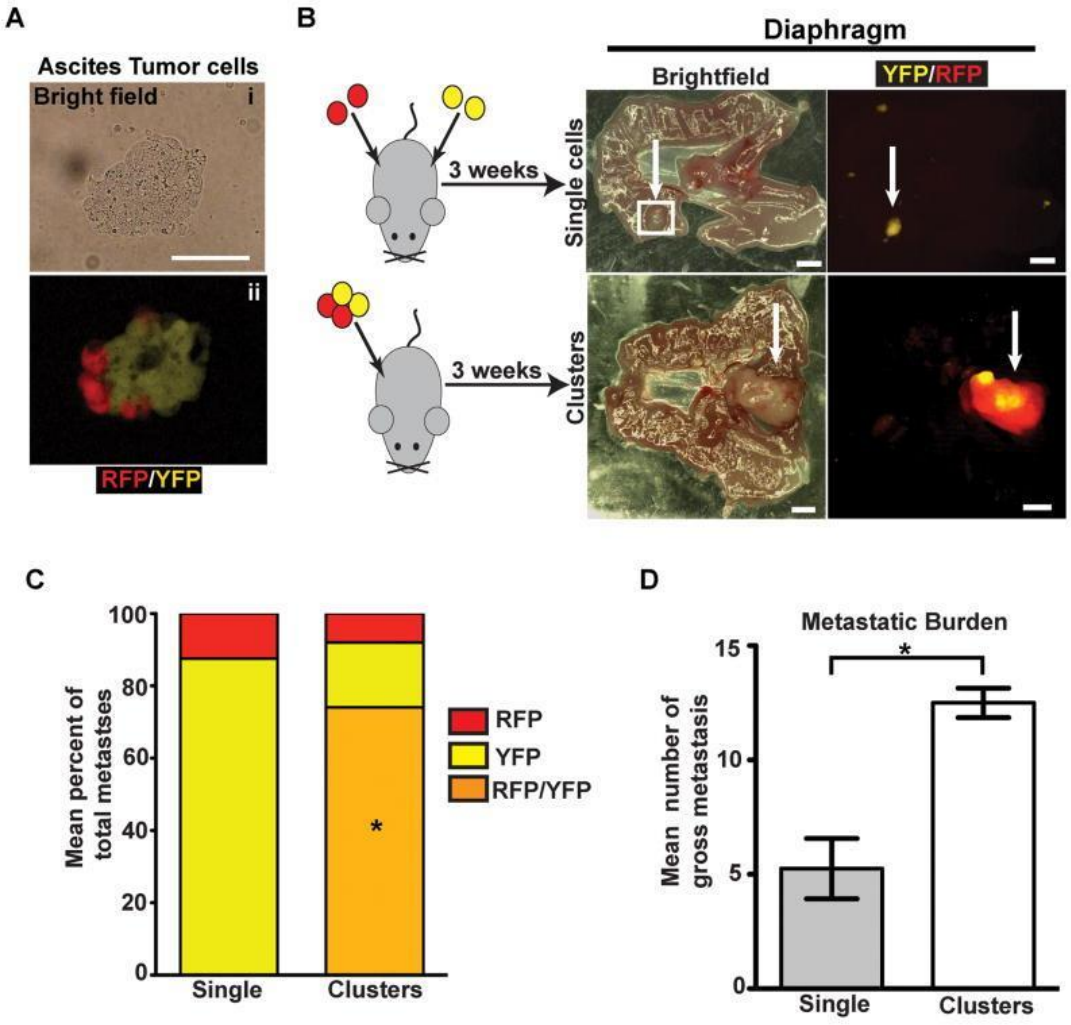

Figure 5 Polyclonal diaphragm metastases are seeded by polyclonal clusters

(A) Bright field (i) and fluorescent (ii) images of a multi-coloured cluster of disseminated tumour cells in the ascites. **(B)** Intraperitoneal injection of red and yellow cells, either as a suspension mixture of single cells (top panel) or two-colour clusters (bottom panel) into NOD SCID mice. Bright-field (left panel) and fluorescent (right panel) stereomicroscope images from mice 3 weeks following injection (n=4 mice for each group) are reported. Monochromatic lesions are either YFP or RFP positive and polychromatic lesions are both YFP and RFP positive. **(C)** Graph showing the mean percentage of total gross monochromatic (RFP or YFP only) or polychromatic (positive for both YFP and RFP) metastases between single cell and cluster injection groups (n=4 mice for each group for a total of 24 lesions counted in the single cell group and 50 lesions counted in the cluster group). No lesions from the single cell injection group were polychromatic. **(D)** Graph showing the mean number of gross metastases in the single cell and cluster injection groups (n=4 mice in each group).
From "Pancreatic Cancer Metastases Harbor Evidence of Polyclonality" [52]

Why are CTC clusters more likely to give rise to metastasis? First, there is evidence suggesting that they have a physical advantage simply because they are bigger than single cells: their large size allows them to remain trapped into capillary beds more easily than single cells. This was shown *in vivo* by labelling CTCs with a fluorescent dye and assessing the circulation time; clusters were cleared from the blood about

three times faster in comparison to single cells, indicating that they remain trapped in the vessels more than single cells [49].

Second, single CTC clusters may be less vulnerable to shear forces, oxidative stresses and immune defences they experience in the bloodstream in comparison to single CTCs [54] and they are more resistant to "anoikis", i.e., the detachment-induced apoptosis [55].

Moreover, their multicellular composition is responsible for the variety of the molecular features that promote stemness and metastasis [56]. In other words, metastasis originated from a CTC cluster can be polyclonal from the start, as demonstrated by Aceto et al, in the paper described above [49], while metastasis derived from a single cell will be clonal. This is relevant since we know that phenotypically and genotypically different populations of cancer cells in a tumour can coexist. Such populations can also cooperate or/and compete determining different properties of the tumour and also different responses to therapy [57]. Indeed, the multiclonality of clusters constitutes an advantage in the adaptation to new microenvironments by augmenting the capacity of a cluster to respond to various different situations and the possibility to resist to anti-tumour therapies [58].

There is evidence that cancer patients with bigger cluster size have shorter survival, independently of the therapeutic strategies [58] and that bigger clusters give rise to more metastatic foci [59]. Since bigger clusters are more likely to be mutationally heterogeneous than smaller clusters [56], such pieces of evidence would support the hypothesis that the multiclonality constitutes an advantage for clusters to metastasise and to resist treatments.

1.3.2 Heterotypic CTC clusters: do they improve the efficiency of metastatization?

In the context of tumour dissemination, not only homotypic CTC clusters, i.e., clusters made by the same type of cells, are important. Recent studies have shown that CTCs can also aggregate with normal (non-cancerous) cells, thus forming heterotypic clusters. The majority of these non-malignant cells are constituted by

cells of the stroma, such as fibroblasts and endothelial cells, immune cells and blood cells. The interaction between CTCs and normal cells has been shown to increase the metastatic potential of CTC clusters. For example, several works reported that when immune cells adhere to CTC clusters, they promote proliferation and consequently metastasis [60, 61]. In those works, it was also demonstrated that the interaction between immune cells and tumour cells does not occur in the bloodstream but in the primary tumour site and, as already known, it is mediated by the secretions of many factors. The interaction between CTC clusters and other types of cells has been reported [62, 63], suggesting that different types of possible heterotypic interactions could be a way to improve the ability of CTC clusters to metastasise.

1.3.3 Metastatic seeds are epithelial or mesenchymal?

As mentioned above, there is evidence that CTC clusters originate from the collective detachment of a group of cells from the primary tumour and from their circulation in the bloodstream as clusters formed by connected cells. In the last two decades, it has been shown that tumour cells can invade and disseminate in various ways, which can be resumed in two major categories: single-cell and collective migration. Tumour invasion could occur by a single cell which acquires migratory capabilities, detaches from the epithelium of the primary tumour site and disseminates through the body, as described in the previous paragraphs. However, more frequently dissemination of tumour cells occurs through collective migration of cohesive cohorts of cells which maintain certain epithelial traits, such as the presence of AJs between cells within the cluster (Fig. 6).

Collective migration of carcinoma cells has been observed and described in different types of carcinomas where this phenomenon underlies various steps of the metastatic cascade. Indeed, primary tumour cells can detach from the epithelium collectively, they can penetrate in groups in the walls of the blood and lymphatic vessels, they can circulate as cohesive clusters and they can extravasate maintaining functional and physical connection between cells [39, 64-67].

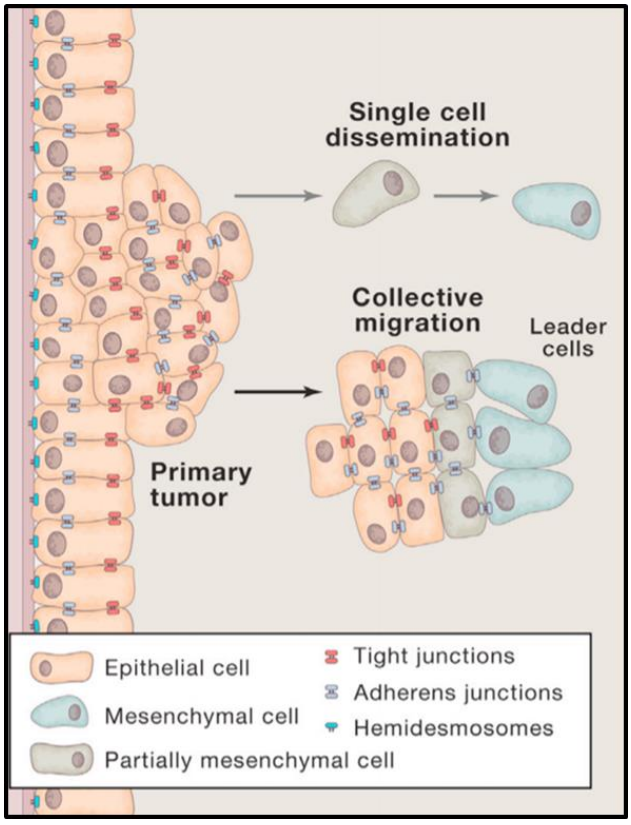

Figure 6 Single-cell migration and collective migration in carcinomas

Dissemination of carcinoma cells can occur through single-cell migration or collective migration. Cells can detach from the primary tumour as single cells which undergo EMT (grey arrow) and switch from an epithelial to a mesenchymal state.
The invasion may also start with the detachment from the epithelium of entire collectives of cells which partially retain epithelial traits (black arrow).
Recent evidence suggests that also the leader cells of the cluster undergo some phenotypical changes related with EMT.
From "Emerging biological principles of metastasis" [32]

The retention of such epithelial features seems to be inconsistent with the concept that tumour cells undergo a complete transition toward a mesenchymal state, since this would determine the loss of cohesive cell-cell interactions. These observations would suggest that EMT is not mandatory for tumour cells to acquire ability to invade adjacent tissues, or that it could occur transiently, or only in some cells within a cluster. Notably, most tumours do not express EMT-related genes. Concordantly, it was shown that in actively invading human tumour organoids of breast cancer no signs of EMT were detected through RNA analysis and lineage marking [68, 69]. Despite the absence of EMT in this model of luminal B breast cancer, the majority of mice develop lung metastasis [70].

Clusters of cells performing collective migration present a complex internal organization, with invasive cells at the leading edge and follower cells which move along thanks to the cell-cell junctions [39]. Several works showed that leading cells at the invasive front exhibit mesenchymal traits, i.e., they are able to move and to degrade the ECM by the expression of various proteases to facilitate the passage of

the whole cluster, they have reduced apico-basal polarity and show actin-rich cellular protrusions. On the other hand, cells in the rest of the cluster continue to express epithelial markers to ensure the cohesiveness between cells [71, 72].

Other works demonstrated that invasive breast cancer cells are characterised by the expression of basal epithelial markers, such as cytokeratin 14, P-cadherin and p63 [39]. Cytokeratin 14 positive tumour cells were detected during all the stages of metastatic cascade, with the exception of the primary tumour and the macrometastases, by the use of multicolour lineage tracing in a common mouse model of breast cancer [40]. This suggests that there are different epithelial programmes that guide tumour growth and tumour dissemination and that the metastatic dissemination process requires changes in the epithelial differentiation state [41]. Moreover, recent studies have demonstrated that epithelial features which are retained during metastatic spread can contribute to its efficiency [39, 40, 49].

This is consistent with recent evidence about the dispensability of EMT in the accomplishment of metastasis [73-76].

Together these studies suggest that even if it has been demonstrated that EMT plays an important role during cancer progression, its requirement and the extent of its contribution in the formation of metastasis is still controversial.

As described, collective cell migration takes part in various steps accomplished by tumour cells to move from the primary site to distant organs. A detailed description of the mechanisms underlying this process will be provided in the next chapter.

CHAPTER 2: COLLECTIVE CELL MIGRATION

2.1 Defining collective migration

Collective migration is a biological phenomenon which consists in the concerted movement of cells. From the evolutionary point of view, it is an ancient mechanism, present in humans as well as in other animals and even in simpler organisms, such as lower eukaryotes [77]. It is of fundamental importance for several biological processes where many cells act in a coordinated way. Many studies describe collective migration during embryonic morphogenesis of higher organisms, e.g., the development of lateral line in zebrafish (*Danio rerio)*, which involves the migration of about a hundred epithelial-like cells [78]; the migration of six-eight border cells towards the developing oocyte in *Drosophila melanogaster* [79] and the collective movement of cells during gastrulation of higher organisms such as chick, *Xenopus*, fish and mouse [80]. Collective movements take place during epithelial regeneration, as in the case of keratinocytes to repair a skin injury [81] and during angiogenesis, which relies on the directed migration of multicellular stalk of endothelial cells in response to VEGF gradient [82]. Collective cell migration is also implicated in disease progression in various pathologies including cancer. Relevantly, the collective cell detachment from primary tumours is associated with the increased efficiency of invasion and metastatization [56, 61, 83].

Collective cell migration is characterized by the physical and functional connection between cells, through the maintenance of cell-cell contacts during the movement. Similarly to what happens in single-cell migration in response to external guidance cues, a front-rear polarity is established within the group of cells. Polarization is associated then to spatially controlled polymerisation and contractility of actomyosin, which are essential phenomena in directing the movement of the cell aggregate.

Cells receive inputs from the environment, which can be both chemical, such as chemotactic gradients of soluble secreted factors or haptotactic gradients towards substrate-bound chemoattractants, and physical, such as in contact guidance, where

the direction is influenced by the geometrical pattern of the substrate, or durotaxis, i.e., the migration toward rigidity patterns. Such guidance inputs could be converging or opposing and need to be integrated by cells to determine the global behaviour of the entire group [84].

Moreover, to move along their migration path and to allow their passage through the stroma, groups of cells require a significant remodelling of the ECM to be operated, considering their large size in comparison to single cells [85]. Spatial remodelling occurs through the matrix degradation, usually through the secretion by the tip-cells first, and the follower cells later, of MMPs [86]. In other cases, cells can exploit pre-existent and least resistant anatomic paths, such as vascular tracks or the lumen of lymphatic vessels [87].

While biological and molecular mechanisms of single-cell migration have been well studied, collective migration has not yet been completely understood. In the context of cancer an important role of collective migration in invasion and dissemination is emerging and interesting questions are still to be answered. Does collective motility confer a selective advantage to cancer cells in comparison to normal cells? Collectives of cells can sense chemotactic gradients and perform directional migration [88-91] and gradient sensing might even be improved in multicellular aggregates with respect to single cells [92-94]. Could this be relevant in the contest of biological and pathological processes? And how do cells in a multicellular cluster communicate to each other?

In this chapter I will discuss the mechanisms underlying collective migration and the guidance cues which influence it, focusing on chemotaxis. The discussion will range over different modalities of collective migration in various systems, with particular reference to cancer.

2.2 Mechanisms of collective migration

2.2.1 Overview of different modes of collective migration

Thanks to the advances in live imaging techniques witnessed in the last two decades, it has been possible to visualize the behaviour of collectively moving cells in different model organisms *in vivo*. This holds true especially for processes like morphogenesis and regeneration which generally are observed in well reproducible sets of cells in model organisms or in precisely controlled biological situations, such as a wound or a limb amputation. It is instead more difficult for cancer progression, which is typically slow, long lasting and unpredictable, therefore not easily amenable to direct imaging. To partially overcome this problem, many *in vitro* experimental models to study collective migration dynamics both in two-dimensional (2D) and in three-dimensional (3D) experimental settings have been developed.

Collective migration occurs with different modalities depending on the organism, the cell and the tissue type and the environment. In many cases, it involves cells of epithelial tissues, both in embryos and in adult organisms.

Collectives of cells might need to migrate through different environments as well, depending on the experimental system considered, and it could be constituted by a matrix or by other cells, thus requiring different types of movements with different cellular speeds, proteolytic activity, cellular interactions and degrees of coordination.

Collective movements can occur by 2D sheets across a tissue or by a multicellular group or strand through a 3D environment [83, 95].

Some of the various different modes of collective migration are sketched in figure 7.

In the first case, cells can migrate as monolayers and form a single-layered or, if they proliferate, a multi-layered epithelium, as in the case of an epidermal layer moving on a 2D ECM, or during the repair of injuries of the intestinal epithelium (Fig. 7a) [96]. In the second case, cells can be tightly associated, as in the primordium of the posterior lateral line in zebrafish, where hundreds of moving and proliferating cells cross the entire length of the body performing a slug-like movement [95]. Alternatively, cells can move as isolated groups that detach from the tissue of origin and migrate elsewhere. This latter modality occurs in *Drosophila melanogaster* during

oogenesis, when border cells migrate as clusters across egg chambers (Fig. 7e) [97] or in some tumours during the invasion into the surrounding stroma by metastatic cells (Fig. 7f) [83]. Alternatively, cells can move as strand-like mass, as poorly differentiated invasive cancer cells (Fig. 7d), or as strands of cells which differentiate to form tubular structures or vascular sprouting (Fig. 7c) [83].

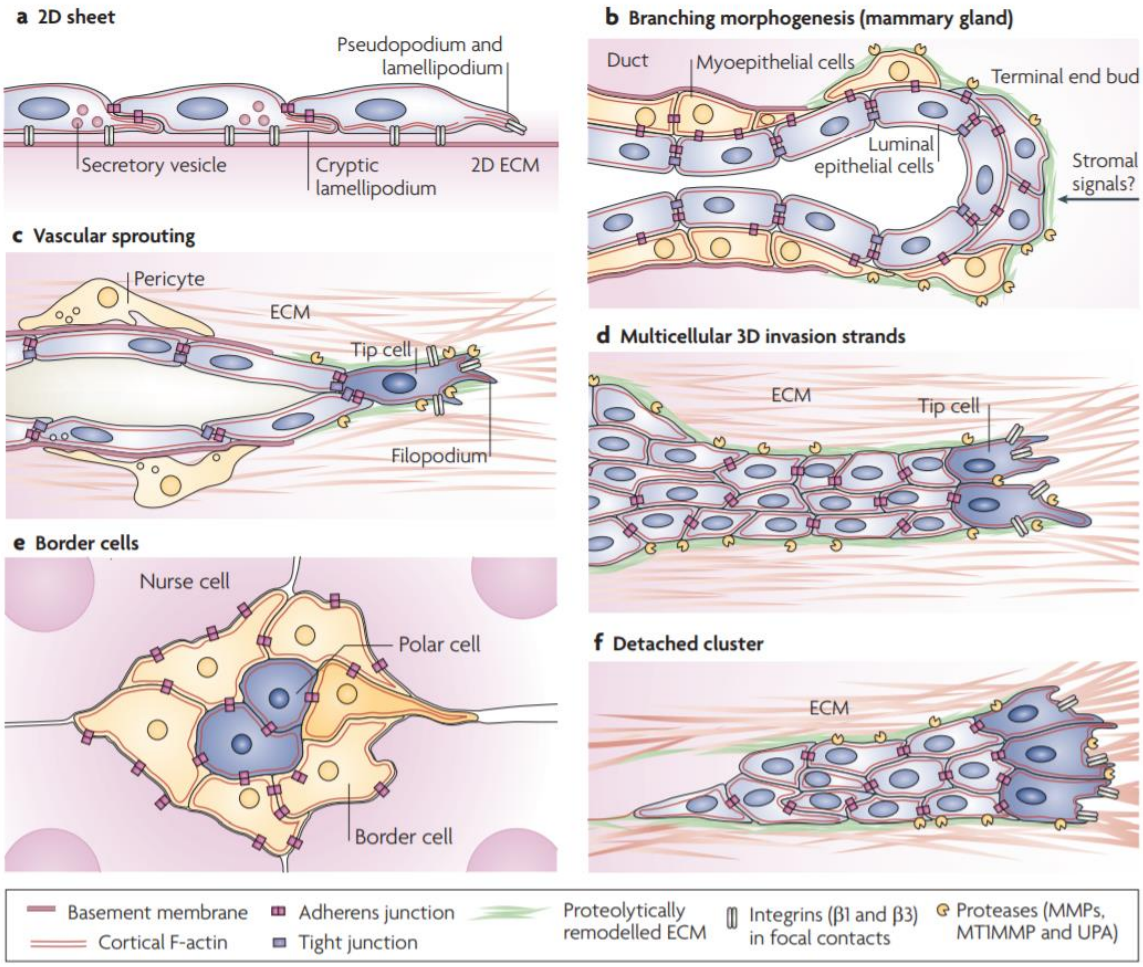

Figure 7 Examples of different modes of collective migration

(a) An epidermal monolayer moving across a 2D ECM substrate. Actin-rich protrusions (pseudopodia, i.e, temporary arm-like membrane extensions, and lamellipodia, i.e., thin sheet-like types of pseudopodia) promote the migration and follower cells connect the migrating group through AJs; the interaction with the BM is provided by integrins. (**b)** Sprouting of the terminal end bud in the developing mammary gland during branching morphogenesis induced by stromal signals. (**c)** Vascular sprouting during vessel formation or regeneration. The migration is determined by a tip cell which follows the guidance track provided by a BM deposited by both endothelial cells and pericytes. (**d)** Poorly differentiated invasive cancer cells invading as multicellular strands through the ECM. (**e)** In *Drosophila melanogaster*, border cells form a small cluster that migrates collectively through the egg chamber. Border cell cluster is made of mobile outer cells and two less mobile polar cells which migrate along cell-cell junctions of nurse cells. (**f)** Collective invasion of cancer cells that detach from the epithelium and move as a small cluster.
From: "Collective cell migration in morphogenesis, regeneration and cancer". [83]

Despite the wide variety of modalities described above, the underlying requirements are shared by all the types of collective migration and consequently share similar or identical molecular mechanisms. The main examples of such requirements are the need for cell-cell linkages, the establishment of a front-rear polarity, and the response to guidance cues. These three processes, through the cytoskeleton remodelling, allow the coordination of all the cells of the ensemble.

2.2.2 The need for cell-cell linkages: cell adhesion mechanisms

The fundamental role of connecting cells to each other and to the substrate is played by cell adhesion. Molecules that participate in this process form a bridge between neighbouring cells through the actin cytoskeleton which is connected across multiple cell bodies allowing the integration of forces generated by every individual cell and displaying therefore a supracellular organization [98-100]. Stable junctions are required to allow cell-cell signalling and cooperation, to attach cells to the tissues and to favour contractility and other mechanical properties. On the contrary, dynamic junctions are necessary to enable the changing of position of cells within a group, to ensure rapid movements and, in general, to allow all the cellular activities which require transient contacts with other cells or with the substrate [101, 102]. The response to the complex and diversified extracellular stimuli requires different levels of cell-cell cooperation and it is achieved through the combination of different adhesion systems and their modulation in time and space.

The proteins that provide those functions in collective migration of many organisms are generically called "cell adhesion molecules" and can be classified into four main groups: cadherins, integrins, selectins, and immunoglobulins superfamily. They are mostly transmembrane receptor proteins formed by three domains: an intracellular domain which interacts with the cytoskeleton, a transmembrane domain and an extracellular domain which interacts with ECM or other adhesion molecules [103].

In the epithelia, the main adhesion structures which allow tissue integrity connecting the actin cytoskeleton of adjacent cells are the AJs which are mainly composed of cadherins [104]. The cadherin superfamily comprises classical and

non-classical cadherins which differ for their functioning and their roles. Cadherins have the mechanical function to bind cells together, forming homophilic interactions with the same type of cadherins on another cell [105]. They also sense changes in tension and activate cytoskeleton responses through the interaction with other proteins, among which catenins [106, 107]. Cadherins associate with actin via other proteins, which function as adaptors, coupling cell-cell interactions with cytoskeleton.

The stability of AJs is controlled by several mechanisms, including endocytosis of both receptor and adaptor proteins and cytoskeletal regulation [108].

Many biological processes involving collective migration rely on AJs. For example, invading epithelial strands during branching morphogenesis retain E-cadherin-based AJs between moving cells, as well as desmosomal and tight junctions (TJs) which are other two important adhesion complexes. Desmosomes are one of the strongest cell-cell adhesion types, and are therefore essential in tissues that experience intense mechanical stress. As AJs, they are formed by cadherins and adaptor proteins [109]. TJs are formed by transmembrane proteins and have mainly the function to seal the cells and create a barrier between different regions of the body [110].

The first classical cadherins identified in vertebrates were E- and N-cadherin [103], which, among other functions, take part in collective invasion of cancer progression, a process that relies on a wide range of cell adhesion mechanisms. During collective migration of epithelial tumours, E-cadherin and β-catenin positive cell-cell junctions were observed, proving that tumour cells retain the expression of epithelial markers during collective migration [39]. Also N-cadherin regulates AJs and cell interactions in cancer invasion [7]. Moreover, during invasion, tumour cells need to pass through the ECM components; to facilitate this process, the expression of stromal proteases is activated and promotes the cleavage of proteins such as cadherins [45], demonstrating the plasticity of the cell adhesion machinery.

Another important class of proteins implied in cell adhesion is constituted by integrins. These proteins are members of a large and complex family of transmembrane glycoproteins. Structurally, they are heterodimeric transmembrane

receptors formed by two subunits, α and β [111]. Through their extracellular domain, they bind to other glycoproteins or to components of ECM, such as laminins, collagen and fibronectin. As cadherins do, even if with different modalities, integrins as well have the crucial function to connect with the actin cytoskeleton through other proteins, consequently activating downstream pathways and constituting a link between the cells and the outside environment [103]. The interactions between cells and ECM mainly occur through integrins.

Integrins can bind to proteins directly, as they do with talin, filamin and vinculin [112], or they can phosphorylate some kinases, including focal adhesion kinases (FAKs), proto-oncogene tyrosine protein kinase (SRC)-family kinases (SFKs) and integrin-linked kinase (ILK) [113] to mediate cell responses. Integrin-dependent adhesions activate two small GTPases, CDC42 and RAC, through adaptor proteins. This signalling promotes the formation of membrane protrusion at the cell front [97].

The pathways activated by integrins not only regulate the movement, but also other several fundamental activities of the cells, including cell proliferation, differentiation, and the generation of cell survival signals thanks to the correct location and the adequate anchorage of the cells [114]. It is well known that many types of both normal and tumour cells require the presence of integrins to remain attached to the ECM and dispose of the survival signals. Tumour cells lacking these linkages will normally detach and undergo the detachment-induced apoptosis called "anoikis". It has been demonstrated that some integrins are involved in the resistance to anoikis of cancer cells, which is one of the escape modes to initiate the metastatic cascade [115].

It is known that integrins play a role both in tumour suppression and in tumour promotion [116]. They have an important function also during tumour invasion when alterations of the integrin signalling have been observed, including the switch between β1 and β3 integrin [101, 117]. The ratio between β1 and β3 integrin is crucial in cancer cells [118]. The inactivation of β1 integrin in normal and malignant mammary epithelial cells (MECs) impairs TGF-β-induced motility, provoking a compensatory expression of β3 integrin in malignant MECs, but not in their normal

counterparts. This compensatory expression of β3 integrin increased the growth of malignant MECs organoids and was able to rescue the growth of tumours and of pulmonary metastasis of β1 integrin-deficient mice, process that is prevented by inactivating β3 integrin [117]. The role of integrins in intercellular contacts and in collective migration is still poorly understood, but there is emerging evidence about their contribution to cell-cell interaction. For example, β1 integrin is necessary to maintain the cell-cell contacts in multicellular melanoma cancer clusters, as demonstrated through the block of its function and the consequent loss of cell-cell cohesion and the switch from a collective to amoeboid single-cell migration [66]. It is also crucial to maintain the integrity of multicellular ovarian carcinoma spheroids [119] and to allow the formation of fibroblast spheroids [120].

An important role in cell adhesion and migration is played also by immunoglobulin superfamily members, which are expressed in many different cell types, such as cells of the nervous system, leukocytes, and epithelial and endothelial cells [105] and often act in association with integrins, cadherins and other adhesion and cytoskeletal proteins [121]. They mediate cell-cell relations by homophilic and heterophilic interactions of their immunoglobulin-line domains [105].

The role of immunoglobulin superfamily members is important in many contexts, including cancer, mainly in situations which require less stable or transient connections between cancer cells [105, 122]. Neural CAM (NCAM) is one of the best studied members of the immunoglobulin superfamily and there is evidence about its role in cell-matrix adhesion during progression of pancreatic and colorectal cancer [105]. Indeed, the loss of NCAM in pancreatic β tumour cells mediates the induction of metastatic dissemination in mouse models, mainly to regional lymph nodes, and tumour cell lines isolated from NCAM-deficient tumours showed defects in cell-matrix adhesion, although cell-cell adhesion was not affected. This constitutes also a further evidence that tumours can form metastases even in the presence of cell-cell adhesion.

Cell adhesion molecules are essential to modulate the response of collective moving groups formed by different types of cells and in a broad range of organisms. They connect the actin cytoskeleton of multiple cell bodies, allowing the distribution of

the forces and the coordination of the movement of the entire moving groups. By the modulation of cell adhesion composition, cells are able to respond to external stimuli and to switch between different types of movements to adapt to the local stimulations.
As explained in the next paragraph, cell adhesion plays an important role also during the establishment of the front-rear polarity.

2.2.3 The establishment of a front-rear polarity

To migrate collectively, a group of cells need to move in the same direction. The control of the directionality is regulated by a range of guidance mechanisms, including chemotaxis, haptotaxis, durotaxis, strain-induced mechanosensing and electrotaxis [84]. These guidance principles often act in parallel and need to be integrated to produce cellular responses.
The first process which is established in cells when cells sense external cues, is the front-rear polarity, which, in many cases, determines the coordination between two populations of cells within the group: leader and follower cells [97].
Cell polarization is a fundamental process also in single-cell migration, where a front to rear polarity axis is established. It determines cytoskeletal rearrangements and a polarized organization of membrane trafficking. Molecular mechanisms which regulate the polarization involve small GTPase proteins of the RHO family. In particular, as mentioned before, RAC and CDC42 induce the formation of membrane protrusions, e.g., lamellipodia and filopodia, at the front, while at the rear signalling pathways involving RHO induce actomyosin contraction [97]. The front to rear orientation is maintained also in collective migration; however, since collectively moving units are formed by many different cells with different positions, the polarization requires different distribution of the signals.
In collective migration, the definition of leader and follower cells is usually determined by the relative position of cells within the group: the leader cells are localized at the front, since they receive more stimuli from the environment, and the followers at the rear. However, as consequence of the stimuli received, the position

of cells can change and the followers can become leaders [81]. Thanks to their position, leader cells have a free edge that can form protrusions, while their lateral and rear sides are designated to establish cell-cell contacts.

It is important to note that the directionality of a group of cells is not always "decided" by cells located at the front and that the proteolytic activity and the generation of traction forces are not functions specifically restricted to front cells. Therefore, a more appropriate definition of the functional role of cells could be "steering cells", while a purely topological definition could see the use of the terms "front cells" and "rear cells", as proposed and discussed by Theveneau et al [123].

The important role of the leaders was demonstrated by the elimination of leader cells or by their separation from the followers; these experiments lead to the impairment of the migration of Madin-Darby Canine Kidney (MDCK) cell culture in collagen [124] and in monolayers [125], perturbing in particular the directionality of the movement.

Leader cells have the role of sensing chemical stimuli, such as chemoattractant, and to consequently promote the movement of the entire collective towards the soluble factor, as will be discussed later. They are also the cells which pave the way to the rest of the group by moving into the 3D environment and modifying the shape of the ECM fibres thanks to the forces exerted through focal adhesions and through the secretion of MMPs. Leader cells interact with the ECM mainly through integrins which receive signals from composition, stiffness and directional cues provided by ECM and lead to cytoskeletal modifications and morphological polarization (i.e., the formation of protrusions), as sketched in figure 8.

The signals transduced by the activation CDC42 and RAC through other proteins such as proteins associated with guanosine exchange factors (GEFs) [126, 127] or FAK and SRC kinases [128] lead to actin polymerization at the leading edge of the plasma membrane, generating the pushing forces necessary to form protrusions [129]. Also the microtubule network and the associated vesicular traffic are polarized, provoking the increase of membrane surface and receptors at the front of the migrating group [130, 131].

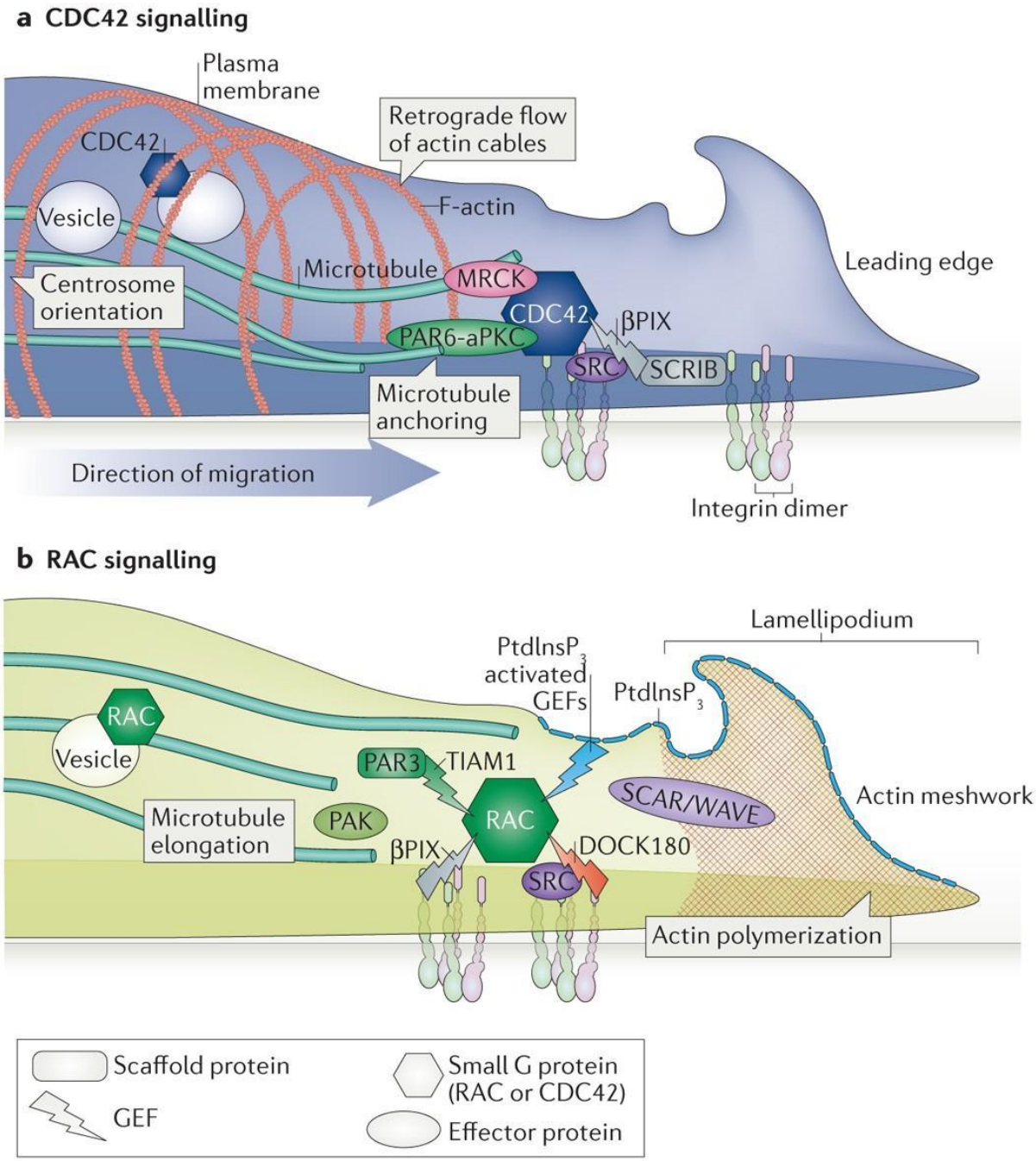

Figure 8 Leader cells receive stimuli from the environment

During the migration of a cohesive group of cells, the leader cells are exposed to environmental cues. While the cell rear is mainly engaged in forming intercellular contacts, the cell front interacts with the ECM or with other cells and receive external stimuli such as chemical factors. Leader cells polarise by integrin-induced signalling cascade which is sketched in the figure.
From: "The front and he rear of collective cell migration". [97]

In different types of collective migration, the number of leader cells can varies depending on the context and on the geometry of the migrating group. There are many cases where collective migration is driven by groups of leader cells. For

example, during dorsal closure in *Drosophila melanogaster*, the collective migration is guided by a row of leader cells located at the front of the group, as shown in figure 9a. In the case of epithelial wound healing process *in vitro*, leader cells are disposed in clusters, as represented in figure 9b. Similarly, during the invasion of cancer cells, small groups of leader cells, but also only one or two leader cells [133], as shown in figure 9d., been observed collective migration [132], In zebrafish, during the migration of the lateral line primordium, leader cells that promote the migration along a chemical gradient of SDF1 are composed of a group of 10-20 cells (Fig. 9e). Conversely, collective migration is driven by one or two leader cells, which are called tip cells, in mammalian angiogenesis or in insect tracheal development [134], as visible in figure 9c. A single leader cell controls the migration of *Drosophila melanogaster* border cells during oogenesis (figure 9f).

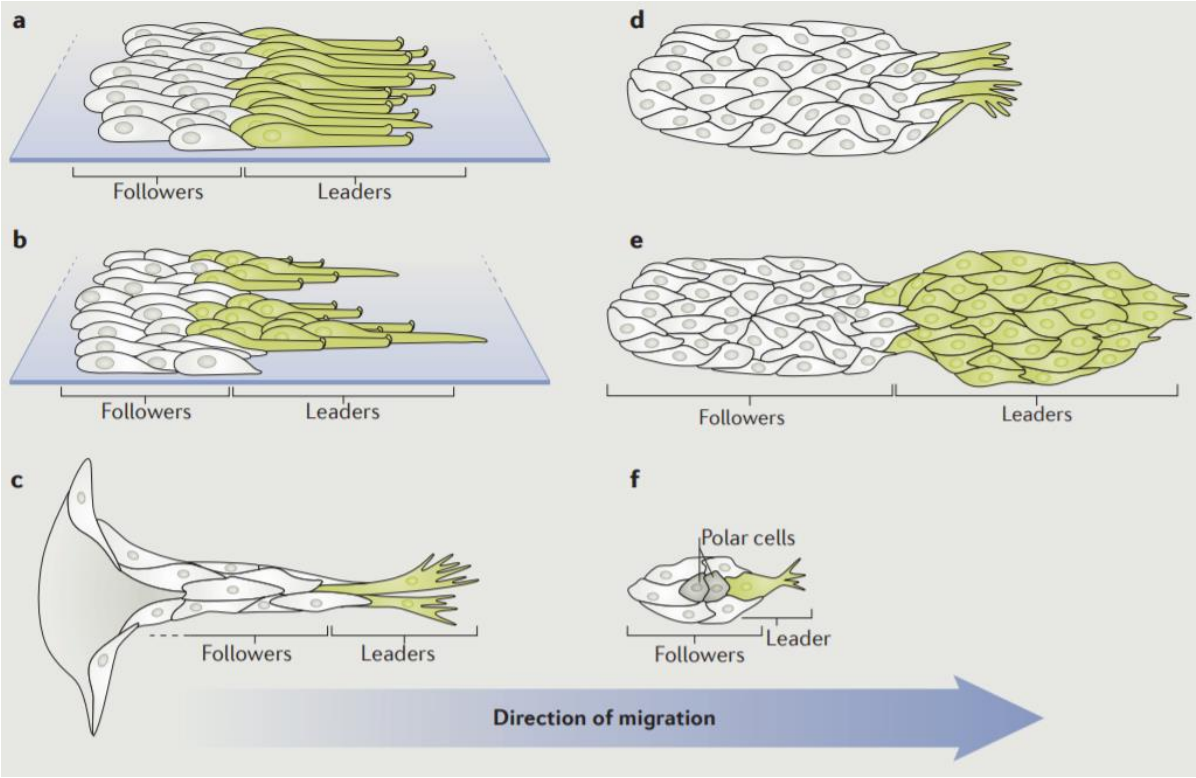

Figure 9 Leader cells in different modes of collective migration

The number of leader cells (green) varies depending on the geometry of the migrating group. The collective migration of cell monolayers, for example during dorsal closure in *Drosophila melanogaster*, is driven by a first row of leader cells **(a)**, or by clustered leader cells localized at the front edge, as is the case during epithelial wound healing *in vitro* **(b)**. One or two leader cells, also called tip cells **(c)**, are sufficient to guide the collective migration of strands of cells or cell groups as observed during cancer invasion **(d)**. During the migration of the lateral line primordium in zebrafish, a group of 10 to 20 leader cells guide cells along SDF1 gradient **(e)**, while a single cell leads the migration of the small cluster of *Drosophila melanogaster* border cells **(f)**.
From: "The front and he rear of collective cell migration". [97]

In clusters or sheets of migrating cells, the leader cells are connected by AJs, linked to thick actin filaments to ensure the transmission of the forces between adjacent cells [135]. As mentioned before, adhesion molecules have a critical role in ensuring the right functioning of the entire group of moving cells. Their maintenance and controlled recycling are important also to prevent too frequent changes of position of the leader cells. There is evidence that the impairment of cadherins is sufficient to dramatically alter collective cell dynamics in different systems, in many cases leading to the detachment of leader cells or blocking the emission of protrusions [136-139].

In the complex regulation of collective migration, follower cells also have active roles. Indeed, the generation of the forces is not only a prerequisite of the leaders [140]; followers influence in indirect manner the polarization of leader cells and consequently of the entire group [97]. The process which allows such polarization is called contact inhibition of locomotion (CIL) and consist in the arrest of the forward locomotion of two colliding cells by the retraction of protrusions at the site of contact and the formation of new protrusions in different directions [141].

Moreover, follower cells participate in establishing and sensing the gradient during chemotaxis, for example expressing decoy receptors to intrinsically generate a chemotactic gradient, as explained below.

2.2.4 The response to guidance cues: chemical guidance through chemotaxis

Chemotaxis is the cell movement through a positive gradient of chemical concentration [142]. The observation that cells are able to follow concentration gradients of soluble chemical factors dates back to the mid-nineteenth century and was made before the word “chemotaxis” was used to describe this phenomenon. First evidence of chemotaxis regarded the mechanisms responsible for the attraction of neutrophils to the sites of infection [143]. Since then, many discoveries have been made showing that chemotaxis is a mechanism present in a wide range of organisms, from simple bacteria to specialized mammalian cells and that it is involved in a variety of functions, even in cancer [144, 145].

In many organisms, in order to move in the direction of the gradient, cells must first perceive the differences in the concentration of the soluble factors across the cell body; then they polarize in that direction and finally migrate along the highest chemoattractant availability (Fig. 10) [144, 146]. Sensing of soluble factors is allowed through cell membrane receptors, which could be both G-protein coupled receptors, as in the case of neutrophils or *Dictyostelium discoideum* cells, and receptor tyrosine kinases (RTKs) as in fibroblasts or in carcinoma cells [145, 147].

Soluble chemical cues involved in chemotaxis include chemokines, cytokines, altered pH or reactive oxygen species (ROS) [148]. Soluble chemotactic molecules bind to their receptors, which are activated and determine downstream signalling which cause cytoskeletal remodelling.

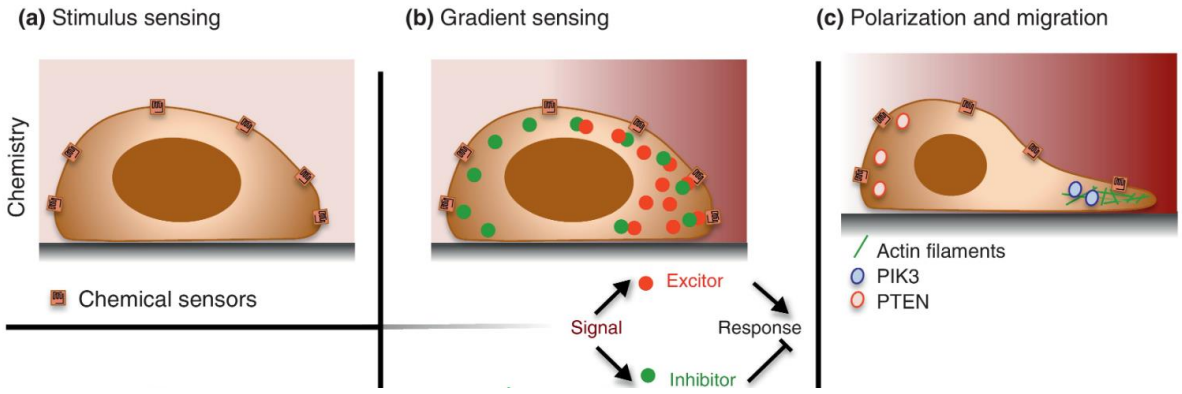

Figure 10 Directed cell migration toward chemical soluble factors

(a) Cells detect soluble factors with specific cell membrane receptors such as G-protein coupled receptors. **(b)** The gradient of soluble chemoattractants is detected. The external cue triggers both a local excitation signal (red dots) that induce polarization and a diffusive inhibitory signal (green dots) that tends to oppose it. **(c)** The activation of the chemotactic pathways ultimately leads to an accumulation of actin filaments and the recruitment of molecules implied in the directed migration, such as PIK3 at the front and PTEN at the back of the cell.
From: "Mechanical guidance of cell migration: lessons from chemotaxis". [146]

One of the first changes promoted by the polarization is the emission of actin-based protrusions.

During tumour cells chemotaxis, two types of protrusions have been detected: leading-edge protrusions [149, 150] and invasive protrusions such as invadopodia and podosomes [151, 152]. It has been reported that the formation of invadopodia and podosomes is consequent to chemotactic stimulation by various cytokines such as EGF and colony-stimulating factor 1 (CSF1) [151, 152]. In 3D cultures they have

been observed at the front of the cell, where they mediate both the directional migration and the degradation of ECM components [149], especially during extravasation [153].

Chemotaxis is typically a paracrine mechanism, where diffusible attractants are secreted by neighbouring cells [145, 154], but can be also autocrine, when it is produced or maintained by cells themselves [90, 148, 155]. This latter case is what usually happens during collective migration: cells within the group can sustain directed migration by internally generating chemotactic gradients throughout the modulation of synthesis, secretion and degradation of proteins at the front and the rear of the migrating group [156, 157]. The gradient can be established and sustained in different ways. For example, cells can secrete a chemotactic molecule near the front, which is perceived by leader cells and allow the migration along the gradient. Cells can also release at the front side enzymes which degrade soluble factors uniformly present in the environment; in this case, is the enzyme which diffuses along the cell group, gradually removing the chemoattractant and establishing a gradient. This mechanism is exploited by melanoma cells, possibly to migrate away from the tumour. Melanoma cells are able to perform chemotaxis toward lysophosphatidic acid (LPA), a strong chemoattractant, when it is distributed homogeneously in the extracellular environment. Indeed, melanoma cells themselves generate a gradient by degrading LPA, determining the presence of low concentrations close to the cells, i.e., within the tumour, and higher concentrations away from them. Consequently, melanoma cells sense the LPA self-generated gradient and migrate accordingly [158].

Finally, cells can modulate the gradient in an indirect manner: they can express migration-inducing receptors in the front of the group and decoy receptors in the rear. Receptors at the rear bind, internalize, and remove chemoattractant molecules, acting as a sink and consequently generating or reinforcing a gradient. This is what happens in zebrafish lateral line primordium where the migration of cells is dependent on the chemoattractant SDF1 gradient. Both SDF1 and its cognate receptor CXCR4 are expressed uniformly by cells of the zebrafish embryo, but the scavenger receptor CXCR7 is expressed only in posterior cells. CXCR7 sequesters

SDF1, causing the generation of a front-rear gradient of SDF1 and consequently promoting the migration of cells toward the anterior end of the primordium [78, 156, 159, 160].

In the last years, evidence about the implication of chemotaxis in cancer progression is increasing. For example, between stromal components and cancer cells the establishment of reciprocal gradients has been observed. During the process known as macrophage-led tumour invasion, tumour cells produce CSF1 to attract macrophages and they in turn secrete EGF to promote the migration of tumour cells toward the blood vessels [161]. This is an example of paracrine chemotaxis, but also self-generated gradients are known to take part in cancer. For example, as demonstrated by Shields et al, to metastasize via the lymphatics, breast cancer and melanoma cell lines produce a self-generated gradient of CCL19 and CCL21 and move chemotactically toward the draining lymphatic, thanks to the autocrine loop between those ligands and their cognate receptor CCR7. This allows cancer cells to reach the lymph nodes even when they are too far to sense any chemotactic cues from the lymphatic. Notably, the more highly invasive cell lines used for the experiment secreted more CCR7 ligands than the other less invasive lines. Moreover, MCF10A, the normal breast cell line they analysed, does not express CCR7 and displayed an insignificant response to the CCL21 gradient, in comparison to the tumour cell lines. Chemotaxis toward the ligand gradient could be abolished with neutralizing antibodies against CCL21 and CCR7 in 3D matrices [162].

2.2.5 Chemotaxis and collective migration: cells can cooperate to sense gradients

Single cells are able to perform chemotaxis but there are physical limits to sensing for example when gradients are shallow (i.e., when the difference in the number of molecules bound to the front and the back of the cell is small compared to the counting fluctuations), cells can fail to chemotax because the gradient sensing is limited by the ligand-receptor binding kinetics. It has been shown that this limit can be overcome in clusters of interacting cells, which can sense shallow gradients [89, 93, 163].

One of the first experiments which showed the capability of groups of cells to sense a gradient more efficiently than single cells and the importance of cell-cell interactions in the measurement of a chemical gradient was made in the early 90s by Winklbauer et al. [164, 165]. They were able to recapitulate *in vitro* what happens during *Xenopus* development when the dorsal mesoderm cells, in close contact with each other, migrate across the blastocoel roof toward the animal pole. By transferring mesoderm explants on a plastic dish (procedure adapted from Nakatsuji et al. [166]), they created a conditioned substrate and observed that mesoderm cells were able to migrate toward the animal pole direction on the conditioned substrate, while single isolated mesoderm cells did not show directional migration.

Many years later, Theveneau et al. [163] demonstrated that neurocrest cells were able to migrate collectively toward a source of SDF1 *in vitro*. They also contributed to elucidate some fundamental aspects of collective chemotaxis, showing that N-cadherin dependent cell contacts are necessary for collective directional migration to occur, since N-cadherin inhibition resulted in the impairment of collective chemotaxis. They provide important notions about the influence of the cluster's size on the gradient sensing, showing that small clusters (two- or three -cell big) were able to sense gradient as efficiently as much bigger clusters (a hundred of cells) did. On the contrary, isolated cells showed a dramatically less efficiency in performing chemotaxis compared to groups of cells. This suggested an important function of cell-cell interactions in the gradient sensing. Moreover, they measured the cell polarity by quantifying the activation of Rac and showed that the cells at the edge of the cluster presented high levels of Rac in the direction of the outside edge and not in that of the chemoattractant, while the inner cells were basically unpolarised.

Recently, Malet-Engra et al. [89] added quantitative information about the mechanisms of collective chemotaxis. They exposed chronic lymphocytic leukaemia-derived cell lines to a controllable gradient of CCL9 or CXCL12, showing that clusters present a higher chemotactic prowess in comparison to single cells. Cell clusters always move chemotactically toward the chemokine gradient, while single cells showed different responses depending on the concentration and the steepness

of the gradient, including no response and chemorepulsion. They also provided an important contribution to the understanding of how cluster size impacts cluster directionality and velocity, through physical modelling and experimental evidence, demonstrating that a minimal cluster size of about 20 cells was required to the onset of cluster chemotaxis.

Despite growing evidence about collective chemotaxis by cell clusters, the reason why they have a higher ability to perform chemotaxis in comparison to single cells still remains to be investigated deeper. The proposed mechanisms are discussed in an interesting paper by B. A. Camley [167], sketched in figure 11 and resumed below.

• **The null model**: this first model is based on the hypothesis that chemotaxis is dependent on cell-cell contact. This means that in the most extreme case, cells would be able to perform chemotaxis only when in contact with their neighbours. However, a critical question is whether isolated cells are not able to sense the gradient or whether their responses do not involve motility and chemotaxis. Some studies demonstrated that single cells are sensitive to the gradient but the response is different in comparison to clusters (e.g., single lymphocytes which are chemorepelled from a chemokine gradient while clusters made of the same cells move toward the gradient [89]). How can cell-cell contact drive the switch toward chemotaxis? Cell-cell contact is not just a mechanical link, but can be coupled with the interchange of signals between adherent cells [121, 168]. For example, cell-cell contact could change the number of receptors expressed on the cell surface or could lead to the expression of receptors with different equilibrium constants, and can change the maintenance of cell memory, which are two important factors for cells to chemotax. Indeed, the gradient sensing accuracy depends on both the number of receptors on the cell surface and on the time that cells take to sense and integrate the signals [169-171], which can be different in single cells and in cell clusters due to different biological requirements (i.e., single cells may need to respond quickly to a gradient changing, and in this case a short memory could be advantageous, while clusters may need to be able to sense a shallow gradient, and different responses could be ideal).

• **"Many wrongs make a right"**: this model is based on the assumption that each cell within a cluster makes its independent estimation of the gradient which can be noisy and not accurate. The final decision of the entire cluster will be the combination of all the single estimations, which will result in a more accurate and less noisy estimation [94, 172].

• **Collective susceptibility**: this model assumes that only a few cells within the cluster sense the gradient, while the rest only follow. For example, when the gradient extends for a length of few cells, it has been shown that migration can be more efficient with fewer leader cells. In such a case, cells farther from the gradient do not sense the gradient and a better result is achieved by following the leaders [173].

• **Collective guidance**: this model provides a gradient sensing based on a cluster-scale measurement. Each individual cell within the group makes a measurement of the local concentration (and not of the gradient as in the case of the "many wrongs" models). The global estimation of the gradient will be the result of a comparison between the individual measurements of the concentration, which can be made by different mechanisms, for example by taking into account the fact that cells which sense a greater signal are those which pull more strongly (the so called "tug-of-war"). This cluster-scale measurement can be advantageous in comparison to a single cell-scale measurement since the difference in concentration between the front and the back of a cluster is greater than the difference in concentration between the two opposite poles of a single cell [172]. This model is supported by experimental evidence that shows that cells at the outer edge of a cluster are polarised away from the clusters and not in the direction of the gradient, as in the case of the malignant lymphocyte clusters [89] and the neural crest cell clusters mentioned above [163] (where polarisation was established by measuring the direction of the protrusions and Rac activation respectively). As a result of "tug-of-war", the cluster moves along the gradient direction.

• **Chemotactic relay and self-generated gradients**: this model is the only one among those described which considers groups of cells that are not connected through cell-cell contact, but that act in a concerted manner (e.g., neutrophils

recruitment to repair a wound [174] or lymphocyte during their homing to tumours [175]). It is based on the hypothesis that cells may secrete or degrade signalling molecules, establishing a communication between separated cells to sense the gradient. One example of this model is represented by the one described in 2.2.4 paragraph regarding the melanoma tumour cells which establish a self-generated gradient of LPA acid [158].

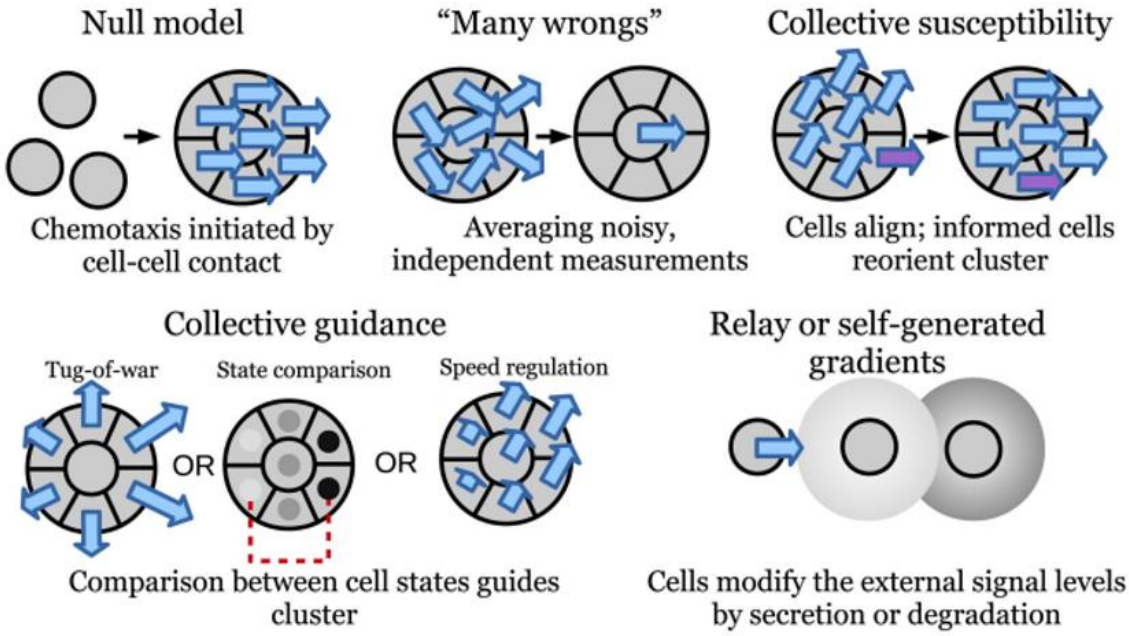

Figure 11 Schematisation of the potential mechanisms underlying collective gradient sensing
Detailed description is provided in the text.
From "Collective gradient sensing and chemotaxis: modeling and recent developments". [167]

In a recent paper from the research group I work with, collective directional migration of the PC-3 cell line was observed in a 3D environment and the dynamics of the movement were explained through a chemotaxis-driven aggregation model [90]. In the next chapter I will discuss the main results of that work and introduce the results of my study that I will detail in the subsequent chapters.

PREVIOUS RESULTS AND RATIONALE OF THE STUDY

In light of what has been discussed so far, an important role of collective directional migration in cancer is emerging. As discussed in the previous chapters, besides the evidence that tumours of epithelial origin originate from the detachment from the primary site and that tumour progression is frequently associated with the acquisition of mesenchymal traits [7], a role for collective phenomena in tumour progression is also very convincing. The observations that CTCs clusters have higher metastatic capability in comparison with single CTCs [41, 49, 52,176] and that heterotypic CTCs clusters show an even greater metastatic potential and survival rates [60, 61] highlight the urgency of further investigation regarding the relevance of collective migration in cancer and the underlying molecular mechanisms. Furthermore, survival and growth of tumour cells in both the primary and metastatic sites are associated with a number of specific alterations of the normal cell functioning, including resistance to apoptotic signals, increased migratory capabilities, paracrine interactions with stroma and stromal cells and auto-sustaining signals [7]. Cell migration away from the primary site in response to external chemical guidance cues has been reported mainly in paracrine settings where secretion is originating in the stroma and the surrounding tissues [15], the blood or lymphatic circulation [24] or an organ [28, 29], as detailed before. Conversely, auto-sustaining signals have been associated with both paracrine and autocrine secretion [177-181]. However, whether autocrine signalling has a role on the migratory properties of cancer cells is much less explored and remains to be fully elucidated.

In this context, the work of Puliafito et al [90] provided an example of how collective migration might have an impact on cancer. The paper presented a 3D biological model to understand collective migration of PC-3 cell lines and demonstrated that chemotaxis-driven aggregation fits very well with the experimental data.

The main results of this work are reported below.

The initial observation regards the phenotypic behaviour of single PC-3 cells or pre-formed spheroids when embedded in a 3D hydrogel, which was recorded by means of time-lapse video-microscopy. Both single cells and pre-formed spheroids grow into larger aggregates and move directionally toward neighbouring clusters through the emission of protrusions, to form larger and larger aggregates in the time-span of several days (spheroids) or weeks (single cells) (Fig. 12). This ability was not observed in other two, less aggressive, prostate cancer cell lines, which, on the contrary, just grow into spheroidal structures, without neither moving nor emitting protrusions.

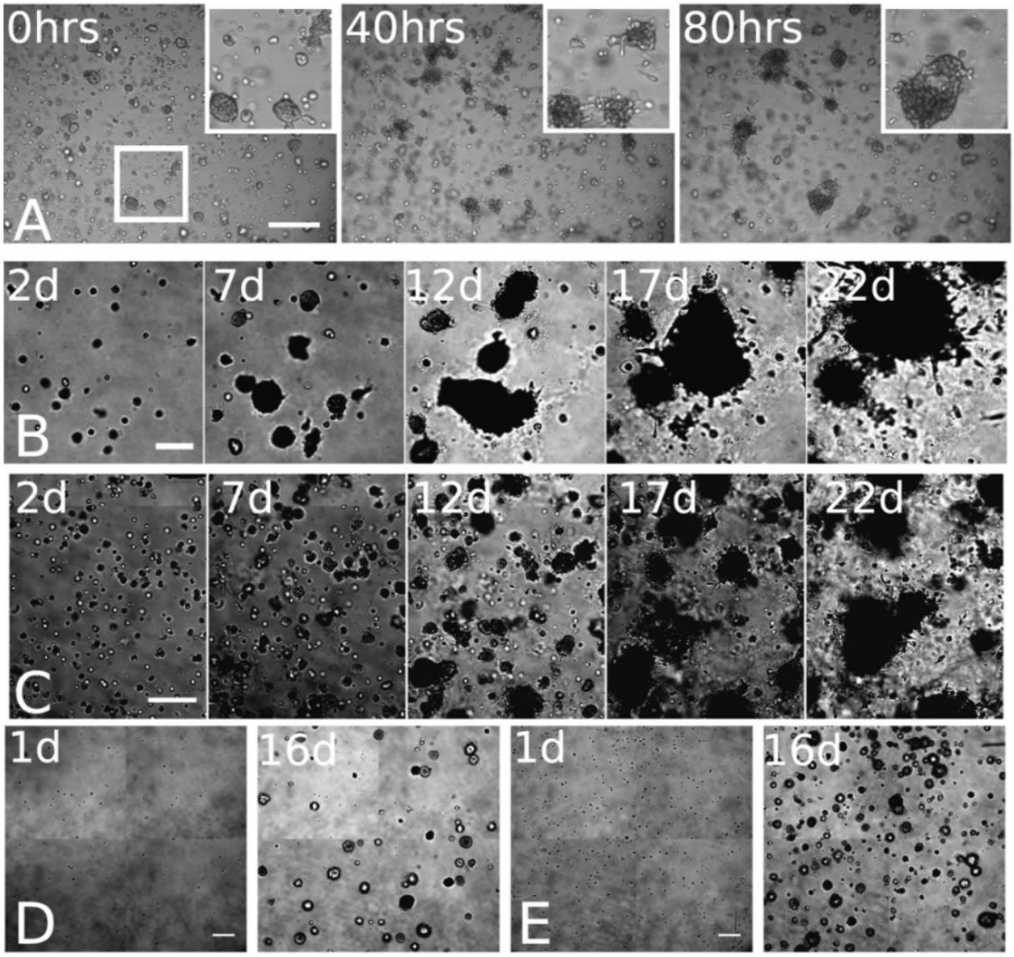

Figure 12 Cancer spheroids grow, migrate and aggregate in 3D cultures

(**A**) PC-3 cells and spheroids were embedded in a 3D hydrogel and observed by means of time-lapse microscopy for days. Representative snapshots at the indicated times are shown. The small white square of the leftmost panel is enlarged to illustrate one aggregation event, were clusters emit protrusions and move directionally to form a bigger cluster. Scale bar is 200 μm. (**B**,**C**) Snapshots of PC-3 single cells seeded at low and high densities respectively and imaged for about three weeks. Seeding densities calculated *a posteriori* are 35 and 113 cells/mm^3 respectively. Scale bar is 200 μm. (**D**,**E**) DU145 cells (a less invasive cell line in comparison with PC-3) were seeded at 23 and 77 cells/mm^3. In this case, cells grow as spheroids, but they do not move or aggregate. Rare merging events are observed whenever clusters come into contact by pure growth.
From "Three-dimensional chemotaxis-driven aggregation of tumor cells" [90]

By measuring the kinetics of aggregation of PC-3 seeded at different initial seeding densities, the authors showed that the behaviour they observed cannot be explained by coalescence due to a random motion. Mathematical arguments on models of active aggregation show that if cells or clusters were to move randomly an inverse proportionality would be observed between the seeding density (and hence the average distance between cells) and the rate of aggregation, measured as the decay time of the number of isolated independent objects in a given fixed volume. Such prediction is clearly inconsistent with the experimental data presented in the paper and calls for a directional rather than random movement.

Further measurements presented in the paper show that the distributions of velocities are dependent on the total number of cells, invoking a mechanism that is

consistent with the sensing of the relative gradient of a diffusible factor. Data are reported in figure 13.

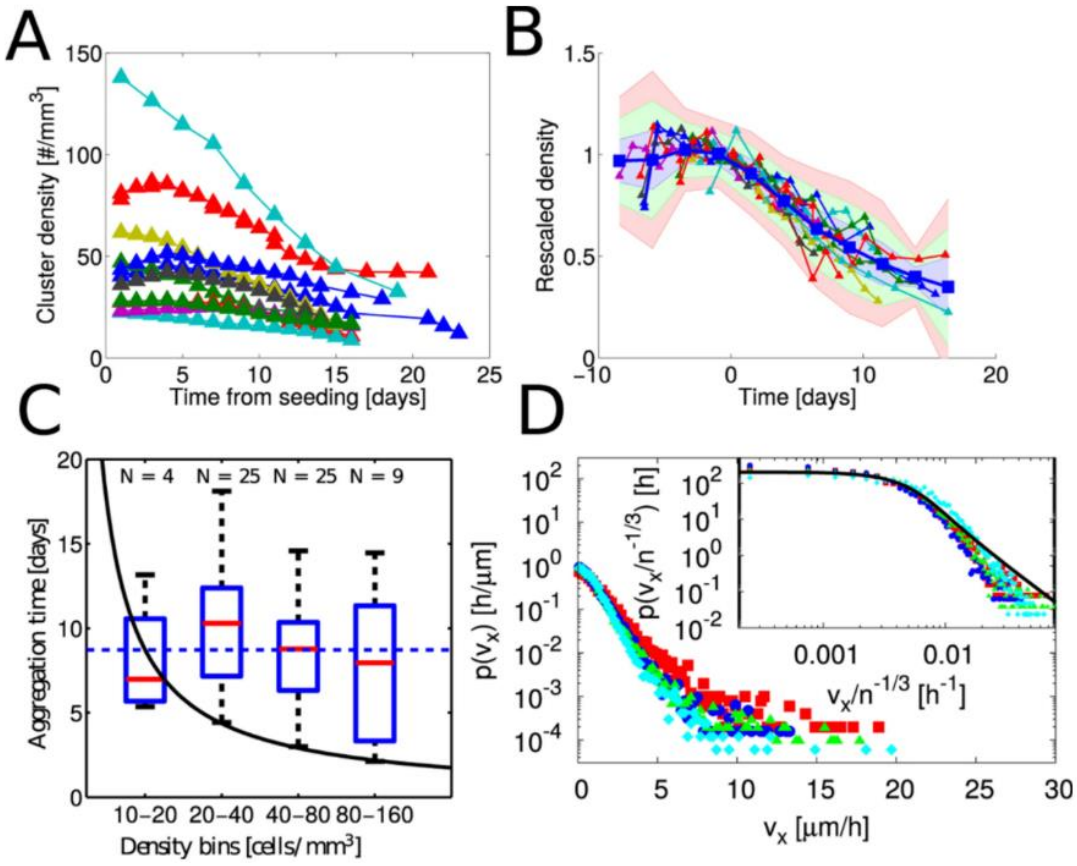

Figure 13 Dynamics of cancer cell spheroids aggregation

(A) The number of separate cells or clusters in the image was measured to calculate density at any time of time-lapse movies of the aggregation assays. Each curve represents a different independent experiment. **(B)** Aggregation curves were fitted independently, rescaled and time-shifted with the values of the obtained parameters. Curves are time-shifted depending on the value of the fit of the lag-times and rescaled according to the fitted seeding density. Shades indicate 1σ (blue), 2σ (red), 3σ (green). **(C)** Halving time of the number of objects in each field of view was measured for several densities (N = 63). The blue dotted line is the median of the data, plotted as a guide to the eye. Each box is the box-plot of the data contained in the corresponding logarithmic bin of cell density. Red lines are medians, blue boxes are 25th and 75th percentiles and whiskers are the most extreme points. The continuous black line represents the function x^{-1}, plotted here as a reference, as this would be the dependence of the time from density in the case of pure random aggregation. **(D)** Velocity of cells and clusters measured at early time-points of the aggregation assay. Densities are 21 cells/mm^3 (red squares), 31 cells/mm^3 (blue circles), 59 cells/mm^3 (green triangles) and 189 cells/mm^3 (cyan diamonds). Here $p(v_x)$ indicates the probability density function (PDF) of the variable v_x. The PDF of the components v_x and v_y of the velocity was found to have heavy tails (power law decay) and to be function of the seeding density. Denser cells move slower on average than sparse cells. The experimental velocity distribution is compared with the predicted Holtsmark distribution (solid line) with width $v_* = 2.8 \cdot 10^{-3}\, n^{-1/3}$ where n is the cluster density.
From "Three-dimensional chemotaxis-driven aggregation of tumor cells". [90]

To explain such results, they hypothesised that collective aggregation of PC-3 was mediated by the chemotaxis of cells toward a gradient of a diffusible factor secreted by cells themselves. Cells and spheroids establish a concentration gradient of the diffusible factor, ruled by the diffusion equation. The concentration field due to local secretion (and degradation) of a diffusible factor is superposed to all other neighboring cells and clusters and produces a spatially complex concentration profile which is locally orienting the direction of migration of cells and clusters which then merge to other clusters. The concentration gradient can therefore be sensed by clusters through the spatially asymmetric activation on the cell surface of receptors to which the ligand binds, and a minimal model of receptor activation is proposed in order to explain the dependence of the velocity on concentration, through density.

The formulated theoretical model of aggregation was in good agreement with the experimental data and the plausibility of their hypothesis was also corroborated by the observation that PC-3 are chemoattracted toward their own conditioned media. This study is one of the few to describe directional migration in collective migration [88, 92]. Importantly, they proposed a new model of cancer growth and opened to some interesting questions regarding the universality of such a phenomenon, its relevance in cancer and the underlying molecular mechanisms. In particular, a relevant question is whether the observed phenomenon is peculiar of the particular

cell line used in the study or whether it is widespread across other cell types and models. A role for cytoskeletal components has not been described in this model and would instead draw some important mechanistic insights. Another underlying question left unanswered is whether the directional migration observed is a result of purely cytoskeletal dynamics, such as for example in a ECM tension driven mechanism, or whether instead it is consistent with receptor-ligand dynamics at a molecular level. Above all, an interesting issue opened by this work is whether collective directional migration has any functional role. An interesting possibility is that this phenomenon might actually bring together different (phenotypically or genetically) clones, having therefore a role in the establishment of tumour heterogeneity and potentially clonal cooperation in cancer.

The work I have carried out during my PhD aimed to address some of these issues. We extended the study to 30 cancer cell lines originating from different tissues, showing that 6 of them can perform collective directional aggregation (CDA) and can actively form heteroclonal aggregates in 3D. Coalescence of distinct cell clusters is mediated by both subcellular and multicellular actin-rich protrusions that directionally extend towards neighbouring aggregates and mediate collective migration. We demonstrated that besides an important role of actin and myosin contractility in CDA, this phenomenon is not molecularly driven by purely cytoskeletal dynamics, but it is compatible with the signalling of upstream receptor-ligand dynamics, as downstream effector inhibition results in an impairment of CDA. The hypothesis that cluster attraction is mediated by soluble attractants is supported by the evidence that conditioned culture media act as chemoattractant, and that cells that respond chemotactically to conditioned media of other cells are also performing collective directional migration towards them.
In the next chapter I will discuss in detail the results I obtained.

MATERIALS AND METHODS

Cell culture

The cancer cell lines used are listed in Table1 (page 50) and were purchased from ATCC. Culture media (all purchased from Sigma-Aldrich), unless otherwise specified, were supplemented with 10% Fetal Bovine Serum (ThermoFisher Scientific), 200 U/ml of penicillin, 200 µg/ml streptomycin (Sigma-Aldrich) and 2 Mm L-Glutamine (Sigma-Aldrich). Cells were kept at 37 °C under 5% CO_2 humidified atmosphere. Cells were counted automatically by using TC20 Automated Cell Counter (BioRad). Medium was replaced three times a week. Each cell line was used up to passage 15. PCR-based Mycoplasma test was performed once a week.

Aggregation assays either starting from single cells or from spheroids were carried out in standard tissue culture plastic dishes (Falcon), multi-well plates (Corning) or imaging dedicated supports (glass-bottom 35 mm dish, Ibidi 81218-200; 96 well-plates Corning; µ-Slide 8 Well Chamber Slide, Ibidi 80827; 2-well silicone inserts, Ibidi 81176).

Cancer cell spheroid formation

Spheroids from cancer cell lines were generated by using the hanging drop technique. The protocol was adapted from the procedures reported in [182, 183]. A methylcellulose stock solution was prepared by dissolving 6 grams of autoclaved methylcellulose powder (M0512 Sigma-Aldrich) into 250 ml of preheated (60°C) serum free culture medium, with the help of a sterile magnetic stirrer, for 2h. 250 ml of 20% FBS culture medium with penicillin/streptomycin was added to a final volume of 500 ml, to obtain a final concentration of 10% FBS, and the solution was mixed overnight at 4°C. The 500 ml were aliquoted and centrifuged at 5000g for 2h at room temperature. The supernatant was collected and used for the spheroid assay, while the pellet was discarded. For spheroid generation, cells were detached,

counted and mixed with 80% culture medium and 20% methylcellulose stock solution to obtain a final concentration of 0.24% methylcellulose. Drops of 30 µl were generated by using a multichannel pipette and laid down onto the inner part of a 150-mm petri dish lid. The lid was carefully reversed to let the cells grow in the hanging drops, under non-adherent culture conditions. Cells were maintained and humidified by adding PBS into the plates and kept in the incubator. After three days, spheroids were carefully harvested by washing out the drops with PBS and collecting the solution into 50 ml tubes. Spheroids were gently spun down at 500 RPM for 5 minutes, the supernatant was removed and spheroids were mixed with Growth Factor Reduced (GFR) Matrigel (Corning) by using wide-bore (and precooled) tips to avoid desegregation.

Spheroids pre-mixed with Matrigel were seeded as described in the following paragraph.

The following number of cells per drop was used to form spheroids of about 200 µm diameter:

ACHN: 100; CFPAC-1: 300; Hs 746T: 100; NCI-H23: 100; MG-63: 100; MDA-MB-231: 300; PC-3: 50; MIA PaCa-2: 300.

3D cell and spheroid culture

For 3D cell culture, cells and pre-aggregated spheroids were mixed at the desired density with GFR-Matrigel diluted with culture media to a final concentration of 8 mg/ml. To avoid the bi-dimensional growth of cells or spheroids underneath (on the plastic bottom of the plates) or on top of the GFR-Matrigel during the 3 week-long assays, a "sandwich" of three layers was prepared as follow: a first layer of GFR-Matrigel was deposed on the bottom of 96- or 48-well plates. A second layer of GFR-Matrigel plus cells or spheroids was added on the top of the previous layer and a third layer of GFR-Matrigel was deposited on top. Each layer was left to polymerize for 10 minutes at 37°C before adding the next layer. Plates were kept on ice to depose the first layer and GFR-Matrigel was manipulated in ice by using precooled tips, to avoid hydrogel solidification. After polymerisation, wells were

filled with culture media (200 µl in 96 well-plates and 500 µl in 48 well-plates) and plates were kept at 37°C. Culture media were replaced three times a week.
The following volumes of Matrigel were used for each of the three layers depending on the culture supports: 96-well plates: 30 µl – 40 µl (including cells) – 30 µl; 48-well plates: 80 µl – 100 µl (including cells) – 80 µl; glass bottom 8 slides: only one layer of 80 µl, to obtain a sufficiently-thin slice suitable for microscopy experiment with short working distance objectives (suitable only for one or two day-long experiments); 2-well silicone inserts: only one layer of 40 µl (same reason).

Drug treatments

To test the effect of pharmacological inhibition, cells and spheroids were seeded in Matrigel as described above and media were replaced with media containing the inhibitors at the desired concentration diluted in DMSO. In the case of single cells, inhibitors were added two days after seeding, while in the case of pre-aggregated spheroids, inhibitors were added a few hours after seeding. Media were replaced three times a week. For actin perturbation we used (Fig. 21) 1 µM Latrunculin A (Sigma-Aldrich); 1 µM Cytochalasin D (Sigma-Aldrich); 100 µM CK666 (Sigma-Aldrich); 10 µM Wiskostatin (Sigma-Aldrich). For Myosin perturbation we used: 100 µM Blebbistatin (Calbiochem); 20 µM Y-27632 (Sigma-Aldrich).
For the results shown in figure 22, the following inhibitors were used PI3K/mTOR inhibitor BEZ235 (Selleckchem) 50 nM, 100 nM and 300 nM; PI3K inhibitor BYL719 (MedChemExpress) 1 µM, 3 µM, 5 µM and 10 µM; AKT inhibitor MK-2206 dihydrochloride (MedChemExpress) 1 µM, 3 µM and 5 µM; MEK inhibitor AZD-6244 (MedChemExpress) 0,5 µM, 1 µM and 3 Mm.

Chemotaxis assay

Chemotaxis was assessed by using 6.4 mm Transwell Permeable Support (Falcon) with 8-µm pore PET membrane inserts. 3×10^4 cells (or 1×10^4 in the case of MG-63 cell line) were seeded on the permeable membrane with 100 µl of medium. Cells

were kept in the incubator over-night to allow the attachment. The following day, cells were gently washed three times with PBS and 400 µl of serum free medium was added. The low compartment was filled with 750 µl of conditioned media. After 24 hours of incubation, non-migrated cells on the upper surface of the membrane were removed with a cotton swab, while cells passed through the membrane were fixed with 2,5 % glutaraldehyde in PBS, washed 2x with PBS and stained with 0.1% crystal violet solution in methanol. Once dry, membranes were imaged on an inverted microscope and images were analysed by means of automatic segmentation as detailed in the Image Analysis section.

To obtain the conditioned media, 2×10^6 cells were seeded into a 10-mm Petri dish with complete media and let attach overnight in the incubator. The following day, cells were washed with PBS and 2 ml of serum free media were added. Conditioned media were collected after 24, 48 and 72 hours and filtered with 0.22-µm filters before being used for the assay.

Plasmids and lentivirus production

Plasmids were purchased from Addgene. LV-GFP and LV-RFP were a gift from Elaine Fuchs (Addgene plasmid #25999 and Addgene plasmid #26001) (Beronja et al. 2010). pLenti.PGK.LifeAct-Ruby.W and pLenti.PGK.LifeAct-GFP.W were a gift from Rusty Lansford (Addgene plasmid #51009 and Addgene plasmid #51010). Lentiviruses were produced by calcium phosphate transfection of lentiviral plasmids together with packaging (pCMVdR8.74) and envelope (pMD2.G-VSVG) plasmids in 293T cells. Supernatant was harvested 24 and 48 h after transfection, filtered with 0.45-µm filters, precipitated (19,000 *g* for 2 h at 20°C), and suspended in PBS at a higher concentration. The multiplicity of infection (MOI) was determined by infecting HeLa cells and by quantifying GFP, RFP or Ruby-positive cells by flow cytometry. All cell lines were infected considering a MOI of 2 viral particles per cell, except MG-63 which required a MOI of 25 viral particles per cell. Positivity to fluorescent proteins was assessed 48 hours after infection.

Imaging methods

Time-lapse experiments were performed on inverted microscopes, either confocal or widefield, equipped with a motorized stage and an incubator to keep the plate stable at 37° and 5% CO_2. For 2 or 3 week-long time-lapse experiments, cells were kept in the incubator and imaged once a day.

To observe the protrusion composition (Fig. 14c), infected cells (with fluorescent H2B and LifeAct) were used to form spheroids, as described above. Spheroids were embedded in Matrigel and after 2 to 3 days culture medium was removed, spheroids were washed twice with PBS and fixed with 4% PFA for 30 minutes. PFA was removed by washing three times with PBS, and samples were kept in PBS for subsequent imaging.

Images throughout the paper are obtained by a number of different techniques and instruments. Temporal grayscale series were obtained by the BioTek Cytation 3 equipped with a 4X objective (Olympus). Fluorescence images were obtained with either a confocal Leica SP8 equipped with dry 20X or immersion 40X or 60X or with a widefield microscope Nikon Ti2 equipped with dry 20X 0.75, immersion 40X 1.15 or 60X 1.4 and a wide field of view monochromatic camera (IRIS 15, Photometrics). Live imaging was performed with an automatic water dispenser for immersion objectives. Fluorescence images were obtained by acquiring z-stacks which were then maximum intensity projected. Widefield fluorescence images were previously deconvoluted with Richardson-Lucy algorithm. In selected images, a Gamma correction was used to increase the contrast of the lower intensity protrusion with the respect to the body of spheroids for visualization reasons. Original images are available upon request. Whole Transwell membranes were acquired by the same widefield microscope with an RGB camera by stitching several images together.

Grayscale images in time-series are obtained by projecting stacks (typically 1mm thick) of single brightfield images taken every 50 μm and then projected onto a single image with extended depth of field (EDF) [184] based on the maximization of the local image variance (with a kernel size of 8um), implemented in Fiji through

the plugin developed by EPFL [185]. Images were handled with custom-written scripts for Fiji or Matlab.

Image analysis

In order to quantify the protrusive fraction of a given time-lapse series we implemented the following image analysis algorithm. A large set of timeseries was fed to a machine learning segmentation software (Ilastik [186, 187]) with different classes for background, bulk and protrusive areas. Multinary images obtained were then processed by a custom written Matlab algorithm to filter out small isolated structures (<50 μm radius) and calculate the ratio between the fraction of the protrusive area in the image to the total cluster occupied region at the first frame, in order to account for the variable number of spheroids in the field of view.

The effect of drug treatments on single cells aggregation assays was quantified as indicated in the figure 22 caption.

The number or independent objects in EDF time series were counted and overlapped objects were checked in the original non projected stack.

In order to obtain quantitative parameters, the number of objects over time was fitted to a sigmoid, shown in figure 17c.

The estimation of the velocity from EDF time series was performed as follows. First images were aligned by means of cross-correlation methods in order to correct for stage offset and gel large scale movement. PIV-based image alignment was implemented in Matlab. After image alignment, segmented images were used to compute area differences at 3 hours in order to consider only relatively fast movements and not overall growth. Such differences between frames were used as an estimation of the velocity by dividing the corresponding area in squared microns by the time interval.

Transwell images were segmented by means of the previously mentioned software Ilastik and binary images were quantified by Matlab custom written scripts.

Statistical and data analysis

The kinetic data of aggregation (Fig. 17a) were fitted to a sigmoid shown in figure 17c. To estimate the doubling times, we fitted the data extracted from the segmentation of single cells or spheroids, and corrected for the dependence on the radius. The total volume of the objects is proportional to the number of cells, therefore the area elevated to the power 3/2 is a pseudo-volume, used as a proxy for the number of cells. Therefore, to extract the doubling time of cells we fitted the area with an exponential A*2^(t/tau) and calculated the doubling time as 2/3tau.
Statistical analysis on the data of chemotaxis assays was performed using GraphPad Prism 8.0.0 software. Statistical significance was assessed by performing a parametric one-tailed t-test with Welch's correction (unpaired). $P \leq 0.05$ was considered significant. When not significant, the p value has been indicated in the figure.

Cell line name	Site of origin	Culture medium
786-O	Renal cell carcinoma	RPMI
A-375	Amelanotic melanoma	DMEM
A-498	Renal cell carcinoma	RPMI
A549	Lung adenocarcinoma	RPMI
ACHN	Papillary renal cell carcinoma; derived from metastatic site: pleural effusion	RPMI
BxPC-3	Pancreatic ductal adenocarcinoma	RPMI
Caki-1	Clear cell renal cell carcinoma; derived from metastatic site: skin	RPMI
Calu-3	Lung adenocarcinoma; derived from metastatic site: pleural effusion	RPMI
Capan-1	Pancreatic ductal adenocarcinoma; derived from metastatic site: liver	ISCOVE 20%
CFPAC-1	Pancreatic ductal adenocarcinoma; derived from metastatic site: liver	RPMI
COV-362	High grade ovarian serous adenocarcinoma; derived from metastatic site: pleural effusion	DMEM
DLD-1	Colon adenocarcinoma	RPMI
DU145	Prostate carcinoma; derived from metastatic site: brain	RPMI
HCT 116	Colon adenocarcinoma	RPMI
HOP-62	Lung adenocarcinoma	RPMI
Hs 578T	Invasive ductal carcinoma, not otherwise specified	RPMI
Hs 746T	Gastric adenocarcinoma; derived from metastatic site: muscle; left leg	DMEM
MDA-MB-231	Breast adenocarcinoma;derived from metastatic site: pleural effusion	DMEM
MG-63	Osteosarcoma	DMEM
MIA PaCa2	Pancreatic ductal adenocarcinoma	RPMI
NCI-H1299	Lung large cell carcinoma; derived from metastatic site: lymph node	RPMI
NCI-H1395	Lung adenocarcinoma	RPMI
NCI-H23	Lung adenocarcinoma	RPMI
OVCAR-8	High grade ovarian serous adenocarcinoma	RPMI
PANC-1	Pancreatic ductal adenocarcinoma	RPMI
PC-3	Prostate carcinoma; derived from metastatic site: bone	RPMI
SK-MES-1	Lung squamous cell carcinoma; derived from metastatic site: pleural effusion	RPMI
SK-OV-3	Ovarian serous cystadenocarcinoma; derived from metastatic site: ascites	McCoy's 5A 10%
U-87MG	Glioblastoma	DMEM
UO-31	Renal cell carcinoma	RPMI

Table1: list of cell lines used in this work, their tissues of origin and their culture media.

RESULTS

Cancer cell lines of different tissues of origin perform collective migration in 3D

In order to verify the universality and recurrence of CDA, we first tested 30 human cancer cell lines for their ability to grow, invade and perform collective directional migration when embedded in a 3D hydrogel. Cell lines were selected on the basis of previous knowledge about the capability to grow as spheroids in a 3D matrix [188-194], which was verified with our experiments.

To this aim single cells were premixed with a hydrogel (Matrigel) in order to obtain a uniform spatial distribution. Cells were observed by means of time-lapse microscopy for approximately three weeks after seeding. In order to monitor a large number of events and to extend our imaging experiments to a large number of samples, we performed extended depth of field (EDF) projections on wide z-stacks (details are given in the Materials and Methods section). Such a technical approach was made necessary by the large range of the time and spatial scales involved in the process, spanning from hours to weeks and from tens of microns to millimetres. Representative snapshots at multiple time-points are shown in figure 14a. Our results show that out of the 30 cell lines tested, 6 cell lines from different tissues of origin (Fig. 14a,b) are able to move within the matrix as multicellular clusters, display active protrusions and multicellular outgrowths (Fig. 14c) and that clusters deriving from distant single cells coalesce to form "multiclonal" aggregates, forming larger and larger objects in the time span of several days (Fig. 14a from the top row to the bottom: MDA-MB-231, PC-3, ACHN, MG-63, NCI-H23 and Hs 746T). Early after seeding, neither significant proliferation nor movement could be detected in our experiments. In a lag-time spanning 1 to 3 days depending on the cell line, the formation of single- and multiple-cell wide outgrowths are observed, as shown in figure 14c, allowing nearby initially separated objects to come into contact and move directionally one towards the other. Such directional migration

events are followed by subsequent reshaping of the new "multiclonal" aggregate into a new structure, that is then compacted and assumes again the shape of a spheroidal cluster, more ordered and rounder in some cell lines (e.g., ACHN, Fig. 14a) and rich in protrusions in others (e.g., MG-63, Fig. 14a). Over the three weeks, cluster active coalescence leads to the formation of larger and larger objects, which reach the size of hundreds of microns. It is worth noting that at sufficiently high densities all cells will present coalescence events due to the high probability of finding two objects close enough to merge due to growth. However, our aggregation assays are designed to obtain an average distance between single cells above 220 μm, thereby minimizing the effect of growth-driven coalescence events.

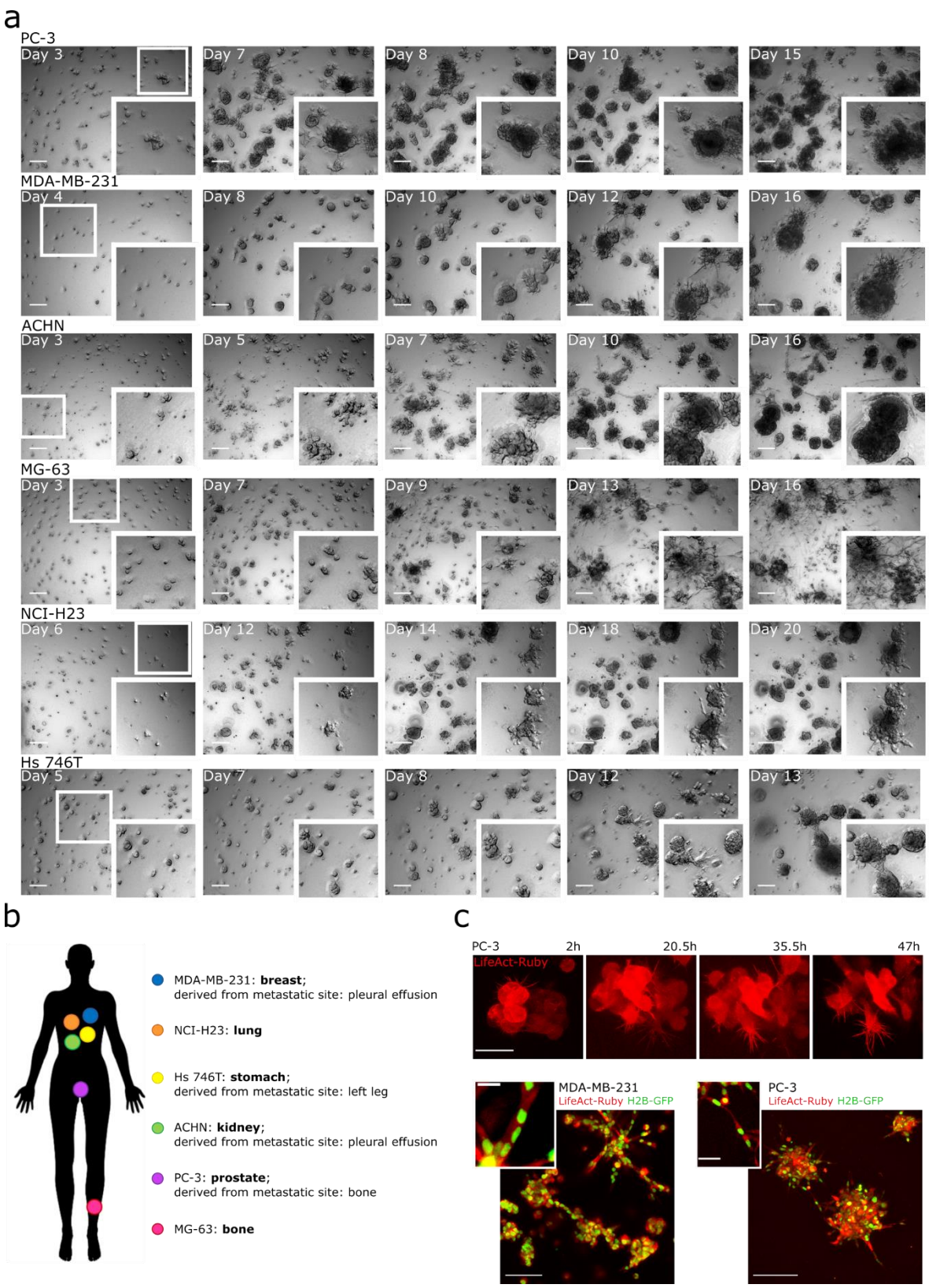
a
PC-3
Day 3
Day 7
Day 8
Day 10
Day 15
MDA-MB-231
Day 4
Day 8
Day 10
Day 12
Day 16
ACHN
Day 3
Day 5
Day 7
Day 10
Day 16
MG-63
Day 3
Day 7
Day 9
Day 13
Day 16
NCI-H23
Day 6
Day 12
Day 14
Day 18
Day 20
Hs 746T
Day 5
Day 7
Day 8
Day 12
Day 13
b
MDA-MB-231: breast;
derived from metastatic site: pleural effusion
NCI-H23: lung
Hs 746T: stomach;
derived from metastatic site: left leg
ACHN: kidney;
derived from metastatic site: pleural effusion
PC-3: prostate;
derived from metastatic site: bone
MG-63: bone
c
PC-3
LifeAct-Ruby
2h
20.5h
35.5h
47h
MDA-MB-231
LifeAct-Ruby H2B-GFP
PC-3
LifeAct-Ruby H2B-GFP

Figure 14 Cancer cells grow, migrate and aggregate in 3D cultures.

(a) Six cancer cell lines from different tissues of origin were seeded as single-cell suspension in a 3D growth assay and imaged by means of bright-field microscopy each day for 2-3 weeks. Representative snapshots at indicated time points are shown. Each image is obtained by creating an extended depth of field (EDF) projection starting from a wide Z stack (around 1mm thick). Each row represents a cell line, from top to bottom: PC-3 (initial seeding density calculated a posteriori: 31 cells/mm3); MDA-MB-231 (22,2 cells/mm3); ACHN (35,1 cells/mm3); MG-63 (84,2 cells/mm3); NCI-H23 (36,2 cells/mm3) and Hs 746T (90,4 cells/mm3). The smaller white squares in the leftmost image of each row are zoomed in the corresponding inserts at the bottom right corner of the images to highlight out aggregation events. Scale bar: 200 µm. **(b)** Sketch of a human silhouette to illustrate the point of origin of each aggregating cancer cell line. **(c)** Confocal microscopy images showing pre-aggregated spheroids of PC-3 (top and bottom-right panels) and MDA-MB-231 (bottom-left panel) infected with LifeAct Ruby (top) or with H2B-GFP/LifeAct-Ruby (bottom) and seeded in Matrigel. Both subcellular protrusions (top) and long multicellular outgrowths (bottom) are well visible. Scale bar top insets: 50 µm; bottom-left inset: 100 µm; enlarge bottom-left inset: 20 µm; bottom-right inset: 200 µm; bottom-right enlarged inset: 50 µm.

In contrast with the set of cell lines shown in figure 14a, other cell lines were able to grow into multicellular spheroids within the matrix, but displayed no visible and measurable signs of directional migration. In such cases coalescence of two or more clusters was only observed when objects came into contact due to growth (Fig. 15a).

a

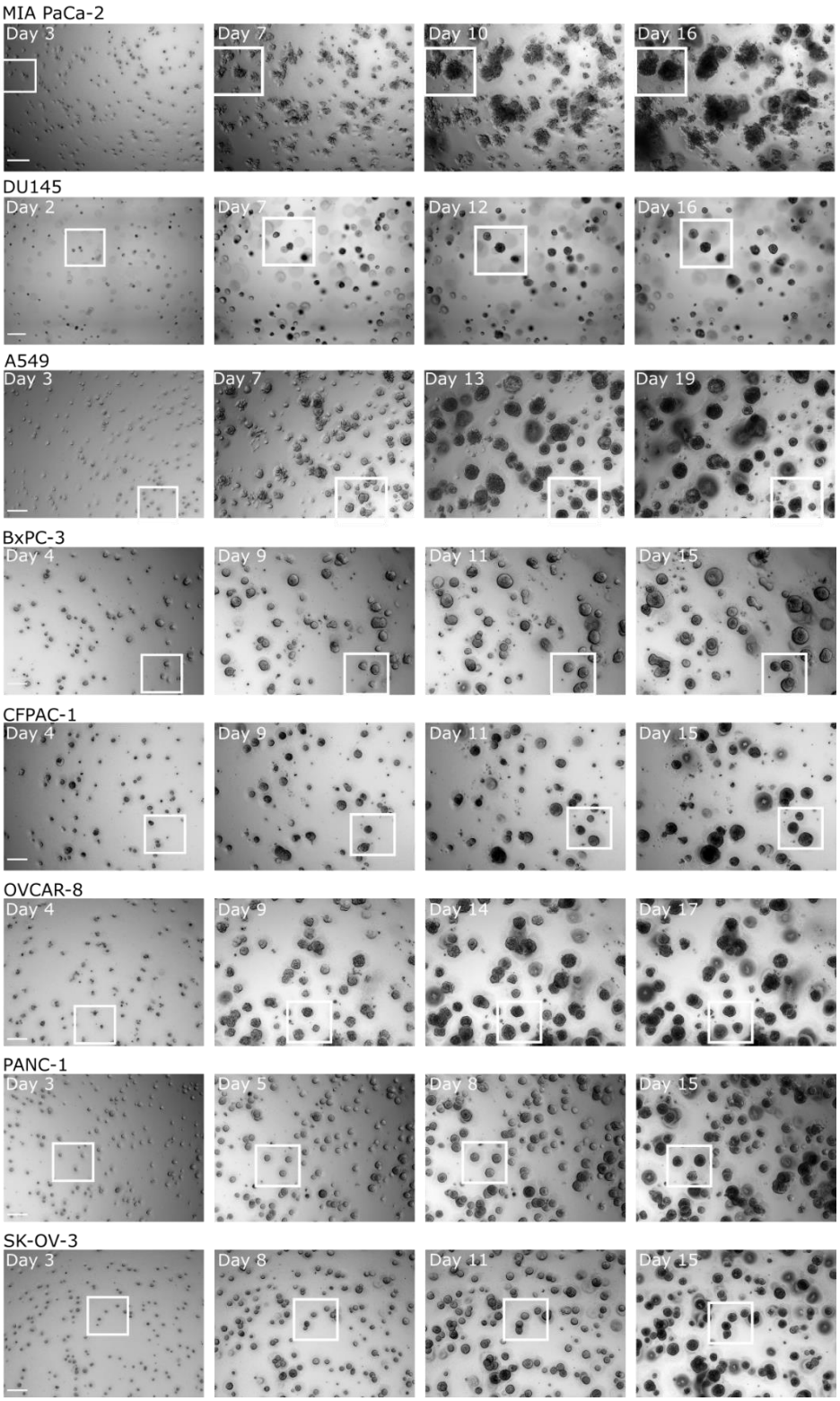
MIA PaCa-2
Day 3
Day 7
Day 10
Day 16
DU145
Day 2
Day 7
Day 12
Day 16
A549
Day 3
Day 7
Day 13
Day 19
BxPC-3
Day 4
Day 9
Day 11
Day 15
CFPAC-1
Day 4
Day 9
Day 11
Day 15
OVCAR-8
Day 4
Day 9
Day 14
Day 17
PANC-1
Day 3
Day 5
Day 8
Day 15
SK-OV-3
Day 3
Day 8
Day 11
Day 15

Figure 15 The ability to perform CDA is not common to all cancer cell lines

(a) Representative snapshots of non-aggregating cell lines, as in Fig. 14a. From top to bottom: MIA PaCa-2 (initial seeding density calculated *a posteriori*: 71 cells/mm^3); DU145 (62,5 cells/mm^3) and A459 (63,7 cells/mm^3); BxPC3 (23,2 cells/mm^3); CFPAC-1 (29,3 cells/mm^3); OVCAR-8 (47,4 cells/mm^3); PANC-1 (59,5 cells/mm^3) and SK-OV-3 (59 cells/mm^3). White squares are meant to indicate clusters that grow without aggregating. Scale bar: 200 µm.

In the vast majority of the cases, non-aggregating cell lines grow into round spheroids, presenting less or shorter outgrowths in comparison with cell lines performing CDA (Fig. 16a).

The phenotypic differences observed among different cell lines associated with their high or low invasiveness (i.e., the emission or long or short outgrowths and the shape more or less rounded) are consistent with what reported in literature [195-197].

To quantitatively confirm the correlation between aggregation and the emission of single cell protrusions and multiple cells wide outgrowths, we counted the fraction of initially seeded cells later involved in at least one event of aggregation (Fig. 16b). We observed that the majority of non-aggregating cell lines only show small percentages of aggregation events (typically less than 10% at the considered densities). One cell line (MIA PaCa-2) was found to have an intermediate behaviour (around 25%). It is worth noting that this cell line has also a mixed morphology, presenting slightly less ordered aggregates than other cell lines. As anticipated, the rate of aggregating cells is never 0% due to the presence of coalescence events that are caused by direct growth-induced contact. On the contrary, aggregating cell lines show an aggregation percentage ranging from about 70% (Hs 746T) to almost 100% (MG-63).

Remarkably, all the aggregating cell lines were originally derived from different cancerous tissues, as sketched in panel 14b. Moreover, different cell lines derived from the same tissue of origin (e.g., PC-3 and DU145: prostate; NCI-H23 and A549: lung) show different behaviours (i.e., aggregate or not), suggesting the absence of a direct correlation between the tissue of origin and the CDA phenotype.

These data suggest that this phenomenon is widespread across cancer types, independently from the tissue of origin and that it is related to phenotypic differences in the morphology of multicellular aggregates growing in a 3D matrix.

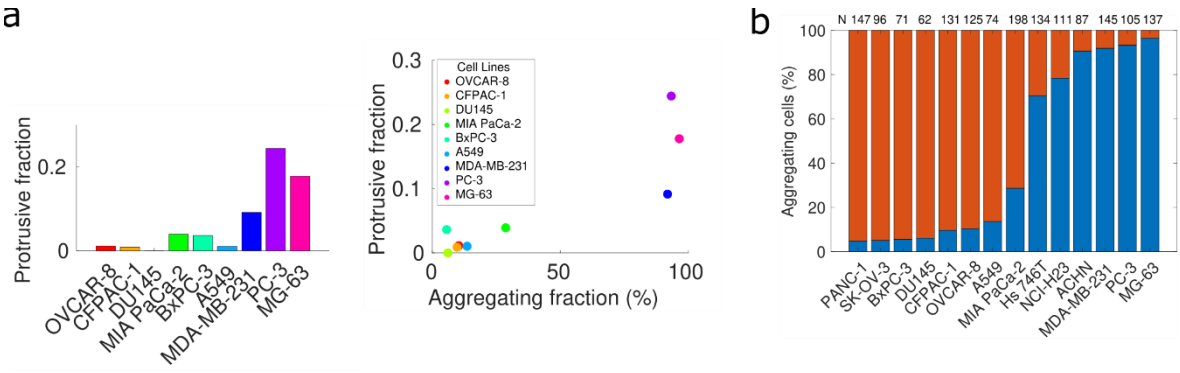

Figure 16 The ability to perform CDA is related to the presence of protrusions and outgrowths

(a) Ratio of protrusions to bulk regions of the spheroid for different cell lines obtained by segmentation of EDF-projected images of aggregation assays at 12 days after seeding. **(b)** Correlation between presence of protrusions/outgrowths and the percentage of aggregating cells shown in panel (c). **(c)** Fraction of cells seeded at the beginning of the assay that are subsequently involved (blue) or not involved (red) in aggregation events over the course of an aggregation assay.

Cluster coalescence is driven by directional collective migration

A fundamental question related to the collective migration observed for such a wide variety of cell lines is whether movement is directional or random, in order to better understand the biological function of such a phenomenon. To this aim, we developed a quantitative high-throughput approach based on the measurement of the number of isolated clusters, or cells, present in a field of view over the course of our time-lapse experiments (Fig. 17a, aggregating cells; Fig. 17b, non-aggregating cells). Each of these time series was fitted to a sigmoid function (see Fig. 17c) in order to extract quantitative information on the dynamics of aggregation in each assay separately.

We first ought to quantify the extent of the aggregation phenomenon in different cell lines and for different initial seeding densities. This measure is given by the ratio between the variation of the number of separated objects (seeding with respect to the end of the assay) and the seeding density in such a way that non-aggregating cells would have a vanishing density fraction and strongly aggregating cells would display values closer to unity. Such values for a set of cell lines are shown in panels 17d and 17e. As expected, aggregating cell lines display a decrease in density which correspond to final densities smaller than half of the initial density (Fig. 17d). In

contrast, non-aggregating cell lines do not show significant decrease in density, as visible also from the curves in figure 17b and in figure 17e. As explained above, a small number of coalescence events can be seen even in non-aggregating cell lines due to the random positioning of the cells at seeding, as shown by the small density fractions plotted in figure 17e.

To verify whether aggregation might be induced by random movement, we measured the effect of the initial distance between cells at seeding (i.e., density) on the dynamics of the aggregation process. If the movement of clusters (or the directionality of protrusions and outgrowths) were random, higher densities would lead to a larger number of aggregation events simply due to the fact that, when cells sit closer, the chance of coming into contact is higher. In particular, this would imply an inverse proportionality between the halving times of the number of objects and the seeding density, as explained in the previous results [90].

We therefore measured the aggregation rates of cell lines at different initial seeding densities, as shown in figure 17f. Our results show that the aggregation halving times are largely independent of initial seeding density, therefore indicating that migration is not random.

Aggregation times show variability across different cell lines and fitted data indicate that ACHN and PC-3 are the fastest to aggregate, with halving times of (7.3±1.0) days and (9.4±0.7) days respectively (mean±std); MG-63, Hs 746T and MDA-MB-231 halve in (13.6±1.0) days; (12.9±1.7) days and (13.0±1.7) days respectively and NCI-H23 is the slowest in the group, with a halving time of (15.5±1.3) days. Overall, this phenomenon occurs on a timescale of the order of a week for all cell lines considered. This is consistent with what previously measured for PC-3 cells [90], and is also significantly different from what observed in liquid overlay cultures, where random movement is predominant [198-200], and the dynamics is much faster, with aggregation times estimated as less than a day.

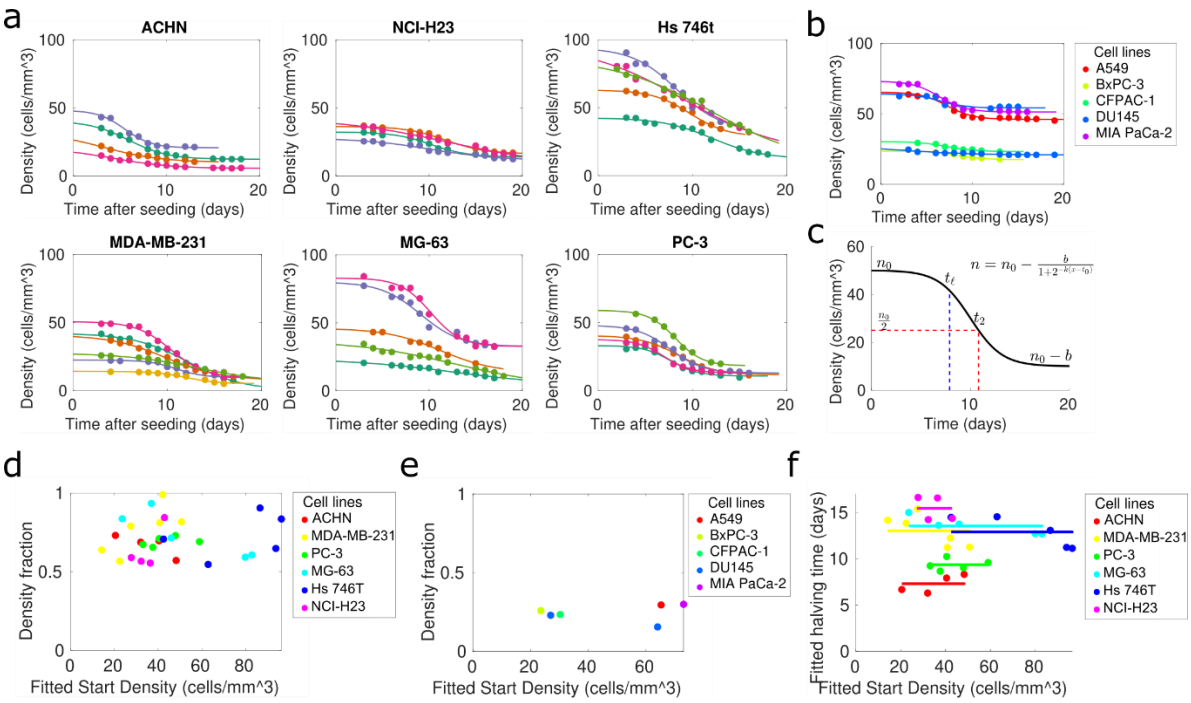

Figure 17 Aggregation kinetics is independent on initial seeding density

(a) The number of separate objects in each EDF-projected image over time is fitted with a sigmoidal curve (see panel c) for different initial seeding density. Each set of lines and points represent a single aggregation assay and points are experimental data, while lines represent the fit. **(b)** Same of (a) but for non-aggregating cell lines. The legend indicates the colours associated to cell lines. **(c)** Plot of the sigmoid function used to fit the data of aggregation kinetics with indicated parameters used in the quantification. The operational definitions of each parameter are: halving time is the time at which the number of objects is half the initial fitted number of objects; lag time t_l is the time corresponding to the first change of convexity of the function; n_0-b is the number of objects at the end of the assay. **(d,e)** The density fraction (difference between number of objects at the beginning and the end of the assay as resulting from the fit parameters divided by the number of objects at the beginning) is plotted for each cell line and initial starting density. **(f)** The plot reports the halving times obtained by the fit parameters of curves shown in panel (a) and plotted as a function of the seeding density.

Aggregation is coupled with proliferation of cells within clusters

To dissect whether proliferation and aggregation occur on the same timescale, we quantified the growth of clusters during the aggregation assays (Fig. 18 a,b) and plotted it against the kinetics of aggregation, as shown in figure 18c and 18d for non-aggregating cell lines. These scatterplots show clearly that separating the effect of proliferation from that of aggregation is a daunting task in aggregation assays starting from monodisperse single-cell size distributions. Therefore, in order to clarify this relationship, and to investigate potential correlations between proliferation and aggregation, we measured the doubling time of spheroids

(calculated from their projected area) as shown in figure 18e and 18f for non-aggregating cell lines. Reported means±std for each cell line are ACHN (0.91±0.24) days; MDA-MB-231 (1.74±0.47) days; PC-3 (1.16±0.51) days; MG-63 (1.67±0.53) days; Hs 746t (5.48±1.04) days and NCI-H23 (2.21±0.26) days. Doubling times for aggregating cell lines are consistent with proliferation rates on flat cultures (1.25 days (ACHN); 1.25 days (MDA-MB-231); 1 day (PC3); 1.25 days (MG-63); 1.6 days (NCI-H23) [201] and 2.8 days for Hs 746T [202]).

Furthermore, coherently with our hypothesis, halving times and doubling time correlate, and faster aggregating cells are found to be on average also more proliferating in our 3D single cell assay (Fig. 18g). These observations hold for all cell lines but for Hs 746T, which show halving times comparable to other cell lines but much slower doubling times. Correlation coefficients for halving and doubling times are indeed $R=0.345$, $p=0.067$ for the complete dataset, and $R=0.752$, $p=2.25\times10^{-5}$ excluding Hs 746T.

These observations are coherent with the notion that it is indeed hard to disentangle the effect of proliferation from that of directional migration in this experimental setup which spans several doubling times for all cell lines.

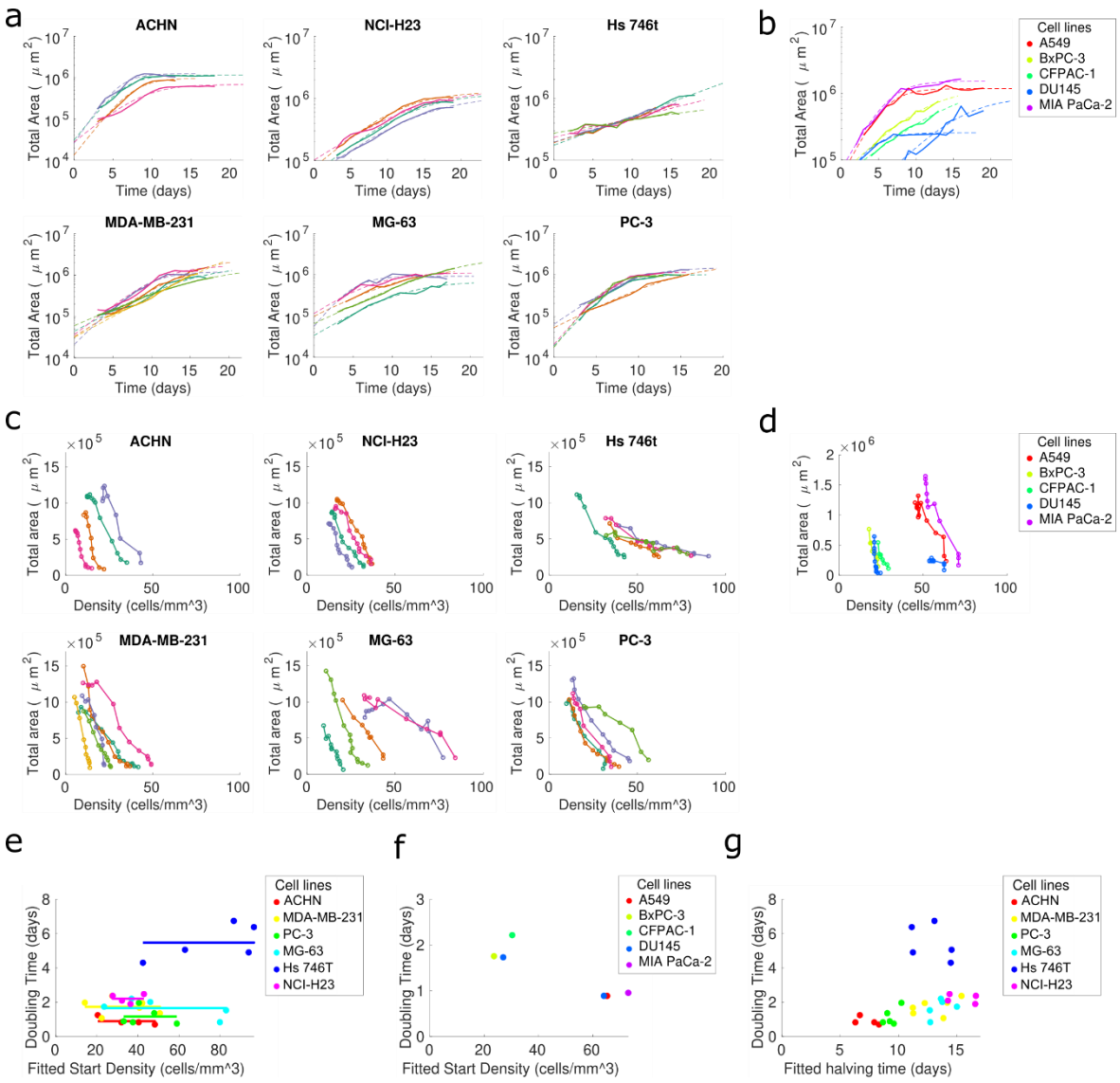

Figure 18 Aggregation kinetics is coupled to cell proliferation rates

(a,b) Timeseries of the total pseudo-volume for each density of the indicated aggregating cell lines (a) and non-aggregating cell lines (b), indicated in the title of the plot or in the legend. Dashed lines represent the fit with a saturating exponential. **(c,d)** Scatter plots reporting fitted starting density vs the total area of the growing spheroids. Each dot represents a single time-point from the aggregation assays. Lines parallel to the y-axis would indicate pure proliferation with no aggregation, while lines parallel to the x-axis would indicate aggregation with no proliferation. **(e,f,g)** The plots report the doubling times, and the scatterplot halving time vs doubling time obtained by the fit parameters of curves shown in panel (a) and plotted as a function of the seeding density. Doubling times were obtained by a separate fit (see details in the Materials and Methods section and growth curves reported in panel 18a,b). Each dot represents an aggregation assay performed with a cell line at a given initial seeding density with colour codes reported in the legend.

In order to further dissect the relationship between proliferation and aggregation, we developed an aggregation assay starting from pre-formed multicellular aggregates, to decrease the relative importance of proliferation. Cell spheroids were

pre-assembled under non-adherent culture conditions and were embedded in the same hydrogel as for single cell assays.

With this experimental setup, the emission of protrusions and collective migration start not later than 24h after seeding. The overall estimated change in the total number of cells over the course of single cell assays was around 10-fold in all cell lines, while spheroid assays involved at most 2-fold changes. Therefore, consistently with the brevity of the assay and the larger structures involved, growth of spheroids during the assay was more limited than in single cell assays. These observations are therefore consistent with the notion that, in pre-assembled spheroids assays, directional migration is occurring on faster scales than growth.

Our experiments show that spheroids seeded in a 3D hydrogel start emitting single cell protrusions and multicellular outgrowths already a few hours after seeding and migrate collectively forming multi-cluster aggregates as shown in figure 19a. All aggregating cell lines recapitulate the same behaviour observed in single cell assays, while non-aggregating cells only show growth, with no signs of collective migration (Fig. 19b).

Despite starting from different initial conditions, the two assays show the same collective migration paradigm, with single and multicellular protrusions mediating the coalescence events as shown in the insets of figure 19a.

To pinpoint the directionality of the movement, we segmented a group of aggregating objects in the images of our time-lapse assay for the entire duration of the aggregation assay and extracted the shape of the projected area occupied by the objects over time (Fig. 19c). Our results show that spheroids move directionally toward each other to form one single cluster at the end of the movie and that spheroid deformation and protrusions occur along the line separating the two objects, albeit with considerable fluctuations in the orientation. This observation is consistent with what observed in other biological settings [203], where protrusions are not statically oriented towards the source, but are dynamically moving, maintaining overall orientation in time.

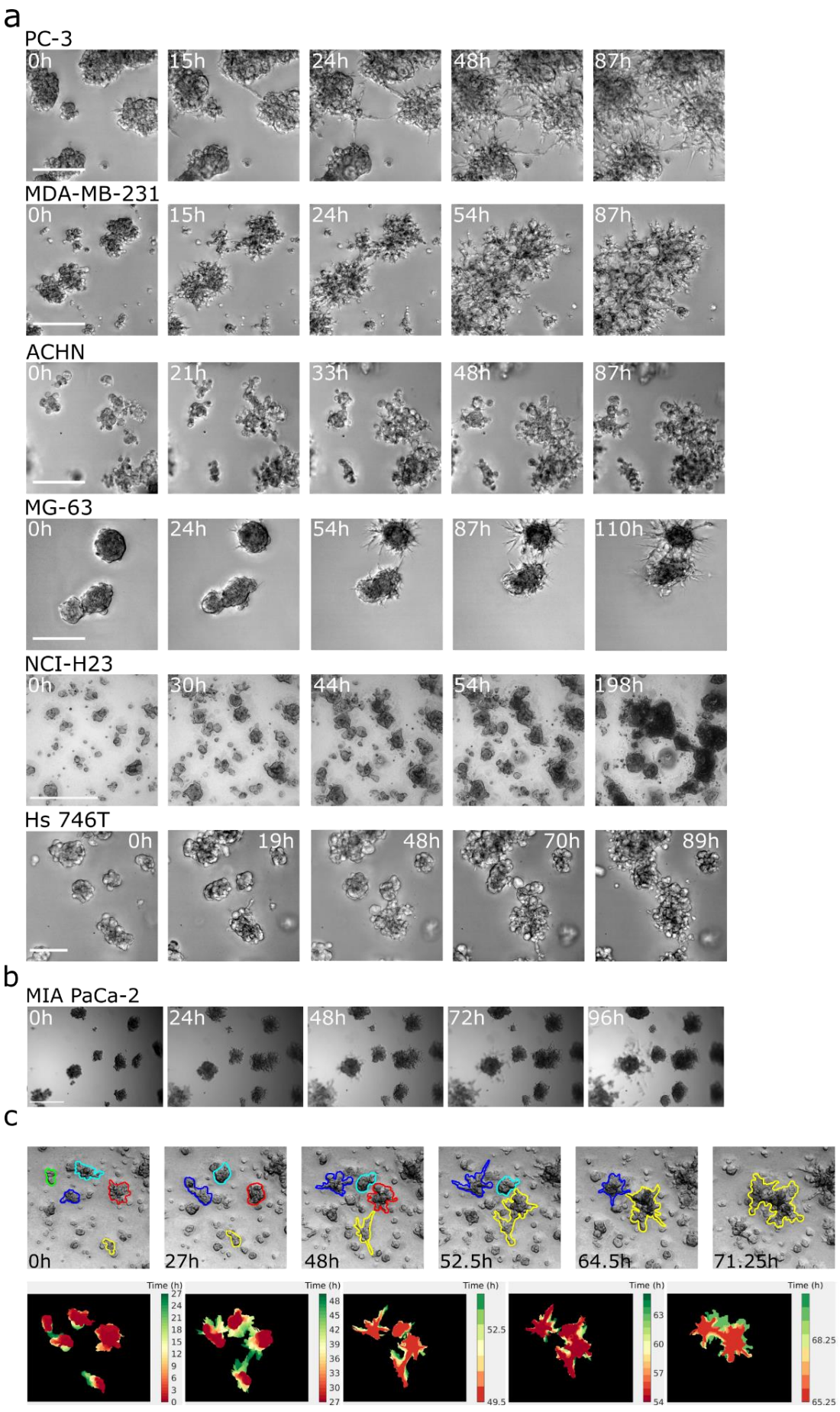
a
PC-3
0h
15h
24h
48h
87h
MDA-MB-231
0h
15h
24h
54h
87h
ACHN
0h
21h
33h
48h
87h
MG-63
0h
24h
54h
87h
110h
NCI-H23
0h
30h
44h
54h
198h
Hs 746T
0h
19h
48h
70h
89h
b
MIA PaCa-2
0h
24h
48h
72h
96h
c
0h
27h
48h
52.5h
64.5h
71.25h
Time (h)
27
24
21
18
15
12
9
6
3
0
Time (h)
48
45
42
39
36
33
30
27
Time (h)
52.5
49.5
Time (h)
63
60
57
54
Time (h)
68.25
65.25

Figure 19 Pre-formed cell spheroids perform CDA

(a) Each row shows representative snapshots of a time-lapse experiment with an aggregation assay performed starting from pre-aggregate spheroids (the same six cell lines showed in Fig. 14a are shown). Seeding density: 2,5 spheroids/mm^3. Scale bar: 500 µm. **(b)** The pre-formed spheroids aggregation assay performed with the MIA PaCa-2 cell line (among the non-aggregating cells). A single merging event is observed when two spheroids come into contact due to growth. Seeding density: 2,5 spheroids/mm^3. Scale bar: 500 µm. **(c)** Top: representative snapshots of an aggregation assay with pre-formed spheroids where 5 clusters were manually segmented and tracked over the course of the assay. Each colour defines the outline of an object, and one of the two colours of two merging objects is retained in an aggregation event. Bottom: the outlines of the spheroids (sampled every 3 hours) as in the top row were superposed with a time dependent colour code (red: earliest time-point; green: latest time-point) in order to highlight the protrusions mediating the aggregation event. Each panel ends when two spheroids merge.

The molecular perturbation of cytoskeletal components impairs the aggregation process

To corroborate the observations on the important role of subcellular and multicellular protrusions reported and discussed in the previous sections, we performed higher resolution microscopy experiments with more specific molecular markers. To this aim we stably expressed LifeAct-GFP or LifeAct-Ruby in a subset of cell lines, and observed single aggregation events. Under these experimental conditions, the actin content of both single and multiple cells outgrowths was well visible in the form of actin filaments.

Cells expressing either LifeAct-GFP or LifeAct-Ruby were seeded as pre-formed spheroids in Matrigel and imaged by means of fluorescence microscopy for several days in order to distinguish the separate contributions of each cluster. Representative snapshots reported in figure 20a show that the aggregation between two neighbouring, initially separated, objects is accompanied by the reciprocal emission of actin-rich protrusions oriented along the longitudinal axis of the two spheroids.

Confocal microscopy time-lapse experiments (Fig. 20b) allowed us to investigate in detail the morphological characteristics and the dynamics of the protrusions. We observed that spheroids of cell lines able to perform CDA, emit actin-rich, long protrusions, which are already visible only a few hours after seeding. Small subcellular protrusions are emitted all around the spheroids (green triangles in Fig. 20b), while longer, several cells-wide, outgrowths develop in the direction of the

neighbouring spheroid (white triangles in Fig. 20b) and allow the two different objects to enter in contact and to subsequently merge.

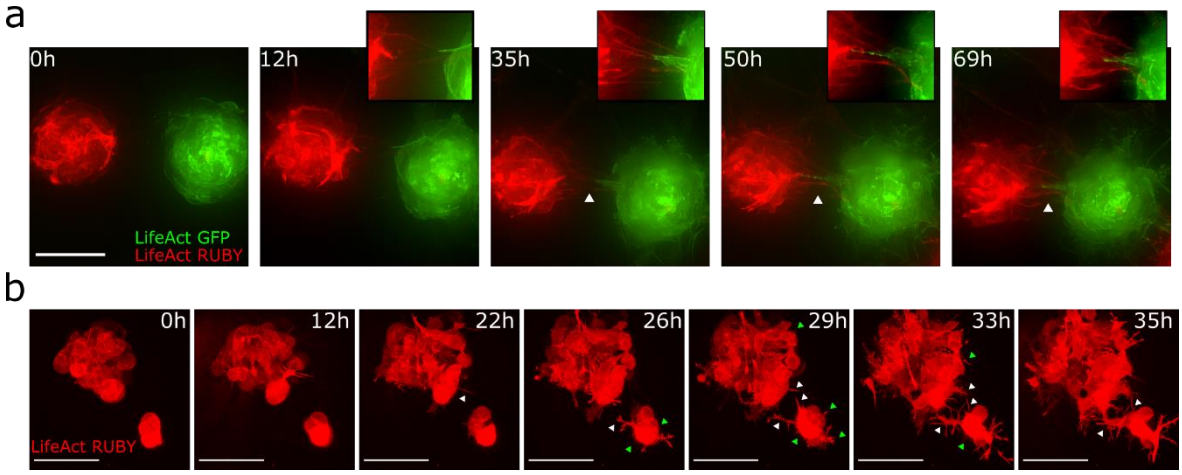

Figure 20 The role of protrusions in CDA

(a) Representative images showing pre-formed spheroids of MG-63 cells transduced with LifeAct-GFP (green) or LifeAct-Ruby (red) expressing lentiviral vectors, embedded in Matrigel. White triangles indicate protrusions between the two spheroids. The region of the images corresponding to protrusions was enlarged and shown in the top-right inserts. Scale bar: 100 µm. **(b)** Representative images of pre-formed spheroids of LifeAct-Ruby expressing MDA-MB-231 embedded in Matrigel. White triangles point at protrusions directed toward the neighbouring object. Green triangles point at smaller protrusions which develop all around the spheroids. Scale bar: 100 µm.

To further confirm the importance of protrusions for directional migration to occur, and to investigate the role of the cytoskeletal machinery in the aggregation process, we tested whether we could perturb CDA by inhibiting crucial cytoskeletal components.

To demonstrate that actin polymerization is required in CDA, we used four inhibitors with different mechanisms of action: Latrunculin A and Cytochalasin D as actin polymerization inhibitors; CK-666 as an actin assembly/branching and Wiskostatin as a WASP inhibitor, perturbing actin polymerization. Likewise, to test the role of myosin II, we used Blebbistatin which is an inhibitor of myosin-II ATPase activity and the ROCK inhibitor Y-27632, which prevents the phosphorylation of myosin II light chain (MLC) mediated by ROCK, a major downstream effector of the small GTPase RhoA.

To perform the experiments, a selected set of cell lines were tested in pre-formed spheroids assays. This choice was necessary to reduce the duration of the assay and

to minimize the effects of the drugs on other important cellular processes. The images of the treated spheroids are reported in figure 21a and show that in all the selected cell lines, both actin and myosin perturbation lead to the impairment of CDA.

In order to appreciate the effect of all these treatments we quantified both the emission of protrusions (Fig. 21b) and the presence of movement (Fig. 21c) by implementing image analysis algorithms based on digital segmentation and tracking.

The effects of actin perturbation on CDA can be appreciated from the representative snapshots of time-lapse experiments (Fig. 21a, from the second to the fifth row of images), where all the treatments blunt the protrusive activity and the capability of the spheroids to move for all cell lines considered. This observation is substantiated by the quantification of the protrusive over bulk projected areas plotted in figure 21b and with the measurements of movement, shown in figure 21c. Notably, no aggregation events are visible following actin inhibition. Taken together these observations confirm the prominent role of actin polymerization and dynamics in the aggregation process.

While a substantial role for actin polymerization was to be expected, given the phenomenological observations, we wondered whether we could see any effect relative to myosin dependent contractility, which has been shown to be a relevant feature in many collective migration models [204-206].

Our data indicate that the inhibition of myosin contractility and, consistently, of MLC activation through the inhibition of ROCK, dramatically impacts the compactness of the spheroids, allowing single cells or at most chains of cells to come out of spheroids, leaving the position of the spheroid bulk unaltered, as shown in figure 21a (last two rows of images at the bottom). This behaviour is corroborated by the quantification of the protrusive over bulk projected area which is much higher than in the control, and with the quantification of movement, which is comparable to control if not higher (Fig. 21b,c). These results are consistent with previously reported observations on the role of myosin in collective migration and represent an interesting molecular insight on the ability of cancer cells to perform

collective versus mesenchymal migration depending on the regulation of myosin contractility.

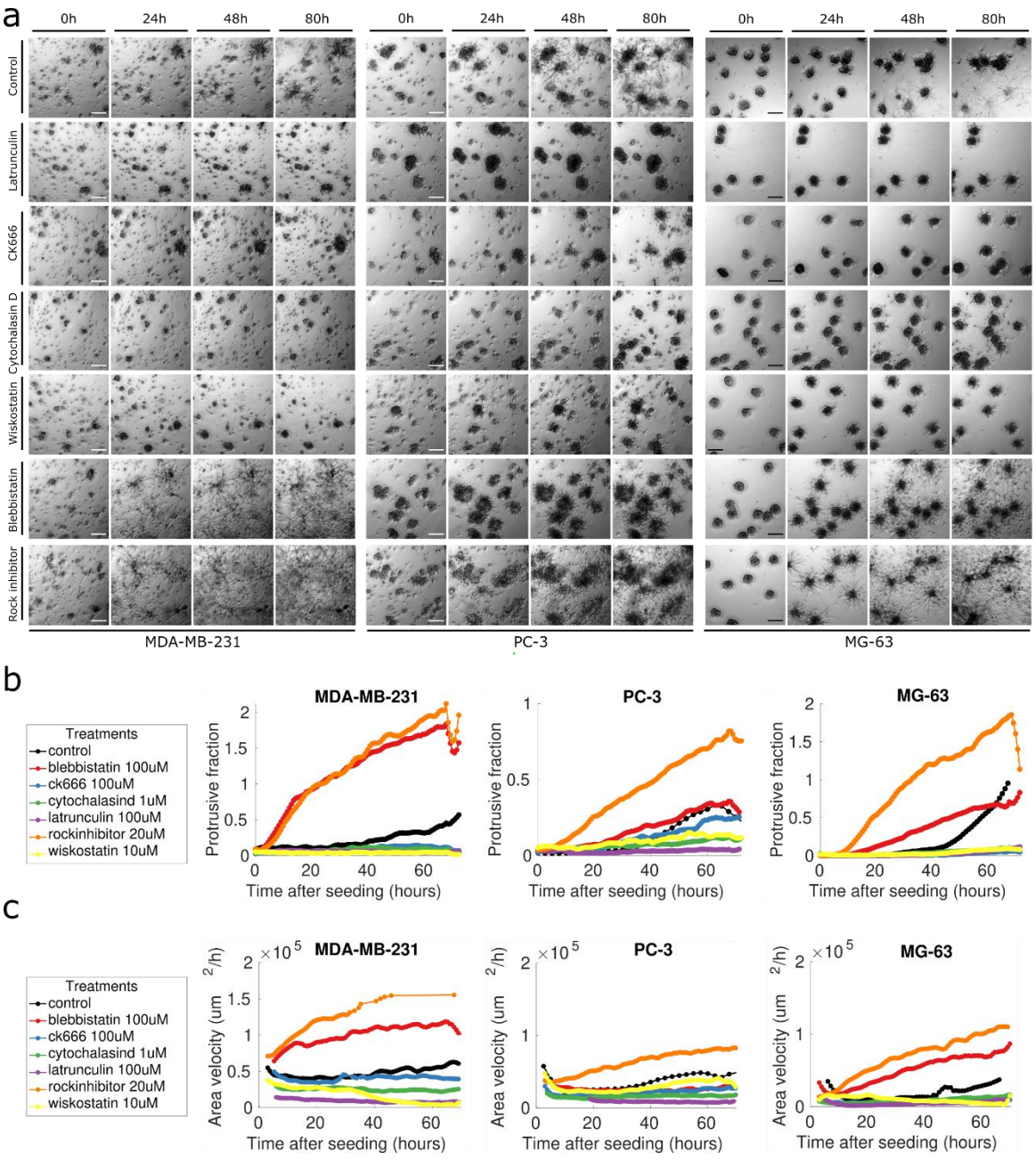

Figure 21 Perturbation of actin and myosin II dynamics impairs collective migration

(a) Pre-formed spheroids of three selected aggregating cell lines were either left untreated or treated with actin or myosin polymerisation inhibitors. (From left to right: MDA-MB-231, PC-3 and MG-63; from top to bottom: untreated, 1 µM Latrunculin A, 100 µM CK666, 1 µM Cytochalasin D, 10 µM Wiskostatin, 100 µM Blebbistatin and 20 µM Y-27632). Snapshots are extracted from time-lapse experiments at 0, 24, 48, and 80 hours after seeding. Seeding density: 2,5 spheroids/mm^3. Scale bar: 200 µm. **(b)** The images corresponding to experiments as those shown in panel (a) were segmented in order to extract the ratio of protrusion to bulk regions for each treatment, as detailed in the legend. **(c)** Area velocity extracted from images as detailed in the Material and Methods section. Each colour represents a different treatment as detailed in the legend.

CDA is perturbed by interfering with the signalling of PI3K/AKT/mTOR and MEK/ERK pathways

A fundamental question for the aggregation process and its driving molecular mechanism is whether this phenomenon is compatible with the signalling of upstream receptor-ligand dynamics or whether it is molecularly driven by purely cytoskeletal dynamics. It is indeed hard to find a unique molecular mediator common to all cell lines which evidently have profoundly different genetic alterations and behaviours. In order to address this question, we inhibited the most important signalling pathways downstream of cell surface receptor signalling, namely PI3K/AKT/mTOR and the MAPK/ERK pathways in order to check the impact of such perturbations with the aggregation phenomenon.

Due to the known involvement of such pathways in cell proliferation, in order to dissect the effect of inhibition on aggregation, we performed the experiments both starting from single cells and from preformed spheroids.

Single cell experiments (reported in Fig. 22a) showed that each inhibitor impacts both proliferation and aggregation, to different extents, as expected. The inhibition of MEK (AZD-6244, Selumetinib) has a clear effect on both aggregation and proliferation in MDA-MB-231 and MG-63 but not in PC-3, where it is essentially not effective.

The PI3K/mTOR inhibition (BEZ235, Dactolisib) causes a reduction of proliferation and aggregation in all the three cell lines, while the pure PI3K inhibition (BYL719, Alpelisib) has only a modest effect on both proliferation and aggregation in MDA-

MB-231, while it impacts more proliferation than aggregation in PC-3 and is effective on both aspects for MG-63.

Strikingly, we found the AKT inhibitor MK-2206 to have the most uniform effect on all three cell lines, acting both on aggregation and proliferation, especially at the highest concentration used.

In general, we found that none of the treatments had a clear effect on aggregation unless bound to an effect on cell proliferation, highlighting a dependence of one effect on the other. This is however consistent with the observation that aggregation is performed by multicellular aggregates, which when proliferation is blunt are much smaller. We found MG-63 to be sensitive to all treatments, while PC-3 cells tend to be less responsive to MEK inhibition and MDA-MB-231 less responsive to PI3K inhibition.

Results obtained by experiments made with pre-formed spheroids (Fig. 22b-c) helped us to visualize a clearer effect on aggregation. To provide quantitative measurements of the behaviour of spheroids following the inhibitions, we employed the same indicators used in the previous section, i.e., the ratio between the protrusive and bulk projected areas and the area velocity. MEK inhibition is effective in impairing protrusion emission and movement in MDA-MB-231 and MG-63 but completely ineffective in PC-3. Conversely, PI3K inhibition had an intermediate effect on PC-3, a strong one in MG-63 and was ineffective on MDA-MB-231. Combined inhibition of PI3K and mTOR was effective in all three cell lines (slightly less on PC-3 as observed in single cell assays). AKT inhibition was the most effective in reducing migration and protrusion emission in all three cell lines. Quantitative results are consistent with what observed in time-lapse experiments shown in figure 22c, where effective treatments blunt aggregation, while intermediate effects correspond to partial aggregation of the spheroids.

The results are therefore consistent with those obtained by single cell assays and show that both the protrusive fraction and the movement of spheroids are reduced or blunted by interfering with the signalling mediators MEK, AKT, PI3K/mTOR. Our results establish a common role for AKT in directional collective migration. The effect of the inhibition of PI3K and MAPK in PC-3 and MDA-MB-231 is instead cell

line dependent, and consistent with the respective genetic backgrounds (PTEN deletion for PC-3 and KRAS and BRAF mutations for MDA-MB-231).

Taken together, these data support the hypothesis that aggregation is mediated by upstream signalling which then reflects into cytoskeletal dynamics, even though cell line specific molecular mechanisms need further investigation. This behaviour is particularly relevant given the conspicuous differences among the three analysed cell lines, i.e., their origin, the type of tumours, their phenotype and their genetic features.

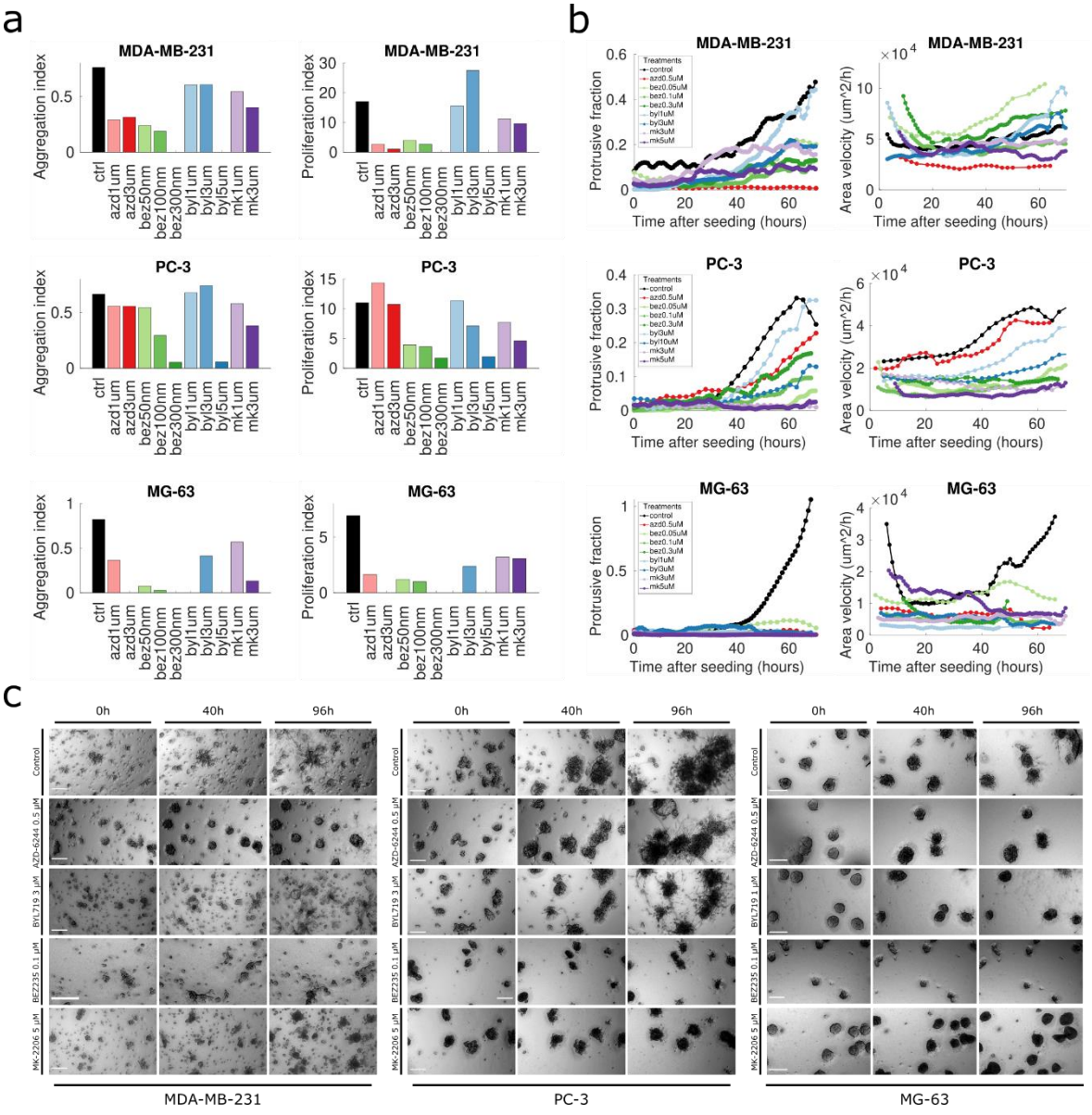

Figure 22 Inhibition of MEK, AKT, PI3K and mTOR affects CDA to different extents

(a1) An aggregation index (equivalent to the density fraction shown in Fig.17d and e) is shown for each inhibitor and each cell line to indicate the impact of each inhibitor on the aggregation process in each cell line. Aggregation assays are started from single cells. **(a2)** A proliferation index (obtained as the ratio between the total area of the spheroids in the images at 15 days and at 3 days after seeding) is shown for each inhibitor and each cell line in order to indicate the impact of each inhibitor on proliferation. Top to bottom: MDA-MB-231, PC-3 and MG-63. **(b1)** The ratio of protrusion to bulk regions in the images for each of the treatments and for the three cell lines is shown. **(b2)** Area velocity extracted from images as detailed in the Material and Methods section. Each colour represents a different treatment as detailed in the legend. **(c)** Pre-formed spheroids seeded in Matrigel were imaged for 4 days. Representative pictures at three time-points (0, 40 and 96 hours) for control and for each inhibitor are shown. Each of the three panels of images corresponds to a cell line; from left to right: MDA-MB-231, PC-3 and MG-63. Each row corresponds to one experimental condition, as reported on the left of each panel; from top to bottom: untreated, MEK inhibitor AZD-6244 0.5 μM, PI3K inhibitor BYL719 1 μM (MG-63) or 3 μM (MDA-MB-231, PC-3), PI3K-mTOR inhibitor BEZ235 0.1 μM, AKT inhibitor MK-2206 5 μM. Scale bar: 200 μm.

CDA is associated with the secretion of autocrine soluble cues in the medium

Previous results in our laboratory indicated that directional collective migration is consistent with the secretion of a soluble factor in the medium, which would stimulate the directional migration along concentration gradients, i.e., collective chemotaxis [90].

To further verify the consistency of the hypothesis of an autocrine loop mediating directional migration driving CDA, we tested the capability of all cell lines to migrate towards their own conditioned media. Conditioned media for each cell line were collected in serum-deprived 2D cultures at 24, 48 and 72 hours of culture and used in a classical chemotaxis assay (Transwell). Results show that conditioned media are all chemoattractant for cells, to different extents depending on the cell line (Fig. 23a-b).

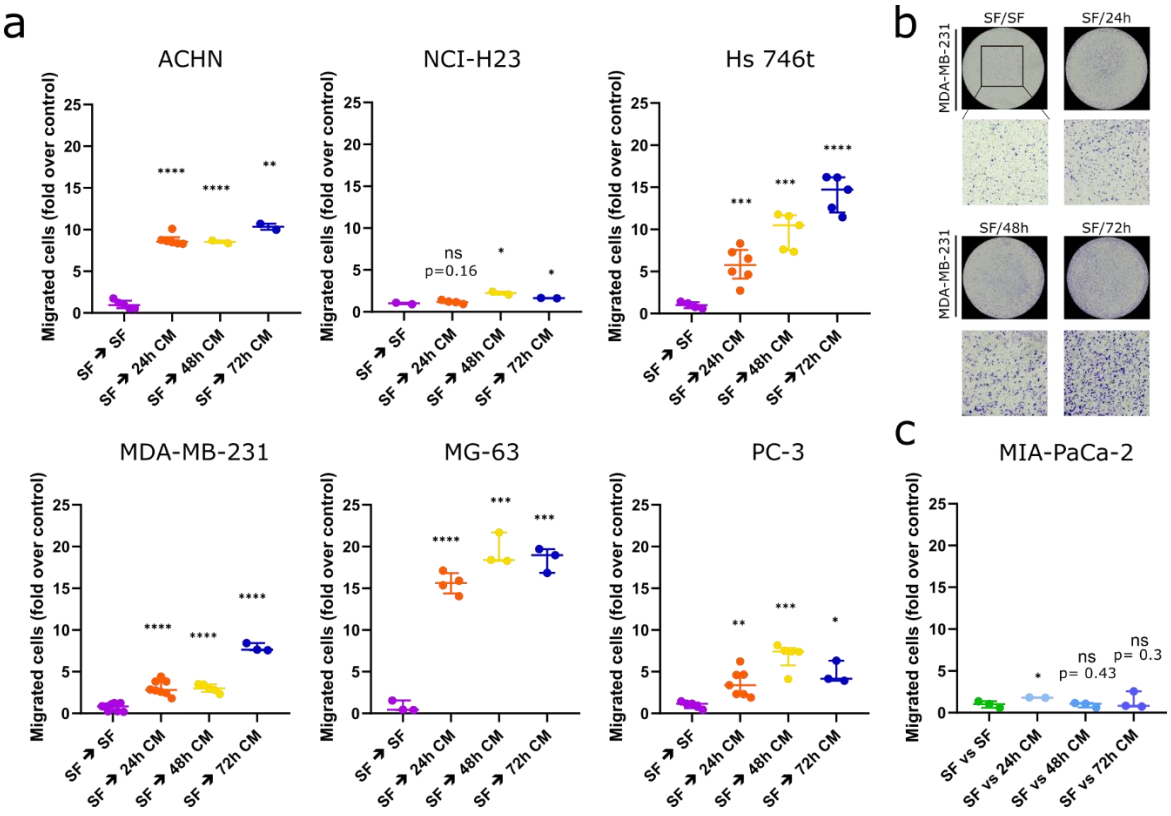

Figure 23 Conditioned media is chemoattractant for aggregating cell lines

(a) The plots report the migrated cells (fold over control) for different cell lines and conditioned media collected at different times. Each point on the plot represents data coming from a whole membrane. Migration of cells from serum free media towards serum free media (SF - SF) was used to normalize data as a control. Data are reported as median (horizontal line) with interquartile range. Statistical significance was assessed by performing a parametric one-tailed t-test with Welch's correction (unpaired); *= $P \leq 0.05$; **= $P \leq 0.01$; ***= $P \leq 0.001$; ****= $P \leq 0.0001$. **(b)** Representative images of membranes corresponding to the experimental conditions reported in the graphs are shown. **(c)** Transwell assay performed with MIA PaCa-2 cells.

We found the chemotactic effect to be higher for later collection times for the majority of the cell lines, peaking at 48 or 72 hours of culture, suggesting that cell produced soluble cues are accumulated over time with degradation rates longer than 72 hours. Notably, MIA PaCa-2 did not show significant attraction towards their own conditioned media, except for a very slight effect of the conditioned media collected at 24 hours, consistently with the fact that this cell line does not show CDA in a 3D assay (Fig. 23c).

A purely chemokinetic effect of conditioned media was excluded by performing the same experiments with the conditioned media in the upper compartment. Results are reported in figure 24a.

a

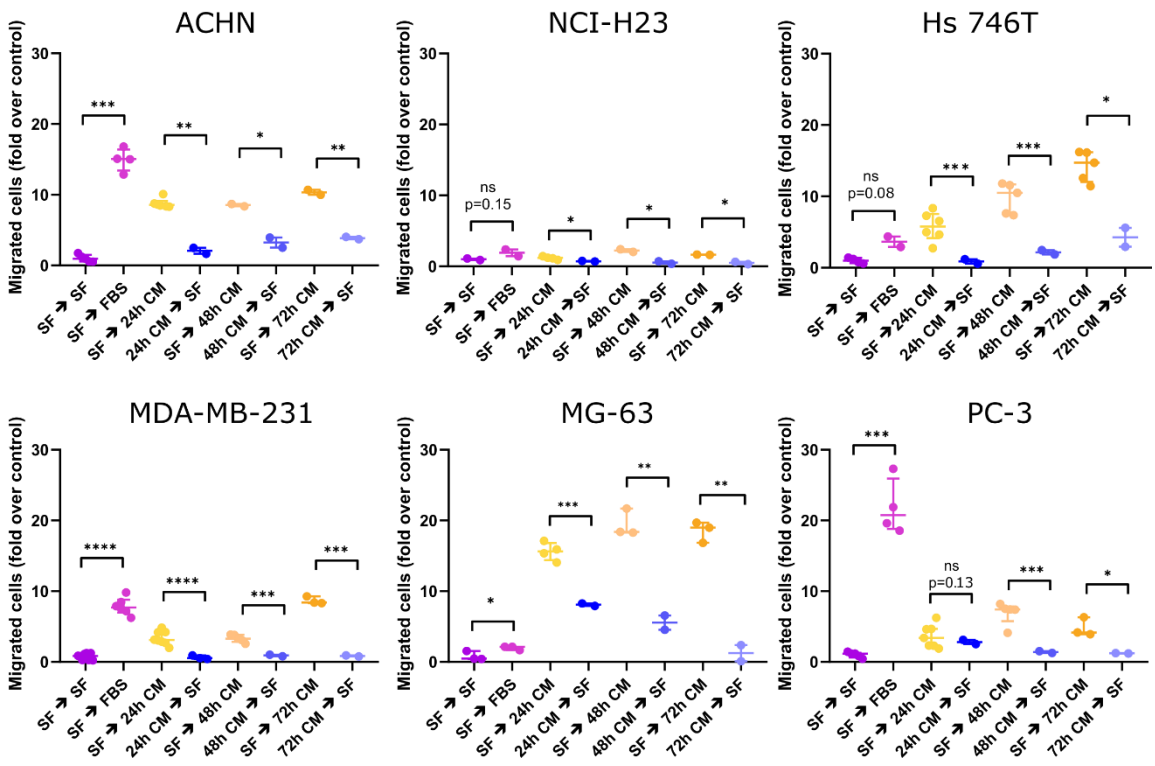

Figure 24 Transwell assay controls

(a) To verify the capability of cells to migrate, we performed a control experiment by adding 1% FBS medium in the lower compartment (violet points) and use migration toward SF medium as control. Furthermore, to exclude purely chemokinetic or proliferative effects we performed the experiments by adding the conditioned medium (24, 48 and 72 hours) in the upper compartment and the serum free medium in the lower compartment. We obtained that indeed the conditioned media has a genuine effect as its presence in the upper chamber did not induce migration as in the previous conditions, or at least not to the same extent (blu-purple points versus yellow-orange points). Statistical significance between the two conditions was assessed by performing a parametric one-tailed t-test with Welch's correction (unpaired); *= $P \leq 0.05$; Conditioned media are not able to attract cells. **= $P \leq 0.01$; ***= $P \leq 0.001$; ****= $P \leq 0.0001$.

These data indicate that all the 6 cell lines secrete chemotactic factors in the culture medium, consistently with the hypothesis that aggregation is mediated by a gradient of diffusible factors.

CDA mediates the formation of heteroclonal cell aggregates

We have shown that cells with a similar or identical genetic background, as those found in a single cell line, can be brought together by CDA. This aspect might potentially be of impact for phenotypic heterogeneity. An even more relevant question along this line is whether such a general mechanism might be able to bring

together cells with a profoundly different genetic background such as for example normal and tumour cells or even clonally distinct tumour cells.

To address this question, we performed aggregation assays with different cell lines by mixing cells expressing different fluorescent markers. Cell nuclei were labelled with fluorescent Histone2b (H2B) constructs and pre-formed spheroids with different cell lines were generated and imaged by means of time-lapse microscopy for several days. Screenshots of three representative couples of cell lines are shown in figure 25a. Our results clearly show that spheroids of different cell lines form heterotypic clusters by performing directional migration. A representative example of the aggregation of heterotypic aggregates is reported in figure 25b-c. Multi-component, i.e., heteroclonal, spheroids are able to migrate collectively and to attract other (both homo- and hetero- typic) spheroids through the emission of multiple cells outgrowths similar to those found in homotypic aggregation events.

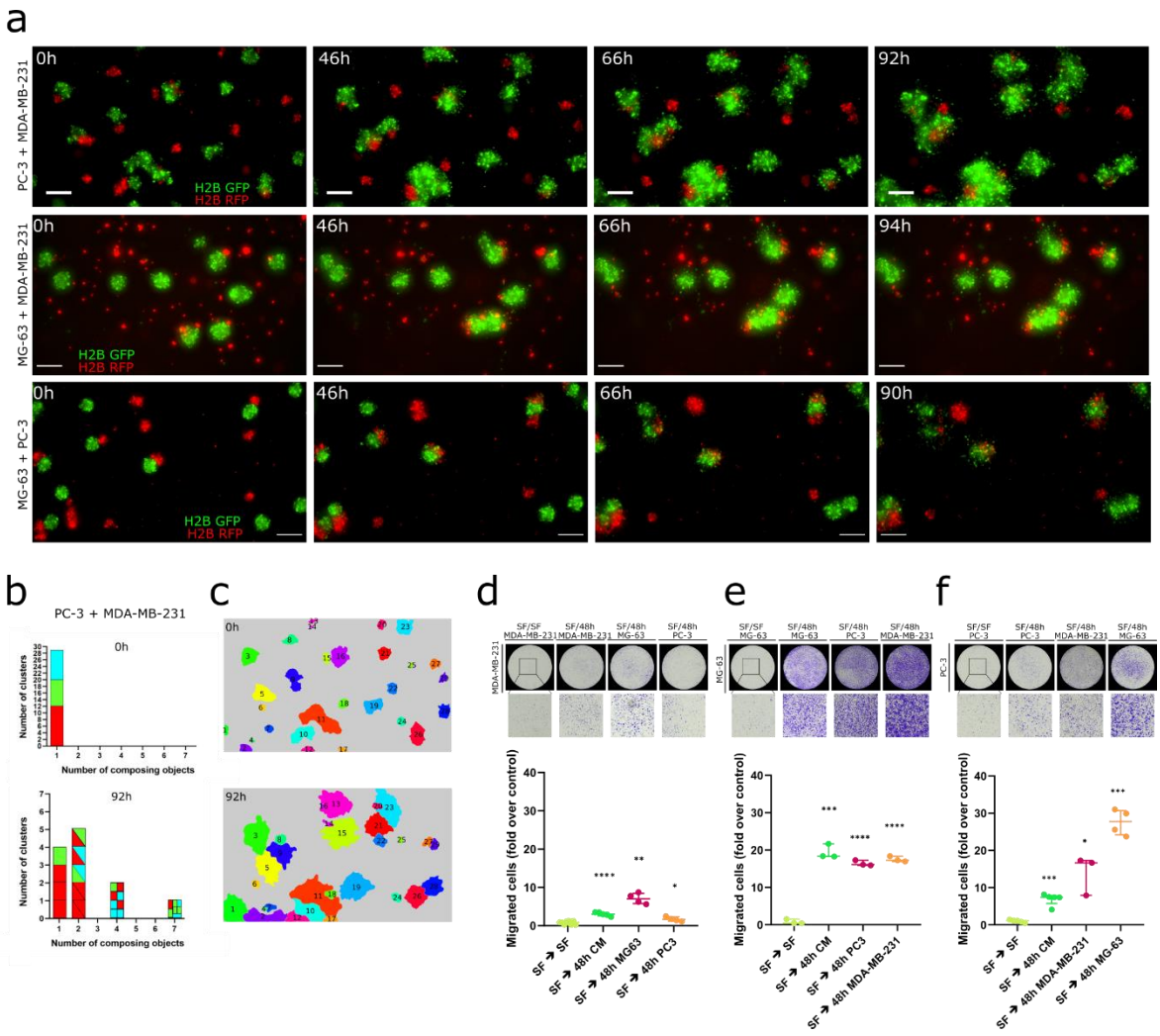

Figure 25 Heterotypic CDA is observed across different cell lines

(a) Snapshots of time-lapse experiments performed with pre-formed spheroids of cell lines couples expressing H2B-RFP (red) or H2B-GFP (green) were seeded in Matrigel. Each row represents (from the top to bottom): H2B-RFP MDA-MB-231 and H2B-GFP PC-3; H2B-RFP MDA-MB-231 and H2B-GFP MG-63; H2B-GFP MG-63 and H2B-RFP PC-3. Scale bar: 200 μm. **(b)** All the graphs and images in this panel refer to the aggregation assay between PC-3 and MDA-MB-231 (top-row images in a). The bar plots show the histogram of the number of composing aggregates of each object for the first (top, 0h) and the last (bottom, 92h) time-frame of the movie for the top row of panel (a), top row. Composing aggregates at frame 1 are conventionally considered as single objects as their aggregation happened before the assay started. **(c)** Images show the segmentation of the first and the last frames of the aggregation assay shown in panel (a), top row. Each object is identified by a numeric label and a unique colour in order to appreciate the aggregation of initially separated objects. **(d,e,f)** Chemotaxis assays (Transwell) performed with the cell line couples represented in panel (a). The plots report the migrated cells (fold over control) of different experiments. Each point on the plot represents a whole membrane. Data are reported as median (horizontal line) with interquartile range. Statistical significance was assessed by performing a parametric one-tailed t-test with Welch's correction (unpaired); *= $P \leq 0.05$; **= $P \leq 0.01$; ***= $P \leq 0.001$; ****= $P \leq 0.0001$. Representative membranes corresponding to the experimental condition reported in the plots are shown on top of each plot.

A necessary underlying condition to the observed behaviour is that conditioned media are able to act as chemoattractant also for other cell lines, notably for those that are involved in heteroclonal aggregation. To verify this hypothesis, we performed Transwell assays with aggregating cell lines and used conditioned media originating from different cell lines, as shown in figure 25 d-f for the couples of cell lines which perform heterotypic aggregation and in figure 26 a-c for all the rest. Our results indicate that the conditioned medium of each of the 6 cell lines act as chemoattractant, to different extents, for all the other cell lines. In particular, the conditioned media collected from the cell line MG-63, which is the cell line with the highest percentage of aggregating cells (as reported in Fig. 16b), is chemoattractant for all the remaining 5 cell lines and has also the greater chemotactic capability, in terms of the number of migrated cells over control, in comparison with conditioned media of other cell lines. On the contrary, the conditioned media of MIA PaCa-2, which show a non-aggregating phenotype, is not effective in all the cases (green experimental points in the graphs of Fig. 26a). Interestingly, the conditioned media collected from MDA-MB-231, MG-63 and ACHN is chemoattractant for MIA PaCa-2 (Fig. 26 b-c).

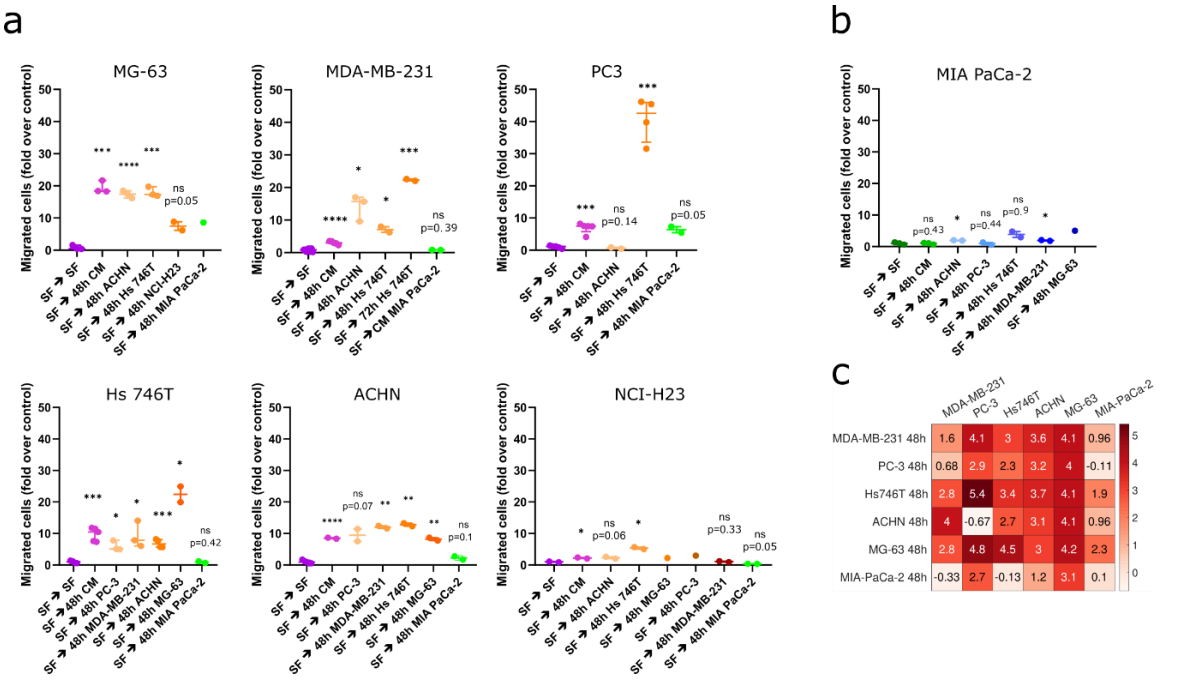

Figure 26 The conditioned medium of aggregating cell lines is chemoattractant for the others

(a,b) Transwell assays performed to test whether the conditioned medium of each of the 6 aggregating cell lines, and MIA PaCa-2 as representative example of a non-aggregating cell line, act as chemoattractant for all the other cell lines. The plots report the migrated cells (fold over control) of different experiments. Each point on the plot represents a whole membrane. Data are reported as median (horizontal line) with interquartile range. Statistical significance was assessed by performing a parametric one-tailed t-test with Welch's correction (unpaired); *= P ≤ 0.05; **= P ≤ 0.01; ***= P ≤ 0.001; ****= P ≤ 0.0001. **(c)** The matrix reports the migrated cells (fold over control) of different Transwell assay experiments performed to test whether the conditioned medium of each of the 6 aggregating cell lines act as chemoattractant for all the other cell lines. Indicated values correspond to the log2 of the median fold-change. Experiments were conducted by seeding onto the Transwell membrane cell lines listed in the column labels and by adding in the lower compartment 48h conditioned media collected from cell lines listed in the row labels.

In order to understand whether subcellular protrusions can be found in heterotypic aggregation as well, we performed time-lapse experiments at high spatio-temporal resolution with pre-formed spheroids made with two different cell lines expressing fluorescent LifeAct. As in the case of homotypic aggregation, we observed that the coalescence between two distinct, initially separate, spheroids of PC-3 and MDA-MB-231 is accompanied by the emission on protrusions, as shown in figure 27a. These data confirm the hypothesis that CDA can drive the formation of heteroclonal aggregates.

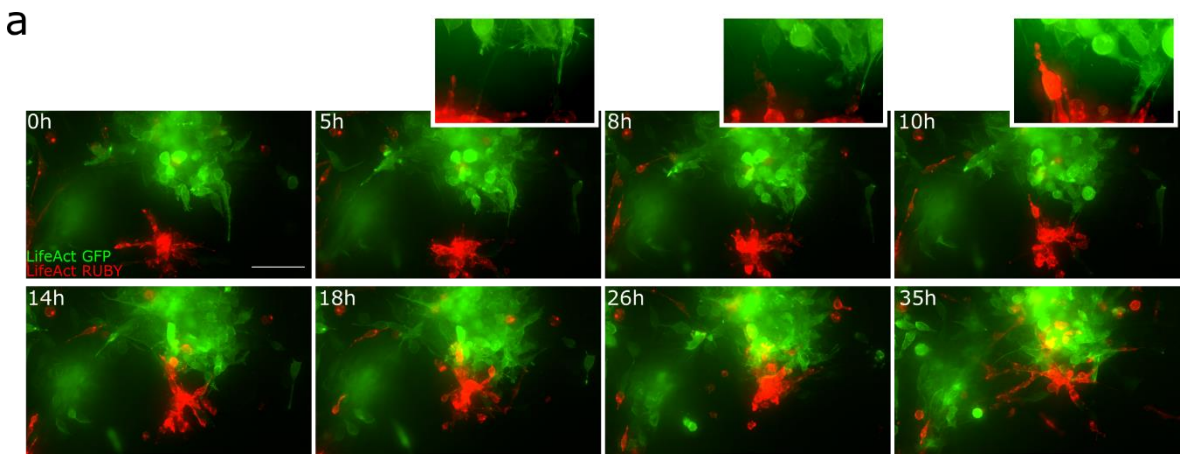

Figure 27 Heterotypic CDA occurs through the emission of protrusions

(a) Representative images of time-lapse movies showing an aggregation event between pre-formed spheroids of LifeAct-Ruby (red) MDA-MB-231 and LifeAct-GFP (green) PC-3 cells in Matrigel. The section of the images corresponding to the area between the two clusters was enlarged to facilitate the visualization of the protrusions and it is shown in the top-right inserts. Time labels indicate hours after seeding. Scale bar: 100 µm.

DISCUSSION

Our study provides a novel 3D model to investigate cancer cell collective migration dynamics and identifies such behaviour as the mechanism driving homo- and hetero-typic aggregation of cancer cell clusters.

We demonstrate that the movement of cells and clusters is directional and mediated by single and multicellular actin-rich protrusions and that molecular inhibition of cytoskeletal dynamics results in impaired CDA. Our results pinpoint a crucial role of myosin II in the retainment of cell-cell contact during cancer collective migration as observed in other biological contexts [204-206].

We hypothesize that cluster-cluster interaction at distance is mediated by soluble cues, such as for example the autocrine secretion of chemoattractants, which would in turn generate spatial gradients mediating directional migration. This hypothesis is supported by the capability of cells to migrate toward their own conditioned media and by the impairment of CDA following the inhibition of cell surface receptors downstream effectors. This result also indicates that aggregation is not purely driven by cytoskeletal dynamics but is compatible with upstream receptor-ligand signalling.

Interestingly, we observed reciprocal aggregation between cells originally derived from different tissues, identifying CDA as a potential mechanism at the basis of the formation of heterogeneous tumours.

The role of chemotaxis in cancer dissemination is documented [145], but mostly involving paracrine mechanisms, e.g., between tumour cells and normal cells [15, 24, 28, 60, 176, 207]. Nevertheless, autocrine loops are widespread across cancer cells [208-214] and chemokines and chemokine receptors are often overexpressed in both metastatic and primary tumour cells, but not in the corresponding normal counterpart [215]. We speculate that expression of such receptors or ligands might determine a higher fitness of cancer cells in comparison to other cellular populations within the primary tumour site, thanks to ligands acting both as chemotactic factors and as mitogens. This would also imply a role for CDA as a self-sustaining mechanism by which cancer cells could augment their survival rate.

It has indeed been proposed that greater metastatic capability of CTC clusters is due to proliferative signals that cells send to each other to improve their survival rates [56]. In light of our findings, we can suppose that such proliferative signals might coincide with (or be associated to) chemotactic signals, conferring a double advantage to CTC clusters. Remarkably, the 6 cell lines which we reported to perform CDA derive both from metastatic sites and from primary tumour sites, suggesting that the capability to migrate in response to chemical cues might in principle be relevant in the primary tumour site, in the dissemination and possibly in the metastasis formation.

The observation that cells originating from spatially distant heterogeneous clones can merge by collective directional migration might be relevant in the context of tumour dissemination as well, as cells expressing even only a receptor for a ligand autocrinely secreted by a separate group of tumour cells, might be attracted during their route from the primary site to distant organs, as already reported for interaction between tumour and normal cells. Such a mechanism might provide a possible explanation of the early acquisition of clonal heterogeneity within the tumour, which represents a big obstacle in the development of effective pharmacological treatments [216].

Our findings are among the few to describe directional migration in collective migration [88, 90, 92, 98]. As already pointed out by previous works, collective chemotaxis might have important differences to single cell chemotaxis in terms of sensing. The detailed mechanisms of transmission of the information on orientation across cells in a multicellular aggregate might rely on purely mechanical signalling among the cells or on chemical intercellular signalling. While these aspects are almost entirely to be elucidated, the dependence of CDA on concentrations and on concentration gradients might be completely different than for single cells, and might result in different dynamical behaviours.

While it has to be expected that the molecular mediators of such phenomenon are not unique, we acknowledge that more detailed molecular studies are required to further investigate the role of such a phenomenon *in vivo* as well as to better understand the role of other concurrent mechanisms such as mechanical forces and

proteolytic activity of tumour cells. Further investigations might help elucidate if and when CDA is relevant during cancer progression and whether there are any significant correlated effects on prognosis.

Notably, the results obtained by inhibiting the signalling pathway effectors might indicate somewhat common mechanisms across cell lines and therefore among different tumours, which, considering the extreme diversity between the analysed cell lines, is an interesting unexpected finding and point at CDA as a rather universal mechanism rather than as a specific aspect of a single cell line or a single molecular mediator.

Our study describes CDA as a novel widespread phenotype and paves the way to further investigation about the biology of such phenomenon and the potential advantage that CDA might have in tumour progression.

ADDITIONAL RESULTS AND FUTURE PERSPECTIVES

A broad effort has been done to identify the molecular mechanisms underlying CDA, but none of the attempts was conclusive or lead to an impairment or a perturbation of CDA. The most important setback in our research was the lack of a strong rationale in the search for a specific ligand/receptor couple responsible for CDA.

First we focused our pursuit on the PC-3 cell line, which was the one for which the CDA phenotype had been best characterised. To overcome the lack of obvious suitable candidates, we exploited the secretome profile of PC-3 published by Sardana et al. [217] and selected secreted ligands whose receptors were expressed as possible candidates [218]. The following ligand/receptor couples were identified and molecularly inhibited (when an inhibitor was available): TGFα/EGFR, EGF/EGFR, SLIT/ROBO, TGF-β/TGFBR, AXL/GAS6.

Particularly worthy of consideration was the couple AXL/GAS6, because of a peculiar behaviour we observed for the MDA-MB-231 cell line, that is herein explained. We noticed that such cell line showed the CDA phenotype when M199 culture medium was used to carry out the experiments, while a prominent reduction of signs of CDA was detected in presence of DMEM or other standard culture media. Among the many differences in the composition of the culture media, the presence only in M199 of menadione bisulfite (a vitamin K precursor), which is necessary for the activation of GAS6, was particularly interesting. Following this line of thought, we tried to block the activity of both AXL and GAS6 by means of pharmacological inhibition and gene silencing. Both the strategies failed to perturb CDA. Moreover, we tried to supplement plain culture media with vitamin K and to block the effect of menadione in M199 by adding warfarin to the medium, but no clear effects on CDA behaviour were disclosed.

We are currently endeavouring to identify the molecular mediators of such a different behaviour by performing an RNA-sequencing experiment to compare the transcriptomic analysis of MDA-MB-231 in 2D versus 3D conditions, in order to rule

out the genes purely associated with the 3D setting, and in DMEM versus M199. Hopefully, but not necessarily, this analysis will bring out molecular candidates which could underlie CDA also in the other aggregating cell lines presented in this work.

Further attempts were made by inhibiting ligand/receptor couples well known in literature for being involved in chemotaxis-driven biological processes, such as CXCR4/CXCL12, repeatedly mentioned through the introduction section and HGF/MET, which are long known for their importance in cancer. Particularly compelling at this regard was the notion that HGF is responsible for the tubulogenesis and the branching of epithelial cells, which brought out the hypothesis of an involvement of such a molecule in CDA. Indeed, even though a wide literature exists about the role of HGF as "scatter factor" [219-221], neither the directionality of the cellular extensions nor the spatio-temporal dynamics of such a process are fully investigated.

In light of these observations, we followed two parallel strategies.

First, we inhibited the aforementioned molecules in a subset of aggregating cell lines, obtaining again no clear effects on CDA.

Second, we built a synthetic model of CDA to verify whether the expression of a ligand in cell lines which express the cognate receptor and which are able to grow and move in a 3D matrix, was sufficient to promote CDA. This approach would also be a proof of concept of our hypothesis on the driving mechanisms of CDA. To this aim, we developed inducible constructs to express the ligand; experiments involving the use of this tool are currently ongoing and will hopefully explore the spatio-temporal dynamics of the gradient sensing, since it will be possible to modulate the amount of the secreted ligand.

Future work shall address the identification of the molecular mediators of CDA, to open the possibility of further investigation about the dynamics of gradient sensing, both to enrich the basic knowledge we have about the collective chemotaxis so far, and to understand whether this phenotype is relevant in the context of cancer.

BIBLIOGRAPHY

1. Mukherjee, S., *The emperor of all maladies : a biography of cancer*. 2011, London: Fourth Estate.
2. Seiler, R., et al., *The earliest known case of frontal sinus osteoma in man.* Clin Anat, 2019. **32**(1): p. 105-109.
3. Chaffer, C.L. and R.A. Weinberg, *A perspective on cancer cell metastasis.* Science, 2011. **331**(6024): p. 1559-64.
4. Fidler, I.J., *The pathogenesis of cancer metastasis: the 'seed and soil' hypothesis revisited.* Nat Rev Cancer, 2003. **3**(6): p. 453-8.
5. Valastyan, S. and R.A. Weinberg, *Tumor metastasis: molecular insights and evolving paradigms.* Cell, 2011. **147**(2): p. 275-92.
6. Talmadge, J.E. and I.J. Fidler, *AACR centennial series: the biology of cancer metastasis: historical perspective.* Cancer Res, 2010. **70**(14): p. 5649-69.
7. Weinberg, R.A., *The biology of cancer*. 2007, New York ; London: Garland Science.
8. Esserman, L.J. and M. Varma, *Should we rename low risk cancers?* BMJ, 2019. **364**: p. k4699.
9. Guan, X., *Cancer metastases: challenges and opportunities.* Acta Pharm Sin B, 2015. **5**(5): p. 402-18.
10. Kessenbrock, K., V. Plaks, and Z. Werb, *Matrix metalloproteinases: regulators of the tumor microenvironment.* Cell, 2010. **141**(1): p. 52-67.
11. Grivennikov, S.I., F.R. Greten, and M. Karin, *Immunity, inflammation, and cancer.* Cell, 2010. **140**(6): p. 883-99.
12. Dirat, B., et al., *Cancer-associated adipocytes exhibit an activated phenotype and contribute to breast cancer invasion.* Cancer Res, 2011. **71**(7): p. 2455-65.
13. DeNardo, D.G., et al., *CD4(+) T cells regulate pulmonary metastasis of mammary carcinomas by enhancing protumor properties of macrophages.* Cancer Cell, 2009. **16**(2): p. 91-102.
14. THOMLINSON, R.H. and L.H. GRAY, *The histological structure of some human lung cancers and the possible implications for radiotherapy.* Br J Cancer, 1955. **9**(4): p. 539-49.
15. Dong, J., et al., *VEGF-null cells require PDGFR alpha signaling-mediated stromal fibroblast recruitment for tumorigenesis.* EMBO J, 2004. **23**(14): p. 2800-10.
16. Hirakawa, S., et al., *VEGF-A induces tumor and sentinel lymph node lymphangiogenesis and promotes lymphatic metastasis.* J Exp Med, 2005. **201**(7): p. 1089-99.
17. Pezzella, F., et al., *Non-small-cell lung carcinoma tumor growth without morphological evidence of neo-angiogenesis.* Am J Pathol, 1997. **151**(5): p. 1417-23.
18. Kuczynski, E.A., et al., *Vessel co-option in cancer.* Nat Rev Clin Oncol, 2019. **16**(8): p. 469-493.
19. Maniotis, A.J., et al., *Vascular channel formation by human melanoma cells in vivo and in vitro: vasculogenic mimicry.* Am J Pathol, 1999. **155**(3): p. 739-52.
20. Bockhorn, M., R.K. Jain, and L.L. Munn, *Active versus passive mechanisms in metastasis: do cancer cells crawl into vessels, or are they pushed?* Lancet Oncol, 2007. **8**(5): p. 444-8.
21. Chiang, S.P., R.M. Cabrera, and J.E. Segall, *Tumor cell intravasation.* Am J Physiol Cell Physiol, 2016. **311**(1): p. C1-C14.
22. Carmeliet, P. and R.K. Jain, *Principles and mechanisms of vessel normalization for cancer and other angiogenic diseases.* Nat Rev Drug Discov, 2011. **10**(6): p. 417-27.
23. Aragon-Sanabria, V., et al., *VE-Cadherin Disassembly and Cell Contractility in the Endothelium are Necessary for Barrier Disruption Induced by Tumor Cells.* Sci Rep, 2017. **7**: p. 45835.
24. Konstantopoulos, K. and S.N. Thomas, *Cancer cells in transit: the vascular interactions of tumor cells.* Annu Rev Biomed Eng, 2009. **11**: p. 177-202.

25. Dua, R.S., G.P. Gui, and C.M. Isacke, *Endothelial adhesion molecules in breast cancer invasion into the vascular and lymphatic systems.* Eur J Surg Oncol, 2005. **31**(8): p. 824-32.
26. Pantel, K. and M.R. Speicher, *The biology of circulating tumor cells.* Oncogene, 2016. **35**(10): p. 1216-24.
27. Nierodzik, M.L. and S. Karpatkin, *Thrombin induces tumor growth, metastasis, and angiogenesis: Evidence for a thrombin-regulated dormant tumor phenotype.* Cancer Cell, 2006. **10**(5): p. 355-62.
28. Sarvaiya, P.J., et al., *Chemokines in tumor progression and metastasis.* Oncotarget, 2013. **4**(12): p. 2171-85.
29. Huang, E.H., et al., *A CXCR4 antagonist CTCE-9908 inhibits primary tumor growth and metastasis of breast cancer.* J Surg Res, 2009. **155**(2): p. 231-6.
30. Luzzi, K.J., et al., *Multistep nature of metastatic inefficiency: dormancy of solitary cells after successful extravasation and limited survival of early micrometastases.* Am J Pathol, 1998. **153**(3): p. 865-73.
31. Massagué, J. and A.C. Obenauf, *Metastatic colonization by circulating tumour cells.* Nature, 2016. **529**(7586): p. 298-306.
32. Lambert, A.W., D.R. Pattabiraman, and R.A. Weinberg, *Emerging Biological Principles of Metastasis.* Cell, 2017. **168**(4): p. 670-691.
33. van Grunsven, L.A., et al., *XSIP1, a Xenopus zinc finger/homeodomain encoding gene highly expressed during early neural development.* Mech Dev, 2000. **94**(1-2): p. 189-93.
34. Arnoux, V., et al., *Erk5 controls Slug expression and keratinocyte activation during wound healing.* Mol Biol Cell, 2008. **19**(11): p. 4738-49.
35. Iwano, M., et al., *Evidence that fibroblasts derive from epithelium during tissue fibrosis.* J Clin Invest, 2002. **110**(3): p. 341-50.
36. Zhang, Y. and R.A. Weinberg, *Epithelial-to-mesenchymal transition in cancer: complexity and opportunities.* Front Med, 2018. **12**(4): p. 361-373.
37. Greenburg, G. and E.D. Hay, *Epithelia suspended in collagen gels can lose polarity and express characteristics of migrating mesenchymal cells.* J Cell Biol, 1982. **95**(1): p. 333-9.
38. Boyer, B., et al., *Rearrangements of desmosomal and cytoskeletal proteins during the transition from epithelial to fibroblastoid organization in cultured rat bladder carcinoma cells.* J Cell Biol, 1989. **109**(4 Pt 1): p. 1495-509.
39. Cheung, K.J., et al., *Collective invasion in breast cancer requires a conserved basal epithelial program.* Cell, 2013. **155**(7): p. 1639-51.
40. Cheung, K.J., et al., *Polyclonal breast cancer metastases arise from collective dissemination of keratin 14-expressing tumor cell clusters.* Proc Natl Acad Sci U S A, 2016. **113**(7): p. E854-63.
41. Cheung, K.J. and A.J. Ewald, *A collective route to metastasis: Seeding by tumor cell clusters.* Science, 2016. **352**(6282): p. 167-9.
42. De Craene, B. and G. Berx, *Regulatory networks defining EMT during cancer initiation and progression.* Nat Rev Cancer, 2013. **13**(2): p. 97-110.
43. Lamouille, S., J. Xu, and R. Derynck, *Molecular mechanisms of epithelial-mesenchymal transition.* Nat Rev Mol Cell Biol, 2014. **15**(3): p. 178-96.
44. Brabletz, T., et al., *Variable beta-catenin expression in colorectal cancers indicates tumor progression driven by the tumor environment.* Proc Natl Acad Sci U S A, 2001. **98**(18): p. 10356-61.
45. Kalluri, R. and R.A. Weinberg, *The basics of epithelial-mesenchymal transition.* J Clin Invest, 2009. **119**(6): p. 1420-8.
46. Kapoor, C., et al., *Seesaw of matrix metalloproteinases (MMPs).* J Cancer Res Ther, 2016. **12**(1): p. 28-35.
47. Virchow, R., *Vorlesungen uber pathologie*. 4th ed. ed. 1871, Berlin: August Hirschwald.
48. Paget, S., *The distribution of secondary growths in cancer of the breast. 1889.* Cancer Metastasis Rev, 1989. **8**(2): p. 98-101.

49. Aceto, N., et al., *Circulating tumor cell clusters are oligoclonal precursors of breast cancer metastasis.* Cell, 2014. **158**(5): p. 1110-22.
50. Pantel, K. and C. Alix-Panabières, *Liquid biopsy and minimal residual disease - latest advances and implications for cure.* Nat Rev Clin Oncol, 2019. **16**(7): p. 409-424.
51. Hou, J.M., et al., *Clinical significance and molecular characteristics of circulating tumor cells and circulating tumor microemboli in patients with small-cell lung cancer.* J Clin Oncol, 2012. **30**(5): p. 525-32.
52. Maddipati, R. and B.Z. Stanger, *Pancreatic Cancer Metastases Harbor Evidence of Polyclonality.* Cancer Discov, 2015. **5**(10): p. 1086-97.
53. Weissenberger, J., et al., *Development and malignant progression of astrocytomas in GFAP-v-src transgenic mice.* Oncogene, 1997. **14**(17): p. 2005-13.
54. Giuliano, M., et al., *Perspective on Circulating Tumor Cell Clusters: Why It Takes a Village to Metastasize.* Cancer Res, 2018. **78**(4): p. 845-852.
55. Al Habyan, S., et al., *Multicellular detachment generates metastatic spheroids during intra-abdominal dissemination in epithelial ovarian cancer.* Oncogene, 2018. **37**(37): p. 5127-5135.
56. Aceto, N., *Bring along your friends: Homotypic and heterotypic circulating tumor cell clustering to accelerate metastasis.* Biomed J, 2020. **43**(1): p. 18-23.
57. Tabassum, D.P. and K. Polyak, *Tumorigenesis: it takes a village.* Nat Rev Cancer, 2015. **15**(8): p. 473-83.
58. Fanelli, M.F., et al., *Evaluation of incidence, significance, and prognostic role of circulating tumor microemboli and transforming growth factor-β receptor I in head and neck cancer.* Head Neck, 2017. **39**(11): p. 2283-2292.
59. Liotta, L.A., M.G. Saidel, and J. Kleinerman, *The significance of hematogenous tumor cell clumps in the metastatic process.* Cancer Res, 1976. **36**(3): p. 889-94.
60. Sprouse, M.L., et al., *PMN-MDSCs Enhance CTC Metastatic Properties through Reciprocal Interactions via ROS/Notch/Nodal Signaling.* Int J Mol Sci, 2019. **20**(8).
61. Szczerba, B.M., et al., *Neutrophils escort circulating tumour cells to enable cell cycle progression.* Nature, 2019. **566**(7745): p. 553-557.
62. Duda, D.G., et al., *Malignant cells facilitate lung metastasis by bringing their own soil.* Proc Natl Acad Sci U S A, 2010. **107**(50): p. 21677-82.
63. Upreti, M., et al., *Tumor-Endothelial Cell Three-dimensional Spheroids: New Aspects to Enhance Radiation and Drug Therapeutics.* Transl Oncol, 2011. **4**(6): p. 365-76.
64. Friedl, P., et al., *Migration of coordinated cell clusters in mesenchymal and epithelial cancer explants in vitro.* Cancer Res, 1995. **55**(20): p. 4557-60.
65. Bronsert, P., et al., *Cancer cell invasion and EMT marker expression: a three-dimensional study of the human cancer-host interface.* J Pathol, 2014. **234**(3): p. 410-22.
66. Hegerfeldt, Y., et al., *Collective cell movement in primary melanoma explants: plasticity of cell-cell interaction, beta1-integrin function, and migration strategies.* Cancer Res, 2002. **62**(7): p. 2125-30.
67. Nabeshima, K., et al., *Cohort migration of carcinoma cells: differentiated colorectal carcinoma cells move as coherent cell clusters or sheets.* Histol Histopathol, 1999. **14**(4): p. 1183-97.
68. Nguyen-Ngoc, K.V., et al., *ECM microenvironment regulates collective migration and local dissemination in normal and malignant mammary epithelium.* Proc Natl Acad Sci U S A, 2012. **109**(39): p. E2595-604.
69. Trimboli, A.J., et al., *Direct evidence for epithelial-mesenchymal transitions in breast cancer.* Cancer Res, 2008. **68**(3): p. 937-45.
70. Guy, C.T., R.D. Cardiff, and W.J. Muller, *Induction of mammary tumors by expression of polyomavirus middle T oncogene: a transgenic mouse model for metastatic disease.* Mol Cell Biol, 1992. **12**(3): p. 954-61.

71. Revenu, C. and D. Gilmour, *EMT 2.0: shaping epithelia through collective migration.* Curr Opin Genet Dev, 2009. **19**(4): p. 338-42.
72. Ye, X., et al., *Distinct EMT programs control normal mammary stem cells and tumour-initiating cells.* Nature, 2015. **525**(7568): p. 256-60.
73. Zheng, X., et al., *Epithelial-to-mesenchymal transition is dispensable for metastasis but induces chemoresistance in pancreatic cancer.* Nature, 2015. **527**(7579): p. 525-530.
74. Fischer, K.R., et al., *EMT is not required for lung metastasis but contributes to chemoresistance.* Nature, 2015. **527**(7579): p. 472-476.
75. Ledford, H., *Cancer theory faces doubts.* Nature, 2011. **472**(7343): p. 273.
76. Friedl, P. and K. Wolf, *Plasticity of cell migration: a multiscale tuning model.* J Cell Biol, 2010. **188**(1): p. 11-9.
77. Weijer, C.J., *Dictyostelium morphogenesis.* Curr Opin Genet Dev, 2004. **14**(4): p. 392-8.
78. David, N.B., et al., *Molecular basis of cell migration in the fish lateral line: role of the chemokine receptor CXCR4 and of its ligand, SDF1.* Proc Natl Acad Sci U S A, 2002. **99**(25): p. 16297-302.
79. Montell, D.J., *Border-cell migration: the race is on.* Nat Rev Mol Cell Biol, 2003. **4**(1): p. 13-24.
80. F., B.M.J. and G.S. F., *Developmental Biology*. 12th ed. 2019: Sinauer Associates.
81. Poujade, M., et al., *Collective migration of an epithelial monolayer in response to a model wound.* Proc Natl Acad Sci U S A, 2007. **104**(41): p. 15988-93.
82. Gerhardt, H., *VEGF and endothelial guidance in angiogenic sprouting.* Organogenesis, 2008. **4**(4): p. 241-6.
83. Friedl, P. and D. Gilmour, *Collective cell migration in morphogenesis, regeneration and cancer.* Nat Rev Mol Cell Biol, 2009. **10**(7): p. 445-57.
84. Haeger, A., et al., *Collective cell migration: guidance principles and hierarchies.* Trends Cell Biol, 2015. **25**(9): p. 556-66.
85. Lintz, M., A. Muñoz, and C.A. Reinhart-King, *The Mechanics of Single Cell and Collective Migration of Tumor Cells.* J Biomech Eng, 2017. **139**(2).
86. Nabeshima, K., et al., *Front-cell-specific expression of membrane-type 1 matrix metalloproteinase and gelatinase A during cohort migration of colon carcinoma cells induced by hepatocyte growth factor/scatter factor.* Cancer Res, 2000. **60**(13): p. 3364-9.
87. Hendrix, M.J., et al., *Molecular plasticity of human melanoma cells.* Oncogene, 2003. **22**(20): p. 3070-5.
88. Ewald, A.J., et al., *Collective epithelial migration and cell rearrangements drive mammary branching morphogenesis.* Dev Cell, 2008. **14**(4): p. 570-81.
89. Malet-Engra, G., et al., *Collective cell motility promotes chemotactic prowess and resistance to chemorepulsion.* Curr Biol, 2015. **25**(2): p. 242-250.
90. Puliafito, A., et al., *Three-dimensional chemotaxis-driven aggregation of tumor cells.* Sci Rep, 2015. **5**: p. 15205.
91. Varennes, J. and A. Mugler, *Sense and Sensitivity: Physical Limits to Multicellular Sensing, Migration, and Drug Response.* Mol Pharm, 2016. **13**(7): p. 2224-32.
92. Varennes, J., B. Han, and A. Mugler, *Collective Chemotaxis through Noisy Multicellular Gradient Sensing.* Biophys J, 2016. **111**(3): p. 640-649.
93. Ellison, D., et al., *Cell-cell communication enhances the capacity of cell ensembles to sense shallow gradients during morphogenesis.* Proc Natl Acad Sci U S A, 2016. **113**(6): p. E679-88.
94. Camley, B.A., et al., *Emergent Collective Chemotaxis without Single-Cell Gradient Sensing.* Phys Rev Lett, 2016. **116**(9): p. 098101.
95. Rørth, P., *Collective cell migration.* Annu Rev Cell Dev Biol, 2009. **25**: p. 407-29.
96. Hwang, S., et al., *E-cadherin is critical for collective sheet migration and is regulated by the chemokine CXCL12 protein during restitution.* J Biol Chem, 2012. **287**(26): p. 22227-40.

97. Mayor, R. and S. Etienne-Manneville, *The front and rear of collective cell migration.* Nat Rev Mol Cell Biol, 2016. **17**(2): p. 97-109.
98. Shellard, A., et al., *Supracellular contraction at the rear of neural crest cell groups drives collective chemotaxis.* Science, 2018. **362**(6412): p. 339-343.
99. Trepat, X. and J.J. Fredberg, *Plithotaxis and emergent dynamics in collective cellular migration.* Trends Cell Biol, 2011. **21**(11): p. 638-46.
100. Maruthamuthu, V., Y. Aratyn-Schaus, and M.L. Gardel, *Conserved F-actin dynamics and force transmission at cell adhesions.* Curr Opin Cell Biol, 2010. **22**(5): p. 583-8.
101. Friedl, P. and R. Mayor, *Tuning Collective Cell Migration by Cell-Cell Junction Regulation.* Cold Spring Harb Perspect Biol, 2017. **9**(4).
102. Collins, C. and W.J. Nelson, *Running with neighbors: coordinating cell migration and cell-cell adhesion.* Curr Opin Cell Biol, 2015. **36**: p. 62-70.
103. Janiszewska, M., M.C. Primi, and T. Izard, *Cell adhesion in cancer: Beyond the migration of single cells.* J Biol Chem, 2020. **295**(8): p. 2495-2505.
104. Shapiro, L. and W.I. Weis, *Structure and biochemistry of cadherins and catenins.* Cold Spring Harb Perspect Biol, 2009. **1**(3): p. a003053.
105. Cavallaro, U. and G. Christofori, *Cell adhesion and signalling by cadherins and Ig-CAMs in cancer.* Nat Rev Cancer, 2004. **4**(2): p. 118-32.
106. Leckband, D.E. and J. de Rooij, *Cadherin adhesion and mechanotransduction.* Annu Rev Cell Dev Biol, 2014. **30**: p. 291-315.
107. De Pascalis, C. and S. Etienne-Manneville, *Single and collective cell migration: the mechanics of adhesions.* Mol Biol Cell, 2017. **28**(14): p. 1833-1846.
108. Delva, E. and A.P. Kowalczyk, *Regulation of cadherin trafficking.* Traffic, 2009. **10**(3): p. 259-67.
109. Garrod, D. and M. Chidgey, *Desmosome structure, composition and function.* Biochim Biophys Acta, 2008. **1778**(3): p. 572-87.
110. Zihni, C., et al., *Tight junctions: from simple barriers to multifunctional molecular gates.* Nat Rev Mol Cell Biol, 2016. **17**(9): p. 564-80.
111. Bachmann, M., et al., *Cell Adhesion by Integrins.* Physiol Rev, 2019. **99**(4): p. 1655-1699.
112. Calderwood, D.A., I.D. Campbell, and D.R. Critchley, *Talins and kindlins: partners in integrin-mediated adhesion.* Nat Rev Mol Cell Biol, 2013. **14**(8): p. 503-17.
113. Desgrosellier, J.S. and D.A. Cheresh, *Integrins in cancer: biological implications and therapeutic opportunities.* Nat Rev Cancer, 2010. **10**(1): p. 9-22.
114. Aksorn, N. and P. Chanvorachote, *Integrin as a Molecular Target for Anti-cancer Approaches in Lung Cancer.* Anticancer Res, 2019. **39**(2): p. 541-548.
115. Vachon, P.H., *Integrin signaling, cell survival, and anoikis: distinctions, differences, and differentiation.* J Signal Transduct, 2011. **2011**: p. 738137.
116. Keely, P.J., *Mechanisms by which the extracellular matrix and integrin signaling act to regulate the switch between tumor suppression and tumor promotion.* J Mammary Gland Biol Neoplasia, 2011. **16**(3): p. 205-19.
117. Parvani, J.G., et al., *Targeted inactivation of β1 integrin induces β3 integrin switching, which drives breast cancer metastasis by TGF-β.* Mol Biol Cell, 2013. **24**(21): p. 3449-59.
118. Pan, B., et al., *β1 and β3 integrins in breast, prostate and pancreatic cancer: A novel implication.* Oncol Lett, 2018. **15**(4): p. 5412-5416.
119. Casey, R.C., et al., *Beta 1-integrins regulate the formation and adhesion of ovarian carcinoma multicellular spheroids.* Am J Pathol, 2001. **159**(6): p. 2071-80.
120. Salmenperä, P., et al., *Formation and activation of fibroblast spheroids depend on fibronectin-integrin interaction.* Exp Cell Res, 2008. **314**(19): p. 3444-52.
121. Juliano, R.L., *Signal transduction by cell adhesion receptors and the cytoskeleton: functions of integrins, cadherins, selectins, and immunoglobulin-superfamily members.* Annu Rev Pharmacol Toxicol, 2002. **42**: p. 283-323.

122. Haeger, A., et al., *Cell jamming: collective invasion of mesenchymal tumor cells imposed by tissue confinement.* Biochim Biophys Acta, 2014. **1840**(8): p. 2386-95.
123. Theveneau, E. and C. Linker, *Leaders in collective migration: are front cells really endowed with a particular set of skills?* F1000Res, 2017. **6**: p. 1899.
124. Yamaguchi, N., et al., *Leader cells regulate collective cell migration via Rac activation in the downstream signaling of integrin β1 and PI3K.* Sci Rep, 2015. **5**: p. 7656.
125. Reffay, M., et al., *Orientation and polarity in collectively migrating cell structures: statics and dynamics.* Biophys J, 2011. **100**(11): p. 2566-75.
126. Osmani, N., et al., *Cdc42 localization and cell polarity depend on membrane traffic.* J Cell Biol, 2010. **191**(7): p. 1261-9.
127. Ellenbroek, S.I., S. Iden, and J.G. Collard, *The Rac activator Tiam1 is required for polarized protrusional outgrowth of primary astrocytes by affecting the organization of the microtubule network.* Small GTPases, 2012. **3**(1): p. 4-14.
128. Scales, T.M. and M. Parsons, *Spatial and temporal regulation of integrin signalling during cell migration.* Curr Opin Cell Biol, 2011. **23**(5): p. 562-8.
129. Krause, M. and A. Gautreau, *Steering cell migration: lamellipodium dynamics and the regulation of directional persistence.* Nat Rev Mol Cell Biol, 2014. **15**(9): p. 577-90.
130. Etienne-Manneville, S., *Microtubules in cell migration.* Annu Rev Cell Dev Biol, 2013. **29**: p. 471-99.
131. Garcin, C. and A. Straube, *Microtubules in cell migration.* Essays Biochem, 2019. **63**(5): p. 509-520.
132. Vignjevic, D., et al., *Fascin, a novel target of beta-catenin-TCF signaling, is expressed at the invasive front of human colon cancer.* Cancer Res, 2007. **67**(14): p. 6844-53.
133. Wolf, K., et al., *Multi-step pericellular proteolysis controls the transition from individual to collective cancer cell invasion.* Nat Cell Biol, 2007. **9**(8): p. 893-904.
134. Weavers, H. and H. Skaer, *Tip cells: master regulators of tubulogenesis?* Semin Cell Dev Biol, 2014. **31**: p. 91-9.
135. Peglion, F., F. Llense, and S. Etienne-Manneville, *Adherens junction treadmilling during collective migration.* Nat Cell Biol, 2014. **16**(7): p. 639-51.
136. Bazellières, E., et al., *Control of cell-cell forces and collective cell dynamics by the intercellular adhesome.* Nat Cell Biol, 2015. **17**(4): p. 409-20.
137. Wilson, A.L., et al., *Cadherin-4 plays a role in the development of zebrafish cranial ganglia and lateral line system.* Dev Dyn, 2007. **236**(3): p. 893-902.
138. Niewiadomska, P., D. Godt, and U. Tepass, *DE-Cadherin is required for intercellular motility during Drosophila oogenesis.* J Cell Biol, 1999. **144**(3): p. 533-47.
139. Cui, Y. and S. Yamada, *N-cadherin dependent collective cell invasion of prostate cancer cells is regulated by the N-terminus of α-catenin.* PLoS One, 2013. **8**(1): p. e55069.
140. Trepat, X., et al., *Physical forces during collective cell migration.* Nature Physics, 2009. **5**: p. 426-430.
141. Abercrombie, M., *Contact inhibition in tissue culture.* In Vitro, 1970. **6**(2): p. 128-42.
142. Lauffenburger, D.A. and S.H. Zigmond, *Chemotactic factor concentration gradients in chemotaxis assay systems.* J Immunol Methods, 1981. **40**(1): p. 45-60.
143. HARRIS, H., *Role of chemotaxis in inflammation.* Physiol Rev, 1954. **34**(3): p. 529-62.
144. Insall, R.H., *Understanding eukaryotic chemotaxis: a pseudopod-centred view.* Nat Rev Mol Cell Biol, 2010. **11**(6): p. 453-8.
145. Roussos, E.T., J.S. Condeelis, and A. Patsialou, *Chemotaxis in cancer.* Nat Rev Cancer, 2011. **11**(8): p. 573-87.
146. Roca-Cusachs, P., R. Sunyer, and X. Trepat, *Mechanical guidance of cell migration: lessons from chemotaxis.* Curr Opin Cell Biol, 2013. **25**(5): p. 543-9.
147. Bagorda, A. and C.A. Parent, *Eukaryotic chemotaxis at a glance.* J Cell Sci, 2008. **121**(Pt 16): p. 2621-4.

148. Majumdar, R., M. Sixt, and C.A. Parent, *New paradigms in the establishment and maintenance of gradients during directed cell migration.* Curr Opin Cell Biol, 2014. **30**: p. 33-40.
149. Packard, B.Z., et al., *Direct visualization of protease activity on cells migrating in three-dimensions.* Matrix Biol, 2009. **28**(1): p. 3-10.
150. Mouneimne, G., et al., *Spatial and temporal control of cofilin activity is required for directional sensing during chemotaxis.* Curr Biol, 2006. **16**(22): p. 2193-205.
151. Zicha, D., et al., *Chemotaxis of macrophages is abolished in the Wiskott-Aldrich syndrome.* Br J Haematol, 1998. **101**(4): p. 659-65.
152. Desmarais, V., et al., *N-WASP and cortactin are involved in invadopodium-dependent chemotaxis to EGF in breast tumor cells.* Cell Motil Cytoskeleton, 2009. **66**(6): p. 303-16.
153. Seano, G. and L. Primo, *Podosomes and invadopodia: tools to breach vascular basement membrane.* Cell Cycle, 2015. **14**(9): p. 1370-4.
154. Tessier-Lavigne, M., *Axon guidance by diffusible repellants and attractants.* Curr Opin Genet Dev, 1994. **4**(4): p. 596-601.
155. Cai, D. and D.J. Montell, *Diverse and dynamic sources and sinks in gradient formation and directed migration.* Curr Opin Cell Biol, 2014. **30**: p. 91-8.
156. Valentin, G., P. Haas, and D. Gilmour, *The chemokine SDF1a coordinates tissue migration through the spatially restricted activation of Cxcr7 and Cxcr4b.* Curr Biol, 2007. **17**(12): p. 1026-31.
157. Aman, A. and T. Piotrowski, *Wnt/beta-catenin and Fgf signaling control collective cell migration by restricting chemokine receptor expression.* Dev Cell, 2008. **15**(5): p. 749-61.
158. Muinonen-Martin, A.J., et al., *Melanoma cells break down LPA to establish local gradients that drive chemotactic dispersal.* PLoS Biol, 2014. **12**(10): p. e1001966.
159. Dambly-Chaudière, C., N. Cubedo, and A. Ghysen, *Control of cell migration in the development of the posterior lateral line: antagonistic interactions between the chemokine receptors CXCR4 and CXCR7/RDC1.* BMC Dev Biol, 2007. **7**: p. 23.
160. Donà, E., et al., *Directional tissue migration through a self-generated chemokine gradient.* Nature, 2013. **503**(7475): p. 285-9.
161. Condeelis, J. and J.W. Pollard, *Macrophages: obligate partners for tumor cell migration, invasion, and metastasis.* Cell, 2006. **124**(2): p. 263-6.
162. Shields, J.D., et al., *Autologous chemotaxis as a mechanism of tumor cell homing to lymphatics via interstitial flow and autocrine CCR7 signaling.* Cancer Cell, 2007. **11**(6): p. 526-38.
163. Theveneau, E., et al., *Collective chemotaxis requires contact-dependent cell polarity.* Dev Cell, 2010. **19**(1): p. 39-53.
164. Winklbauer, R. and M. Nagel, *Directional mesoderm cell migration in the Xenopus gastrula.* Dev Biol, 1991. **148**(2): p. 573-89.
165. Winklbauer, R., et al., *Cell interaction and its role in mesoderm cell migration during Xenopus gastrulation.* Dev Dyn, 1992. **195**(4): p. 290-302.
166. Nakatsuji, N. and K.E. Johnson, *Conditioning of a culture substratum by the ectodermal layer promotes attachment and oriented locomotion by amphibian gastrula mesodermal cells.* J Cell Sci, 1983. **59**: p. 43-60.
167. Camley, B.A., *Collective gradient sensing and chemotaxis: modeling and recent developments.* J Phys Condens Matter, 2018. **30**(22): p. 223001.
168. Klezovitch, O. and V. Vasioukhin, *Cadherin signaling: keeping cells in touch.* F1000Res, 2015. **4**(F1000 Faculty Rev): p. 550.
169. Hu, B., et al., *Physical limits on cellular sensing of spatial gradients.* Phys Rev Lett, 2010. **105**(4): p. 048104.
170. Hu, B., et al., *How geometry and internal bias affect the accuracy of eukaryotic gradient sensing.* Phys Rev E Stat Nonlin Soft Matter Phys, 2011. **83**(2 Pt 1): p. 021917.

171. Segota, I., et al., *High fidelity information processing in folic acid chemotaxis of Dictyostelium amoebae.* J R Soc Interface, 2013. **10**(88): p. 20130606.
172. Varennes, J., et al., *Emergent versus Individual-Based Multicellular Chemotaxis.* Phys Rev Lett, 2017. **119**(18): p. 188101.
173. McLennan, R., et al., *Neural crest migration is driven by a few trailblazer cells with a unique molecular signature narrowly confined to the invasive front.* Development, 2015. **142**(11): p. 2014-25.
174. Lämmermann, T., et al., *Neutrophil swarms require LTB4 and integrins at sites of cell death in vivo.* Nature, 2013. **498**(7454): p. 371-5.
175. Sackstein, R., T. Schatton, and S.R. Barthel, *T-lymphocyte homing: an underappreciated yet critical hurdle for successful cancer immunotherapy.* Lab Invest, 2017. **97**(6): p. 669-697.
176. Wrenn, E.D., et al., *Regulation of collective metastasis by nanolumenal signaling.* Cell, 2020. **183**(2): p. 395-410.
177. Scheel, C., et al., *Paracrine and autocrine signals induce and maintain mesenchymal and stem cell states in the breast.* Cell, 2011. **145**(6): p. 926-40.
178. Heasley, L.E., *Autocrine and paracrine signaling through neuropeptide receptors in human cancer.* Oncogene, 2001. **20**(13): p. 1563-9.
179. Hoelzinger, D.B., T. Demuth, and M.E. Berens, *Autocrine factors that sustain glioma invasion and paracrine biology in the brain microenvironment.* J Natl Cancer Inst, 2007. **99**(21): p. 1583-93.
180. Ben-Jonathan, N., et al., *Prolactin as an autocrine/paracrine growth factor in human cancer.* Trends Endocrinol Metab, 2002. **13**(6): p. 245-50.
181. Thomas, S.K., J. Lee, and G.L. Beatty, *Paracrine and cell autonomous signalling in pancreatic cancer progression and metastasis.* EBioMedicine, 2020. **53**: p. 102662.
182. Ayuso, J.M., et al., *Study of the Chemotactic Response of Multicellular Spheroids in a Microfluidic Device.* PLoS One, 2015. **10**(10): p. e0139515.
183. Naber, H.P., et al., *Spheroid assay to measure TGF-β-induced invasion.* J Vis Exp, 2011(57).
184. Forster, B., et al. *Extended Depth-of-Focus for Multi-Channel Microscopy Images: A Complex Wavelet Approach*. in *2nd IEEE International Symposium on Biomedical Imaging: Nano to Macro (IEEE Cat No. 04EX821)*. 2004. Arlington, VA, USA.
185. Forster, B., et al., *Complex wavelets for extended depth-of-field: a new method for the fusion of multichannel microscopy images.* Microsc Res Tech, 2004. **65**(1-2): p. 33-42.
186. Berg, S., et al., *ilastik: interactive machine learning for (bio)image analysis.* Nat Methods, 2019. **16**(12): p. 1226-1232.
187. Sommer, C., et al. *ilastik: Interactive Learning and Segmentation Toolkit*. in *Eighth IEEE International Symposium on Biomedical Imaging (ISBI)*. 2011. Chicago Illinois, USA.
188. Zoetemelk, M., et al., *Short-term 3D culture systems of various complexity for treatment optimization of colorectal carcinoma.* Sci Rep, 2019. **9**(1): p. 7103.
189. Vinci, M., et al., *Advances in establishment and analysis of three-dimensional tumor spheroid-based functional assays for target validation and drug evaluation.* BMC Biol, 2012. **10**: p. 29.
190. Hehlgans, S., et al., *Caveolin-1 mediated radioresistance of 3D grown pancreatic cancer cells.* Radiother Oncol, 2009. **92**(3): p. 362-70.
191. Arai, K., et al., *Proteomic approach toward molecular backgrounds of drug resistance of osteosarcoma cells in spheroid culture system.* Proteomics, 2013. **13**(15): p. 2351-60.
192. Han, K., et al., *CRISPR screens in cancer spheroids identify 3D growth-specific vulnerabilities.* Nature, 2020. **580**(7801): p. 136-141.
193. Feng, H., et al., *Homogeneous pancreatic cancer spheroids mimic growth pattern of circulating tumor cell clusters and macrometastases: displaying heterogeneity and crater-like structure on inner layer.* J Cancer Res Clin Oncol, 2017. **143**(9): p. 1771-1786.
194. Tofani, L.B., et al., *Establishment and characterization of an in vitro 3D ovarian cancer model for drug screening assays.* Biotechnol Prog, 2020. **36**(6): p. e3034.

195. Gayan, S., A. Teli, and T. Dey, *Inherent aggressive character of invasive and non-invasive cells dictates the in vitro migration pattern of multicellular spheroid.* Sci Rep, 2017. **7**(1): p. 11527.
196. Härmä, V., et al., *A comprehensive panel of three-dimensional models for studies of prostate cancer growth, invasion and drug responses.* PLoS One, 2010. **5**(5): p. e10431.
197. Kenny, P.A., et al., *The morphologies of breast cancer cell lines in three-dimensional assays correlate with their profiles of gene expression.* Mol Oncol, 2007. **1**(1): p. 84-96.
198. Enmon, R.M., et al., *Dynamics of spheroid self-assembly in liquid-overlay culture of DU 145 human prostate cancer cells.* Biotechnol Bioeng, 2001. **72**(6): p. 579-91.
199. Enmon, R.M., et al., *Aggregation kinetics of well and poorly differentiated human prostate cancer cells.* Biotechnol Bioeng, 2002. **80**(5): p. 580-8.
200. Adenis, L., et al., *Experimental and modeling study of the formation of cell aggregates with differential substrate adhesion.* PLoS One, 2020. **15**(2): p. e0222371.
201. *ExPASy Cellosaurus database*. Available from: https://web.expasy.org/cellosaurus/.
202. *The Landscape of Cancer Cell Line Metabolism*. Available from: https://www.metabolomicsworkbench.org/data/study_textformat_view.php?STUDY_ID=ST001142&ANALYSIS_ID= AN001875.
203. Varnum-Finney, B.J., E. Voss, and D.R. Soll, *Frequency and orientation of pseudopod formation of Dictyostelium discoideum amebae chemotaxing in a spatial gradient: further evidence for a temporal mechanism.* Cell Motil Cytoskeleton, 1987. **8**(1): p. 18-26.
204. Mishra, A.K., et al., *Coordination of protrusion dynamics within and between collectively migrating border cells by myosin II.* Mol Biol Cell, 2019. **30**(19): p. 2490-2502.
205. Combedazou, A., et al., *Myosin II governs collective cell migration behaviour downstream of guidance receptor signalling.* J Cell Sci, 2017. **130**(1): p. 97-103.
206. Omelchenko, T. and A. Hall, *Myosin-IXA regulates collective epithelial cell migration by targeting RhoGAP activity to cell-cell junctions.* Curr Biol, 2012. **22**(4): p. 278-88.
207. Goswami, S., et al., *Macrophages promote the invasion of breast carcinoma cells via a colony-stimulating factor-1/epidermal growth factor paracrine loop.* Cancer Res, 2005. **65**(12): p. 5278-83.
208. Heldin, C.H., *Autocrine PDGF stimulation in malignancies.* Ups J Med Sci, 2012. **117**(2): p. 83-91.
209. Ungefroren, H., *Autocrine TGF-β in Cancer: Review of the Literature and Caveats in Experimental Analysis.* Int J Mol Sci, 2021. **22**(2).
210. Marek, L., et al., *Fibroblast growth factor (FGF) and FGF receptor-mediated autocrine signaling in non-small-cell lung cancer cells.* Mol Pharmacol, 2009. **75**(1): p. 196-207.
211. Mercurio, A.M., et al., *Autocrine signaling in carcinoma: VEGF and the alpha6beta4 integrin.* Semin Cancer Biol, 2004. **14**(2): p. 115-22.
212. Patsialou, A., et al., *Invasion of human breast cancer cells in vivo requires both paracrine and autocrine loops involving the colony-stimulating factor-1 receptor.* Cancer Res, 2009. **69**(24): p. 9498-506.
213. Yi, E.H., et al., *STAT3-RANTES autocrine signaling is essential for tamoxifen resistance in human breast cancer cells.* Mol Cancer Res, 2013. **11**(1): p. 31-42.
214. Graeber, T.G. and D. Eisenberg, *Bioinformatic identification of potential autocrine signaling loops in cancers from gene expression profiles.* Nat Genet, 2001. **29**(3): p. 295-300.
215. Müller, A., et al., *Involvement of chemokine receptors in breast cancer metastasis.* Nature, 2001. **410**(6824): p. 50-6.
216. Dagogo-Jack, I. and A.T. Shaw, *Tumour heterogeneity and resistance to cancer therapies.* Nat Rev Clin Oncol, 2018. **15**(2): p. 81-94.
217. Sardana, G., et al., *Proteomic analysis of conditioned media from the PC3, LNCaP, and 22Rv1 prostate cancer cell lines: discovery and validation of candidate prostate cancer biomarkers.* J Proteome Res, 2008. **7**(8): p. 3329-38.

218. Puto, L.A., C. Benner, and T. Hunter, *The DAXX co-repressor is directly recruited to active regulatory elements genome-wide to regulate autophagy programs in a model of human prostate cancer.* Oncoscience, 2015. **2**(4): p. 362-72.
219. Stoker, M. and M. Perryman, *An epithelial scatter factor released by embryo fibroblasts.* J Cell Sci, 1985. **77**: p. 209-23.
220. Baldanzi, G. and A. Graziani, *Physiological Signaling and Structure of the HGF Receptor MET.* Biomedicines, 2014. **3**(1): p. 1-31.
221. Comoglio, P.M. and C. Boccaccio, *Scatter factors and invasive growth.* Semin Cancer Biol, 2001. **11**(2): p. 153-65.